

**Synthesis and Characterization of Novel Stationary Phases for
Model and Catalytic Reactions in Interphases and
New Polysiloxane Matrices**



**Synthese und Charakterisierung von neuartigen Stationärphasen
für Modell- und katalytische Reaktionen in Interphasen
und neuer Polysiloxan-Matrices**

DISSERTATION

der Fakultät für Chemie und Pharmazie
der Eberhard-Karls-Universität Tübingen

zur Erlangung des Grades eines Doktors
der Naturwissenschaften

2001

vorgelegt von

Stefan Brugger

Tag der mündlichen Prüfung:

29. Mai 2001

Dekan:

Prof. Dr. H. Probst

1. Berichterstatter:

Prof. Dr. E. Lindner

2. Berichterstatter:

Prof. Dr. H. A. Mayer

Meinen Eltern, Andreas und Anja

Die vorliegende Arbeit wurde am
Institut für Anorganische Chemie II der
Eberhard–Karls–Universität Tübingen
unter der Leitung von
Herrn Professor Dr. rer. nat. Ekkehard Lindner
angefertigt.

Meinem Doktorvater,
Herrn Prof. Dr. Ekkehard Lindner,
danke ich herzlich für die Themenstellung,
für die Bereitstellung ausgezeichneter Arbeitsbedingungen,
für wertvolle Anregungen und Diskussionen
sowie sein stetes Interesse an dieser Arbeit.

Mein besonderer Dank gilt Herrn Prof. Dr. Hermann A. Mayer für die in allen Bereichen freundschaftliche Zusammenarbeit, die NMR–Ausbildung und zahlreichen hilfreichen Diskussionen.

Ferner danke ich herzlich:

Dem „Kordinator“ Dr. Klaus Eichele für sehr hilfreiche NMR–Anregungen.

Dem „Festkörper NMR–Team“ Dr. Frank Höhn, Dr. Andreas Baumann, Dr. Joachim Büchele und Dipl. Chem. Michael Marzini sowie Dr. Jürgen Wegmann und Dr. Stefan Bachmann für die gute und freundschaftlich Zusammenarbeit an den NMR Spektrometern.

Herrn Dr. Ulf Kehrer, Frau Heike Dorn und Frau Angelika Ehmman für Hochauflösungs–NMR–Messungen.

Herrn Dipl. Chem. Stefan Steinbrecher, Institut für Angewandte Physik der Universität Tübingen, für die SEM– und EDX–Messungen und deren Auswertung, sowie Herrn Dipl. Chem. Michael Seiler, Institut für Physikalische Chemie der Universität Stuttgart, für die EXAFS–Messungen.

Dem letzten wahren „Interphasler“ Dipl. Chem. Thomas Salesch für BET–Untersuchungen und die sehr freundschaftliche Zusammenarbeit, sowie Herrn Peter Wegner für die ausgezeichnete Ausstattung der Katalysenstation.

Den Herrn Dr. Ulf Kehrer und Dipl. Chem. Michael Henes für die ausgezeichnete und sehr kollegiale Zusammenarbeit in 8M20.

Frau Roswitha Conrad, Frau Barbara Saller, Frau Brigitte Schindler und Herrn Dr. Hans–Dieter Ebert, sowie allen technischen und wissenschaftlichen Angestellten, die zum Gelingen dieser Arbeit beigetragen haben.

Mein ganz persönlicher Dank gilt meiner Freundin Anja Maurer, die durch ihre moralische Unterstützung einen sehr grossen Anteil am Gelingen dieser Dissertation hat.

CONTENTS

1. INTRODUCTION	1
2. GENERAL SECTION	3
2.1 General Remarks	3
2.1.1 Concept of the Interphase	3
2.1.2 Sol–Gel Process	4
2.1.3 Solid State NMR Spectroscopy	5
2.1.3.1 Relaxation Times, Cross Polarization Constants and Line Widths	5
2.2 Synthesis, Characterization and Accessibility Studies on Sol–Gel Processed Diphosphine Ligands	8
2.2.1 Introduction	8
2.2.2 Sol–Gel Processing of $\mathbf{1(T^0)}$ with Different Amounts of the Co–condensing Agents $\mathbf{D^0-C_6-D^0}$ and $\mathbf{Ph(1,4-C_3D^0)_2}$	8
2.2.3 Solid State NMR Spectroscopic Investigations	10
2.2.3.1 ^{29}Si CP/MAS NMR Spectroscopy	10
2.2.3.2 ^{31}P and ^{13}C CP/MAS NMR Spectroscopy	13
2.2.4 Studies on the Dynamic Behavior of the Xerogels by ^{29}Si and ^{31}P Solid State NMR Spectroscopy	14

2.2.5 Accessibility Studies on the P–Centers in the Polysiloxane–Bound	
Diphosphines Ib and Id	16
2.2.5.1 Behavior toward H ₂ O ₂	16
2.2.5.2 Behavior toward S ₈	16
2.2.5.3 Behavior toward CH ₃ I.....	18
2.2.5.4 Behavior toward (NBD)Mo(CO) ₄	18
2.2.5.5 Behavior toward (COD)PdCl ₂	18
2.2.6 SEM Images and EDX Measurements.....	20
2.2.7 Conclusion	21
2.3 Novel Sol–Gel Processed Rhodium(I) Complexes: Synthesis, Characterization and	
Catalytic Reactions in Interphases.....	23
2.3.1 Introduction.....	23
2.3.2 Synthesis of the Monomeric Rhodium(I) Complex 2(T⁰)	23
2.3.3 Sol–Gel Processing of 2(T⁰)	24
2.3.4 Solid State NMR Spectroscopy	26
2.3.4.1 ²⁹ Si CP/MAS NMR Spectroscopy.....	26
2.3.4.2 ³¹ P and ¹³ C CP/MAS NMR Spectroscopy	29
2.3.5 EXAFS Structure Determination of the Rhodium(I) Complexes IIa , IIb , and IIc	29
2.3.6 Studies on the Dynamic Behavior of the Xerogels IIa – i by Solid State NMR	
Spectroscopy.....	31
2.3.6.1 Mobility of the Matrix	31
2.3.6.2 Mobility of the Reactive Center.....	32
2.3.7 Accessibility Studies of the Anchored Rhodium(I) Complexes by Catalytic	
Hydrogenation of 1–Hexene	33
2.3.8 Surface Area and EDX Measurements.....	37

2.3.9 Conclusion	40
2.4 Synthesis, Sol–Gel Processing, and Investigations on the Mobility of Novel	
D– and T–bifunctionalized Co–condensing Agents..... 41	
2.4.1 Introduction.....	41
2.4.2 Preparation of the Monomeric Precursors 3(D⁰) , 4(T⁰) , 5(D⁰) , and 6(T⁰)	41
2.4.3 Sol–gel Processing of 3(D⁰) , 4(T⁰) , 5(D⁰) , and 6(T⁰)	42
2.4.4 Solid State NMR Spectroscopic Investigations	43
2.4.4.1 ²⁹ Si CP/MAS NMR Spectroscopy.....	43
2.4.4.2 ¹³ C CP/MAS NMR Spectroscopy.....	47
2.4.5 Studies on the Dynamic Behavior of the Polysiloxanes by Solid State and	
Suspension State NMR Spectroscopy.....	47
2.4.6 Surface Area Measurements, SEM Images and EDX Measurements	52
2.4.7 Conclusion	54
3. EXPERIMENTAL SECTION.....	56
3.1 General Remarks.....	56
3.1.1 Reagents	56
3.1.2 Elemental Analyses, IR and Mass Investigations	56
3.1.3 NMR Spectroscopy in Solution	57
3.1.4 Solid State NMR Measurements.....	57
3.1.5 Suspension NMR Measurements	58
3.1.6 EXAFS Measurements	59
3.1.7 SEM and EDX Investigations.....	59
3.1.8 Catalysis.....	60

3.2 Preparation of the Compounds	61
3.2.1 Synthesis of the Monomers	61
3.2.1.1 Preparation of the Rhodium(I) Complex 2(T⁰)	61
3.2.1.2 Synthesis of the Co-condensing Agents 3(D⁰) , 4(T⁰) , 5(D⁰) , and 6(T⁰)	62
3.2.2 Synthesis of the Xerogels Ia – d	65
3.2.3 Synthesis of the Xerogels I_Ab and I_Ad	67
3.2.4 Synthesis of the Xerogels I_Bb and I_Bd	68
3.2.5 Synthesis of the Xerogels I_Cb and I_Cd	69
3.2.6 Synthesis of the Xerogels I_Db and I_Dd	70
3.2.7 Synthesis of the Xerogels I_Eb and I_Ed	71
3.2.8 Synthesis of the Xerogels IIa – i	72
3.2.9 Synthesis of the Xerogels IIIa, b , IVa, b , Va, b , and VIa, b	76
4. REFERENCES	80
5. SUMMARY	84

1. Introduction

In the last years polymer-supported catalysts have evolved into an area of intensive research with the goal to combine the advantages of homogeneous and heterogeneous catalysis¹⁻³. But the anchoring of reactive centers to inorganic or organic polymers entails several momentous disadvantages such as high metal loss ('leaching') or inhomogeneity of the reactive centers⁴. As an efficient alternative for the reduction or even elimination of these handicaps 'Chemistry in Interphases' was recently introduced². Interphases are systems in which a stationary phase and a mobile component penetrate each other on a molecular scale. An ideal interphase, which is provided with a swellable polymer, affords a solution-like state. Therefore interphases are able to imitate homogeneous conditions, because the active centers become highly mobile simulating the properties of a solution and hence accessible for substrates⁵⁻⁸.

For the generation of stationary phases several T-functionalized silanes of the type Fn-Si(OR)_3 were sol-gel processed with or without co-condensation agents⁹⁻¹⁴. The functional group Fn generally represents either a ligand or a metal complex. These reactive centers are distributed across the entire carrier matrix. The co-condensing agents play an important role in controlling the density and the distance of the reactive centers^{3,10,15,16}. Frequently applied co-condensing agents are alkoxysilanes such as Si(OEt)_4 (\mathbf{Q}^0), MeSi(OMe)_3 (\mathbf{T}^0), and $\text{Me}_2\text{Si(OMe)}_2$ (\mathbf{D}^0)^{13,17-21}. D-groups show high mobility in interphases but they have the disadvantage to be washed out during the sol-gel process. By way of contrast Q-groups cannot be washed out but they lack of the necessary mobility. By the development of D-bifunctionalized organosilanes $\text{MeSi(OMe)}_2(\text{CH}_2)_z(\text{MeO})_2\text{SiMe}$ ($\mathbf{D}^0\text{-C}_z\mathbf{D}^0$, $z = 6, 8, 14$)²² and

$$\text{MeSi(OMe)}_2(\text{CH})_z(\text{C}_6\text{H}_4)(\text{CH}_2)_z(\text{MeO})_2\text{SiMe} \quad (\mathbf{Ph(1,4-C}_z\mathbf{D}^0)_2,$$

$z = 3, 4$)²³ the advantages of Q- and D-groups have been successfully combined. They are not washed out during the sol-gel process and the reactive centers show a high mobility.

The objective of this study is the accessibility and catalytic application of reactive centers anchored to different D-bifunctionalized polysiloxane based inorganic-organic hybrid materials. The synthesis and characterization of sol-gel processed diphosphines and their accessibility by small and bulky reactants is reported in the first part of this thesis. The preparation, sol-gel processing, characterization, and catalytic application in hydrogenation of cationic rhodium(I) complexes is in the focus of the second chapter of this work. In the third part it is the objective to investigate the synthesis and sol-gel processing of novel D- and T-bifunctionalized co-condensing agents and the dynamic properties of the corresponding novel inorganic-organic hybrid materials. The most detailed information about the structure and the dynamic properties of these materials is obtained by multinuclear solid state NMR spectroscopy²⁴⁻²⁷. ²⁹Si NMR spectroscopy enables the characterization of the carrier matrix, the degree of condensation, and the stoichiometric composition of the hybrid materials. ¹³C and ³¹P NMR spectroscopy allow an insight into the hydrocarbon regions of the backbone and the reactive centers, respectively. To get structural information of the atomic distances in the coordination sphere of the active metal center EXAFS spectroscopical measurements are undertaken and in order to have an insight into the morphology and elemental composition of the materials SEM imaging and EDX measurements are performed.

2. General Section

2.1 General Remarks

2.1.1 Concept of the Interphase

The inorganic–organic hybrid materials are considered to build highly swellable stationary phases consisting of a chemically and thermally inert carrier matrix (e.g. TiO_2 , polysiloxane, organic polymer), spacer units (PEG, alkyl chains, combined alkyl phenyl systems) and the reactive centers (ligand or transition metal complex). These materials have the advantages of nearly unlimited modifiability, reduced leaching of functional groups and controlling the density of the reaction centers ².

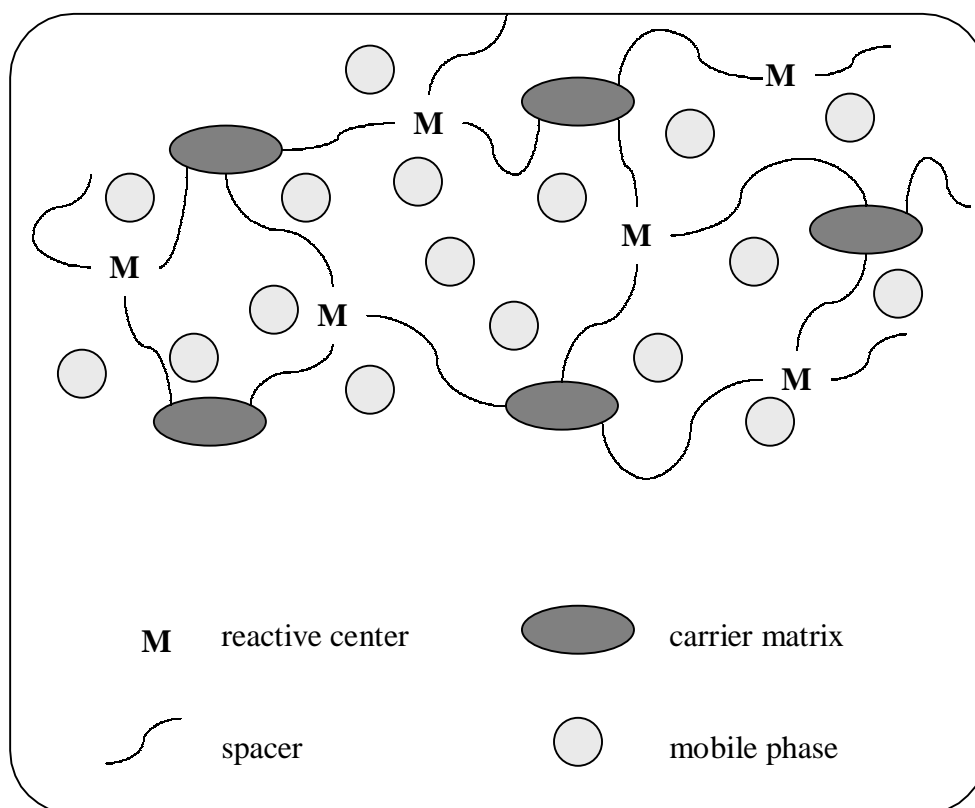


Figure 1 Schematic description of an interphase.

The formation of such an interphase takes place, if a mobile component (e.g. a solvent or a reactant) is added. Then the stationary phase and the mobile phase are able to penetrate each other on a molecular scale without forming a homogenous phase (Figure 1). Therefore interphases are able to imitate homogenous conditions, because the active centers become highly mobile simulating the properties of a solution and hence they are accessible for substrates.

2.1.2 Sol–Gel Process

The sol–gel process is a method to generate the carrier matrix of such interphases by controlled hydrolysis and condensation of suitable precursor molecules (e.g. functionalized alkoxy silanes or metal alkoxides) at mild conditions^{10,28}.



By varying the monomeric sol–gel precursors, the kind of sol–gel catalyst and the solvent, the obtained two– or three–dimensional polysiloxane networks are stationary phases, in which the polarity and swelling capability of the matrix and the density and mobility of the reactive centers can be tuned in a wide range.

2.1.3 Solid State NMR Spectroscopy

Due to the amorphous nature of these inorganic–organic hybrid materials, solid state NMR spectroscopy is the most important method to investigate the structure and dynamic behavior of such copolymers. In rather short times spectra of different NMR active nuclei (^{13}C , ^{29}Si and ^{31}P) incorporated into several sites of the matrix can be recorded routinely by the combination of cross polarization (CP) and magic angle spinning (MAS) ^{29–31}. The comparison of the chemical shifts in the CP/MAS spectra with those obtained from corresponding homogeneous monomers in high resolution spectra establishes the integrity of the polysiloxane–bound species. By modification of the basic cross polarization experiment an access to several dynamic parameters (T_{1X} , $T_{1\rho\text{H}}$, and T_{XH}), which are very sensitive to motion in different time scales, is guaranteed ^{32,33}.

2.1.3.1 Relaxation Times, Cross Polarization Constants and Line Widths

By measuring the spin–lattice relaxation time of the protons in the rotating frame ($T_{1\rho\text{H}}$) the mobility of the materials in the kHz region is revealed. An enhanced mobility in this region influences the dipolar coupling among the protons. This reduced dipolar coupling results in different $T_{1\rho\text{H}}$ values for various sites in the material ³⁴. However, the relaxation constant $T_{1\rho\text{H}}$ is an averaged quantity for all protons within domains of 1 – 2 nm in diameter, whenever an efficient spin diffusion process is present. An unambiguous discussion of the dynamic properties of materials based on relaxation parameters ($T_{1\rho\text{H}}$) is only possible, if the corresponding correlation time τ_c is known.

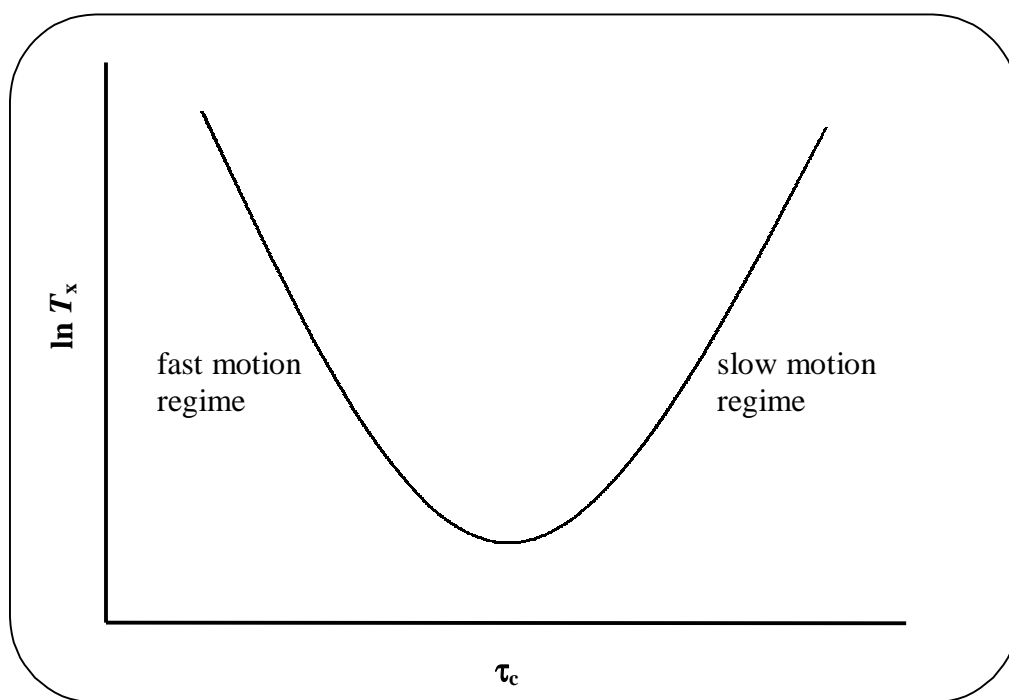


Figure 2 Correlation–time curve.

The correlation–time curve (Figure 2) exhibits two branches, the so called slow (right), and fast motion regime (left). The discrimination between the two cases is possible by temperature dependent measurements. In the slow motion regime an increasing temperature correlates with decreasing relaxation times whereas in the fast–motion regime the values of the relaxation rates increase with increasing temperature (shorter τ_c)²⁴.

The cross polarization constant T_{XH} is influenced by the number of protons and their distance from the observable hetero nuclei and the rigidity of the heteronuclear coupled spin systems (e. g. silicon and protons). If the number and distances of protons surrounding the hetero nucleus in different materials is equal or similar the cross polarization constant T_{XH} is only governed by the mobility. Higher T_{XH} values indicate a more inefficient transfer of magnetization of the protons to the hetero atoms and thus a faster motion.

The line widths of resonances (e.g. ^{31}P) in the solid state are induced by a variety of different interactions, such as heteronuclear dipolar coupling, chemical shift dispersion, and chemical shift anisotropy (CSA). If the local environments of certain nuclei under consideration are identical or at least very similar, the changes of the line widths of signals in the CP/MAS NMR spectra are caused exclusively by the variable flexibilities of the materials.

2.2 Synthesis, Characterization and Accessibility Studies on Sol-Gel Processed Diphosphine Ligands

2.2.1 Introduction

In this part of the thesis the T-functionalized 1,3-bis(diphenylphosphinyl)propane (dppp) [$\mathbf{1}(\mathbf{T}^0)$] with a spacer unit of six methylene groups was sol-gel processed with the D-bifunctionalized co-condensation agents $\mathbf{D}^0\text{-C}_6\text{-D}^0$ and $\mathbf{Ph}(\mathbf{1,4-C}_3\mathbf{D}^0)_2$ in two different ratios. The mobility of the dppp ligand $\mathbf{1}(\mathbf{T}^0)$ in these novel inorganic-organic hybrid polymers and the accessibility of the phosphorus centers were investigated by heteronuclear cross-polarization magic-angle spinning (CP/MAS) solid state NMR spectroscopy and typical phosphine reactions, respectively.

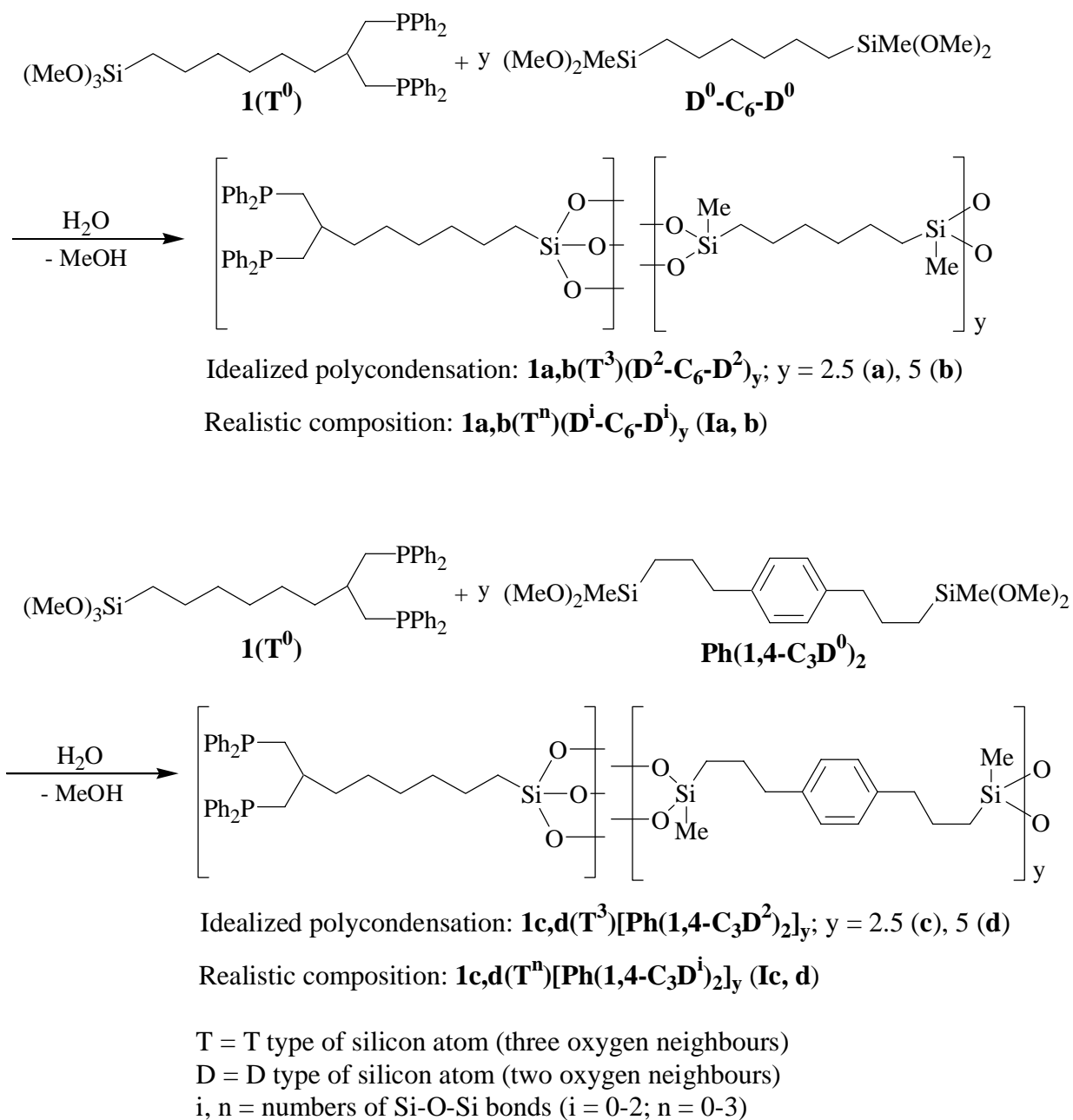
2.2.2 Sol-Gel Processing of $\mathbf{1}(\mathbf{T}^0)$ with Different Amounts of the Co-condensing Agents $\mathbf{D}^0\text{-C}_6\text{-D}^0$ and $\mathbf{Ph}(\mathbf{1,4-C}_3\mathbf{D}^0)_2$

The diphosphine-containing xerogels **Ia** – **d** (Table 1) were prepared by sol-gel processing of the monomeric T-functionalized diphosphine $\mathbf{1}(\mathbf{T}^0)$ with variable amounts of the co-condensation agents $\mathbf{D}^0\text{-C}_6\text{-D}^0$ and $\mathbf{Ph}(\mathbf{1,4-C}_3\mathbf{D}^0)_2$ (Scheme 1).

Table 1 Sol-gel processing and labeling of the xerogels **I**

Diphosphine	Co-condensation agent	ideal T/D ratio	Compound	Xerogel
$\mathbf{1}(\mathbf{T}^0)$	$\mathbf{D}^0\text{-C}_6\text{-D}^0$	5	$\mathbf{1a}(\mathbf{T}^n)(\mathbf{D}^i\text{-C}_6\text{-D}^i)_{2.5}$	Ia
$\mathbf{1}(\mathbf{T}^0)$	$\mathbf{D}^0\text{-C}_6\text{-D}^0$	10	$\mathbf{1b}(\mathbf{T}^n)(\mathbf{D}^i\text{-C}_6\text{-D}^i)_5$	Ib
$\mathbf{1}(\mathbf{T}^0)$	$\mathbf{Ph}(\mathbf{1,4-C}_3\mathbf{D}^0)_2$	5	$\mathbf{1c}(\mathbf{T}^n)[\mathbf{Ph}(\mathbf{1,4-C}_3\mathbf{D}^i)_2]_{2.5}$	Ic
$\mathbf{1}(\mathbf{T}^0)$	$\mathbf{Ph}(\mathbf{1,4-C}_3\mathbf{D}^0)_2$	10	$\mathbf{1d}(\mathbf{T}^n)[\mathbf{Ph}(\mathbf{1,4-C}_3\mathbf{D}^i)_2]_5$	Id

The properties of these materials strongly depend on the reaction conditions during the sol-gel process such as concentration of the monomers, type of solvent and kind of catalyst. All sol-gel processes were carried out in a mixture of THF/MeOH with an excess of water and $(n\text{-Bu})_2\text{Sn}(\text{OAc})_2$ as catalyst. To guarantee reproducible materials uniform reaction conditions were maintained.



Scheme 1 Structure, idealized and realistic compositions of the sol-gel materials **Ia – d**.

2.2.3 Solid State NMR Spectroscopic Investigations

2.2.3.1 ^{29}Si CP/MAS NMR Spectroscopy

As a result of an incomplete condensation the ^{29}Si CP/MAS NMR spectra of the above-mentioned xerogels reveal signals of various substructures with corresponding D^i - and T^n -functions. Average chemical shifts are $\delta = -2.2$ (D^0), -13.6 (D^1), -22.4 (D^2), -60.3 (T^2), and -68.3 (T^3). They remain unchanged with respect to the stoichiometric ratio between the co-condensation agent and the functionalized diphosphine. All silicon atoms in the polysiloxane matrix are in direct proximity of protons, thus silyl species are detectable via cross polarization^{27,35,36}. The signals in the ^{29}Si CP/MAS spectra of the copolymers **Ia** – **d** are located in the typical range for D- and T-silyl functions and their substructures D^0 – D^2 and T^2 – T^3 (Figure 3).

For **Ia** – **d** realistic D/T-ratios and high degrees of condensation were determined by generally known methods^{22,23,37-39} ranging from 81 to 94 % for D- and T-species with exception of **Ic**. In this case the D-functions show a rather low degree of condensation (72 %), which correlates with a high amount of D^0 -species (Table 2). However, these D^0 -groups, that are attached to the polymer network via the second silyl function of the monomeric co-condensation agent, cannot be washed out during solvent processing.

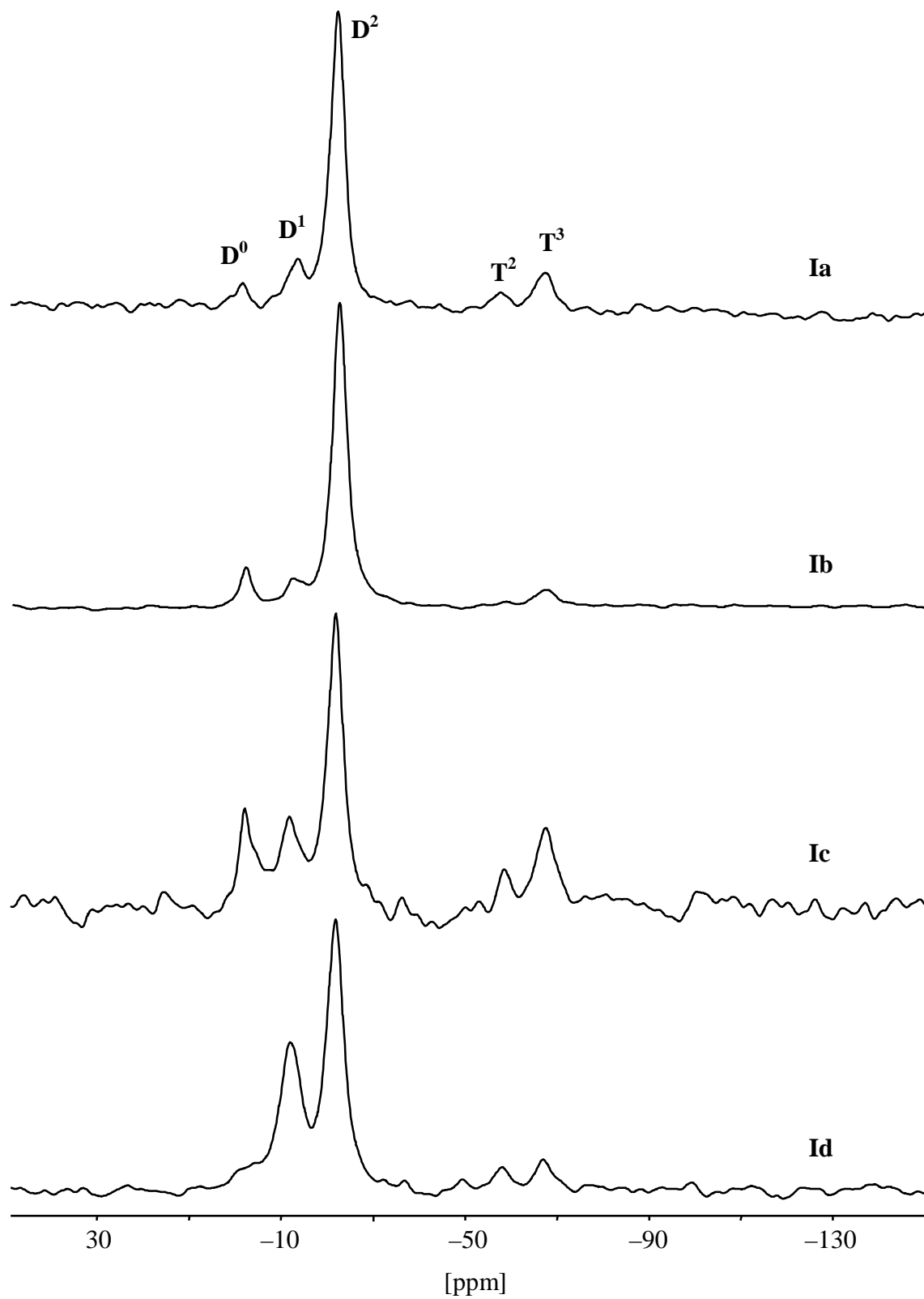


Figure 3 ^{29}Si CP/MAS spectra of the xerogels **Ia** – **d**.

Table 2 Relative I_0 , T_{SiH} , and $T_{1\rho\text{H}}$ data of the silyl species in the xerogels **Ia – d**

Xerogel	relative I_0 data of D and T species ^a					degree of condensation [%]		real T/D moiety ^a	$T_{\text{SiH}}[\text{ms}]^{\text{b}}$					$T_{1\rho\text{H}}[\text{ms}]^{\text{c}}$
	D ⁰	D ¹	D ²	T ²	T ³	D	T		D ⁰	D ¹	D ²	T ²	T ³	
Ia	7.9	7.9	100	6.0	18.7	85	88	1: 4.5	1.71	0.69	1.21	0.70	1.03	3.22
Ib	8.5	11.6	100	2.1	9.4	88	94	1:10.5	1.86	1.04	1.13	0.94	0.82	2.27
Ic	29.4	31.7	100	11.3	26.9	72	90	1: 3.8	0.83	0.80	1.00	0.97	0.56	1.38
Id	<i>d</i>	47.7	100	13.4	14.2	84	81	1:10.7	<i>e</i>	0.83	1.32	0.79	0.52	2.61

^a Determined via deconvolution of ²⁹Si CP/MAS NMR spectra ($T_c = 5$ ms). ^b Determined by contact time variation. ^c Determined via ²⁹Si with the experiment according to ref.⁴⁰. ^d Species not detectable. ^e Intensity too low for a precise determination of T_{SiH} .

2.2.3.2 ^{31}P and ^{13}C CP/MAS NMR Spectroscopy

In the ^{31}P CP/MAS NMR spectra of the polysiloxane-bound diphosphines **Ia** – **d** only one signal is observed with chemical shifts between -22.1 and -22.6 ppm. This result reminds of the monomeric ligand measured in solution⁴¹. No other phosphine species is detectable in the freshly synthesized polymers, but exposure to air leads to the formation of phosphine oxides. The half linewidths of the ^{31}P signals decrease dramatically with rising temperature, indicating that the materials are mobile on the NMR time scale (Figure 4).

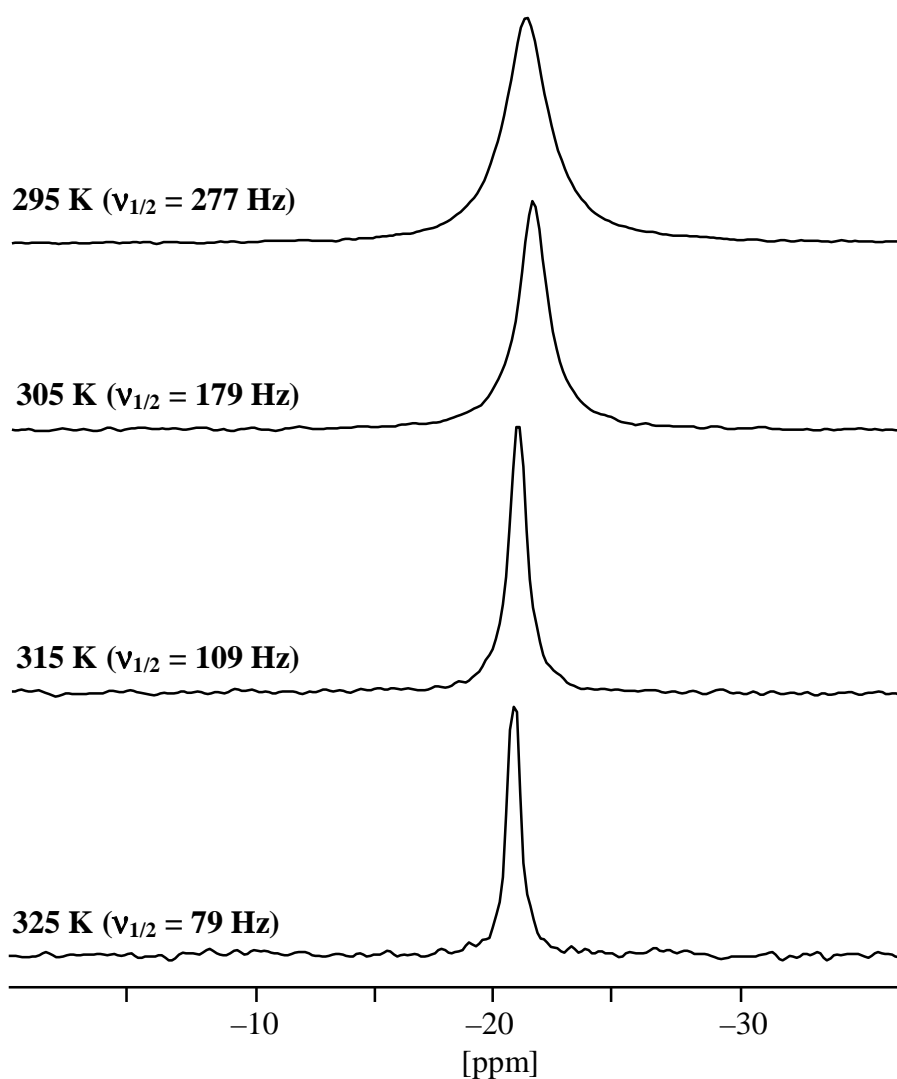


Figure 4 ^{31}P CP/MAS spectra of **Ic** at various temperatures.

Whereas the ^{13}C CP/MAS NMR spectra of the hybrid polymers **Ia, b** display three broad signals in the aromatic region (140 – 120 ppm) originating from the phenyl carbon atoms of the ligand, the resonances of the different methylene units can not unequivocally be assigned. Four major signals (33.3, 23.2, 17.8, and -0.2 ppm) dominate this region, which are attributed to the co-condensation agent $\text{D}^i\text{-C}_6\text{-D}^i$. In the case of the hybrid polymers **Ic, d** all main signals (139.4, 128.9, 39.1, 25.1, 16.8, and -0.3 ppm) stem from the co-condensation agent $\text{Ph}(1,4\text{-C}_3\text{D}^i)_2$. A weak signal at around 50 ppm is characteristic for Si-OMe functions, indicating a high degree of hydrolysis.

2.2.4 Studies on the Dynamic Behavior of the Xerogels by ^{29}Si and ^{31}P Solid State NMR Spectroscopy

To optimize the stationary component for the employment in interphases, it is necessary to get detailed informations on the dynamic properties of the materials and reactive centers.

The spin-lattice relaxation times of the protons in the rotating frame ($T_{1\rho\text{H}}$), which are characteristic for motions in the kHz region, were determined via ^{29}Si and ^{31}P ⁴⁰. In all cases the observed decays of the magnetization were monoexponential. Thus the relaxation mechanism is spin-diffusion controlled and the materials are considered as homogenous. The formation of domains larger than 1 – 2 nm in diameter is excluded. In the solid state the xerogels **Ia – d** do not differ significantly in the relaxation time $T_{1\rho\text{H}}$ and cross polarization parameters T_{PH} and T_{SiH} (Tables 2 and 3).

Table 3 $T_{1\rho\text{H}}$ (via ^{31}P) and T_{PH} parameters of **Ia – d**

Xerogel	$T_{1\rho\text{H}}$ [ms] ^a	T_{PH} [μs] ^b
Ia	1.73	498
Ib	1.67	552
Ic	1.17	534
Id	2.44	477

^a Determined via ^{31}P according with the experiment according to ref. ⁴⁰. ^b Determined via contact time variation.

Temperature dependent studies demonstrate that the $T_{1\rho\text{H}}$ relaxation times of **Ia – d** show a different behavior with increasing temperature (Table 4). Due to the decreasing $T_{1\rho\text{H}}$ values in the applied temperature range, **Ia** resides on the slow motion regime of the correlation time curve and it is therefore the material with the lowest mobility. The trend of the $T_{1\rho\text{H}}$ values of compounds **Ib** and **Id** point to a similar behavior. First they decrease with increasing temperature, then they pass through a minimum to increase again with raising temperature. Therefore these two materials are located in the medium motion regime of the correlation time curve and their mobilities are comparable. The $T_{1\rho\text{H}}$ values of **Ic** increase in the applied temperature range, which means that this material is located on the fast motion regime of the correlation time curve and shows the highest mobility, which can be correlated with the lowest degree of condensation.

Table 4 Temperature dependence of the $T_{1\rho\text{H}}$ values

Xerogel	$T_{1\rho\text{H}}$ [ms] ^a				
	295K	305 K	315 K	325 K	335 K
Ia	0.54	0.42	0.28	0.09	0.06
Ib	0.46	0.28	0.61	0.90	<i>b</i>
Ic	0.63	0.84	1.23	1.67	<i>b</i>
Id	1.73	0.99	0.73	0.86	1.68

^a Determination via ^{31}P with the experiment according to ref. ⁴⁰. ^b Not determined.

2.2.5 Accessibility Studies on the P-Centers in the Polysiloxane-Bound Diphosphines **Ib** and **Id**

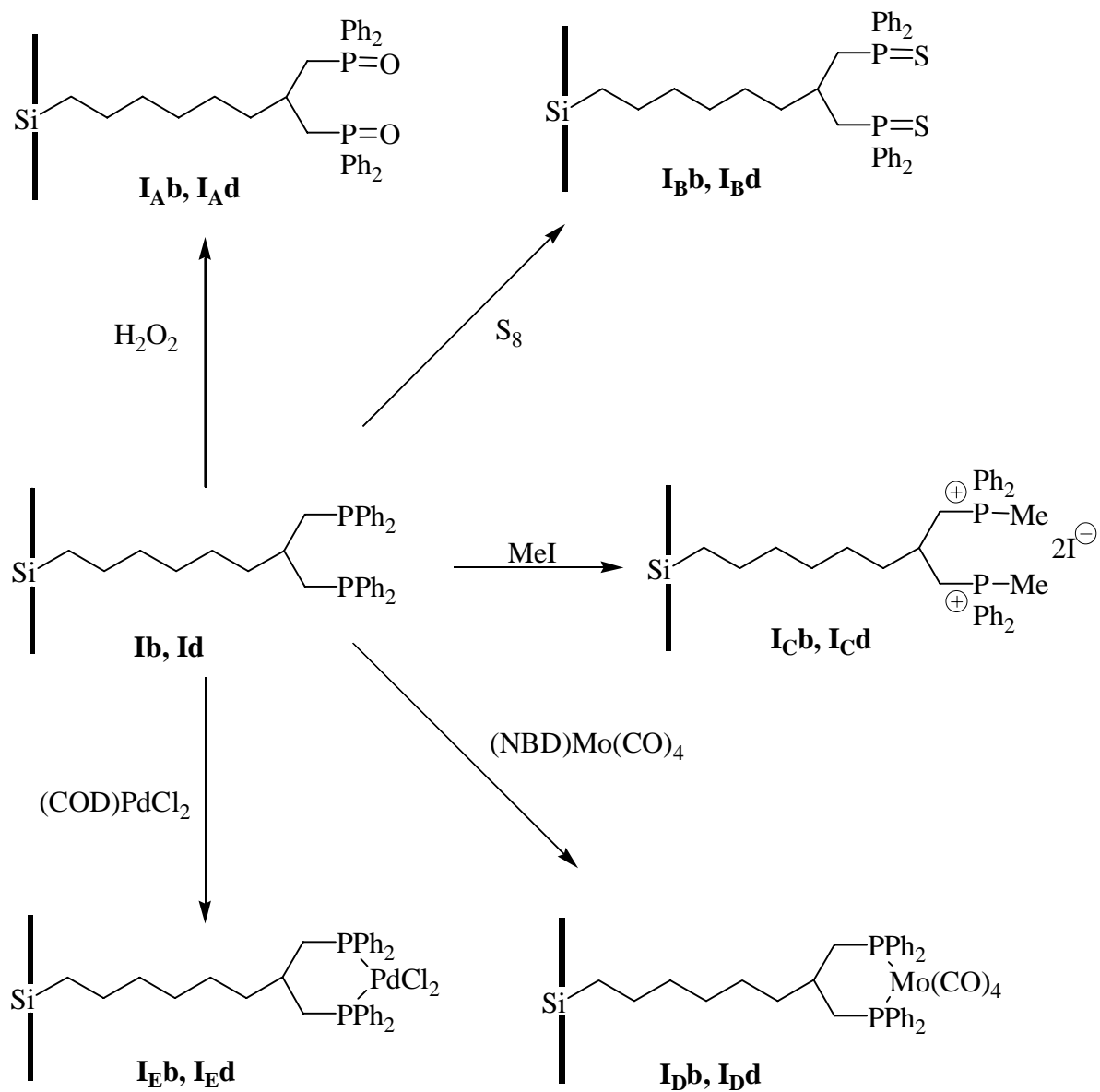
To investigate the accessibility of phosphorus centers in interphases the polymer-bound diphosphines **Ib** and **Id** were subjected to various classical phosphine reactions (Scheme 2).

2.2.5.1 Behavior toward H₂O₂

As an initial probe the polymer-supported diphosphines **Ib** and **Id** were oxidized with H₂O₂. For this reaction both materials were swollen in *i*-propanol and treated with an excess of an aqueous solution of H₂O₂. After stirring overnight at room temperature the corresponding polysiloxane-bound phosphine oxides **I_Ab** and **I_Ad** were obtained. In the ³¹P CP/MAS spectra of **I_Ab**, **d** one isotropic signal is observed at 30.5 ppm and 31.5 ppm, respectively. These chemical shifts are comparable to that of the oxide of 1,3-bis(diphenylphosphinyl)propane in solution and confirms a quantitative reaction in both cases ⁴².

2.2.5.2 Behavior toward S₈

Polymers **I_Bb**, **I_Bd** with thiophosphoryl centers were obtained when **Ib** and **Id** were heated with a suspension of S₈ in toluene at 80 °C. In both cases the reactions proceeded quantitatively. The ³¹P CP/MAS spectra of **I_Bb** and **I_Bd** display one signal each at 38.5 ppm, which is similar to the chemical shift of related diphosphine sulphides ⁴³.



Scheme 2 Model reactions in the interphase.

2.2.5.3 Behavior toward CH₃I

Upon treatment of a suspension of **Ib** and **Id** in CH₂Cl₂ with methyl iodide both phosphorus atoms were quaternized with the formation of the xerogels **I_{Cb}** and **I_{Cd}**. Their ³¹P CP/MAS spectra show one peak at about 22 ppm. As a special feature of the ¹³C CP/MAS spectra of **I_{Cb}** and **I_{Cd}** the *ipso*-C atom are shifted to 122.5 and 121.9, respectively ⁴⁴.

2.2.5.4 Behavior toward (NBD)Mo(CO)₄

The accessibility of diphosphines in interphases by rather bulky molecules was examined with the example of (NBD)Mo(CO)₄. If **Ib** and **Id** are swollen in CH₂Cl₂ and reacted with stoichiometric amounts of (NBD)Mo(CO)₄ at ambient temperature **I_{Pb}** and **I_{Pd}** were obtained as light yellow solids. The IR spectra (in KBr) of **I_{Pb}** and **I_{Pd}** display only three of the four expected CO absorptions for local C_{2v} symmetry, which is agreement with ref. ⁴⁵. In the ³¹P CP/MAS spectra of **I_{Pb}** and **I_{Pd}** one isotropic peak is observed at approximately 25 ppm, which is in the range of the ³¹P chemical shift of the corresponding (dppp)Mo(CO)₄ complex ⁴⁶. Two small signals at 215 and 211 ppm in the ¹³C CP/MAS NMR spectra of **I_{Pb}** and **I_{Pd}** are assigned to the carbonyl C atoms (Figure 5). No signals originating from NBD are detectable.

2.2.5.5 Behavior toward (COD)PdCl₂

At ambient temperature the reaction of the gels **Ib** and **Id** swollen in CH₂Cl₂ with (COD)PdCl₂ afforded the yellow polymers **I_{Eb}** and **I_{Ed}**. Both complexes may be regarded as precursors for the generation of the corresponding polysiloxane-supported bis(acetonitrile)(dppp)Pd complex, which was applied in the co-polymerization of ethene and CO ⁸. A quantitative reaction is confirmed by the ³¹P CP/MAS spectra of both materials,

which show only one peak at approximately 17 ppm. In each ^{13}C CP/MAS spectra no resonances of COD are found.

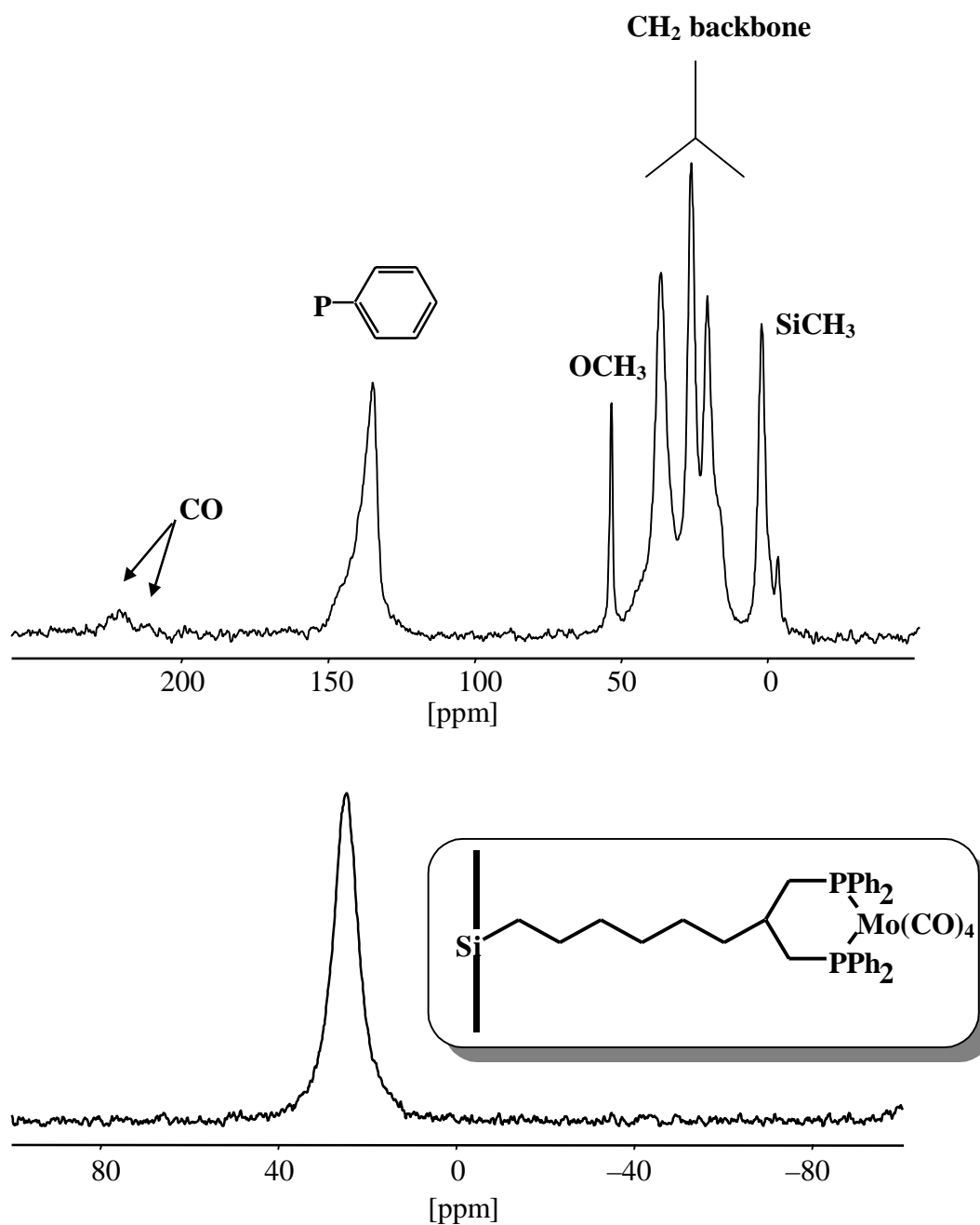


Figure 5 ^{13}C CP/MAS spectrum (top) and ^{31}P CP/MAS spectrum (bottom) of **1Db**.

2.2.6 SEM Images and EDX Measurements

SEM images of **Ib** and **Ic** are depicted in Figure 6. Their morphologies do not differ significantly. The topology seems to be terraced and due to the brittleness both materials are crumbly with sharp fractured edges.

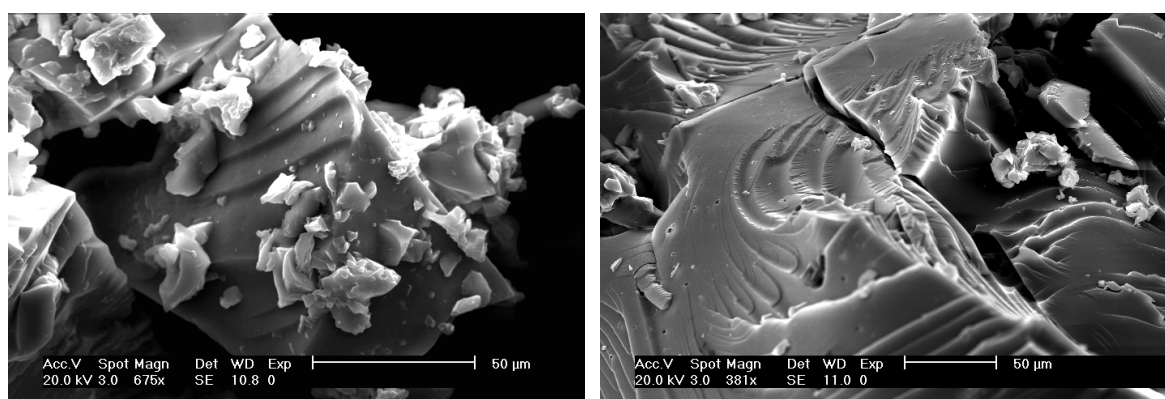


Figure 6 SEM images of **Ib** (left) and **Ic** (right).

Figure 7 reveals typical EDX spectra of **Ia** and **Id** including peak assignment. A qualitative analysis confirms the presence of carbon, oxygen, silicon, and phosphorus. For purposes of quantification, however, the measured composition has to be compared to theoretical values calculated excluding hydrogen, since hydrogen is a single electron atom and thus does not emit characteristic X-rays. Due to uncertainties in fundamental parameters at low X-ray energies and spectrometer calibration correct quantification of light elements is a principal problem in EDX. Although errors of up to 5 % have to be taken into account, oxygen, silicon, and phosphorus can be detected and quantified directly, which is not possible with chemical elemental analysis. In Table 5 the results of quantification of the EDX measurements are summarized and compared to reference data from NMR measurements.

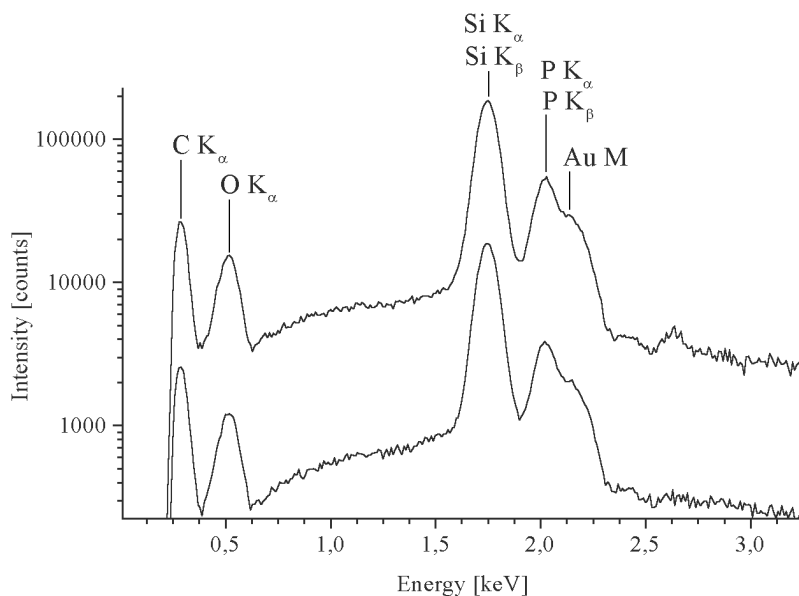


Figure 7 EDX spectra of **Ia** (top) and **Id** (bottom). The spectrum of **Ia** is offset by a factor of 10 for clarity. Assignment of the characteristic X-ray peaks is indicated. Due to the necessity of a conducting coating the Au M-line is also observed. Partial overlap of the P K-line and Au M-line introduces uncertainties to quantification.

Table 5 EDX data of **Ia – d**

Xerogel	Reference data ^a				EDX [ZAF correction] ^b				EDX [$\phi(\rho z)$ -correction] ^b			
	Composition [%] ^c				Composition [%] ^c				Composition [%] ^c			
	C	O	Si	P	C	O	Si	P	C	O	Si	P
Ia	66.4	10.3	16.6	6.8	67.8	10.1	15.7	6.4	68.0	10.0	15.8	6.2
Ib	61.0	13.0	21.8	4.2	64.7	13.8	17.8	3.7	64.7	14.9	16.9	3.5
Ic	73.0	8.1	12.9	6.0	72.2	8.8	13.3	5.7	72.1	9.8	12.7	5.4
Id	68.9	10.3	17.5	3.3	69.3	8.6	17.1	5.0	69.5	9.5	16.3	4.7

^a Derived from NMR data according to ref. ²². ^b Calculated according to ref. ⁴⁷. ^c Calculated excluding hydrogen.

2.2.7 Conclusion

Four different xerogels **Ia – d** were synthesized, in which the T-functionalized 1,3-bis(diphenylphosphinyl)propane [**1(T⁰)**] with a spacer of six methylene units was

incorporated into a polysiloxane matrix. The backbone of the matrices was modified by employment of the different co-condensing $\text{MeSi}(\text{OMe})_2(\text{CH}_2)_6(\text{OMe})_2\text{SiMe}$ ($\mathbf{D}^0\text{-C}_6\text{-D}^0$) and $\text{MeSi}(\text{OMe})_2(\text{CH}_2)_3(\text{C}_6\text{H}_4)(\text{CH}_2)_3(\text{OMe})_2\text{SiMe}$ [$\mathbf{Ph(1,4-C}_3\mathbf{D}^0)_2$] in two different ratios. According to solid state NMR experiments, the realistic stoichiometries do not differ significantly from the applied T/D-ratios and the materials are found to be homogeneous. The formation of domains larger than 1 – 2 nm in diameter can be excluded. Studies on the mobility of the matrix and the reactive centers reveal, that the materials with the phenyl ring in the backbone are slightly more mobile due to the lower degree of condensation. The examination of the accessibility of the incorporated phosphorus centers within these two different types of carrier matrices was carried out by classical phosphine reactions. It was possible to demonstrate that all P-centers were readily accessible by small (e.g. H_2O_2) or even bulkier molecules (e.g. $(\text{NBD})\text{Mo}(\text{CO})_4$) which is an important precondition for a successful employment of this ligand in catalytic processes.

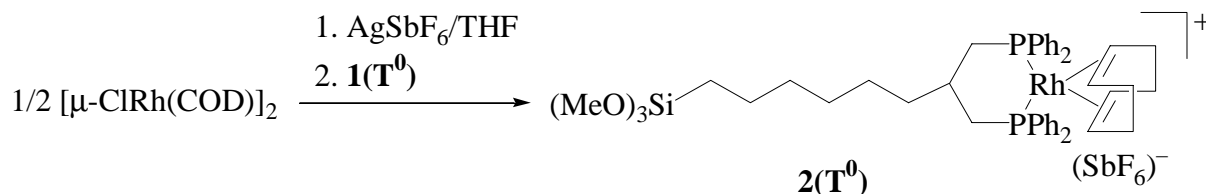
2.3 Novel Sol–Gel Processed Rhodium(I) Complexes: Synthesis, Characterization and Catalytic Reactions in Interphases

2.3.1 Introduction

In this part of the thesis the synthesis and characterization of novel cationic rhodium(I) complexes anchored to polysiloxane–based inorganic–organic hybrid materials is reported. The rhodium centers in these complexes are coordinated to the modified 1,3–bis(diphenylphosphinylpropane) ligand (dppp) [**1**(T^0)]. The monomeric T–silyl substituted complex **2**(T^0) was sol–gel processed with different ratios of the D–bifunctionalized co–condensation agents $D^0-C_6-D^0$ and $Ph(1,4-C_3D^0)_2$. Structural and dynamic investigations of these novel stationary phases were carried out by multinuclear solid state NMR spectroscopy. An exemplary examination of the coordination sphere of the rhodium(I) center was performed by means of EXAFS–spectroscopy, since this method operates in the case of amorphous materials like interphases^{8,22}. The morphology of the materials was investigated by scanning electron microscopy (SEM) and the elemental distribution is revealed by EDX–spectroscopy. Finally the accessibility of this polysiloxane–bound complexes was investigated by catalyzed hydrogenation of 1–hexene.

2.3.2 Synthesis of the Monomeric Rhodium(I) Complex **2**(T^0)

The cationic rhodium(I) complex **2**(T^0) was obtained in good yields as a orange–yellow microcrystalline powder by reaction of the diphos ligand **1**(T^0) with a half equivalent of $[\mu-ClRh(COD)]_2$ and one equivalent of $AgSbF_6$ (Scheme 3). Complex **2**(T^0) was characterized by 1H , $^{13}C\{^1H\}$, $^{31}P\{^1H\}$, and ^{103}Rh NMR spectroscopy and mass spectrometry.



Scheme 3 Synthesis of $\mathbf{2}(\text{T}^0)$.

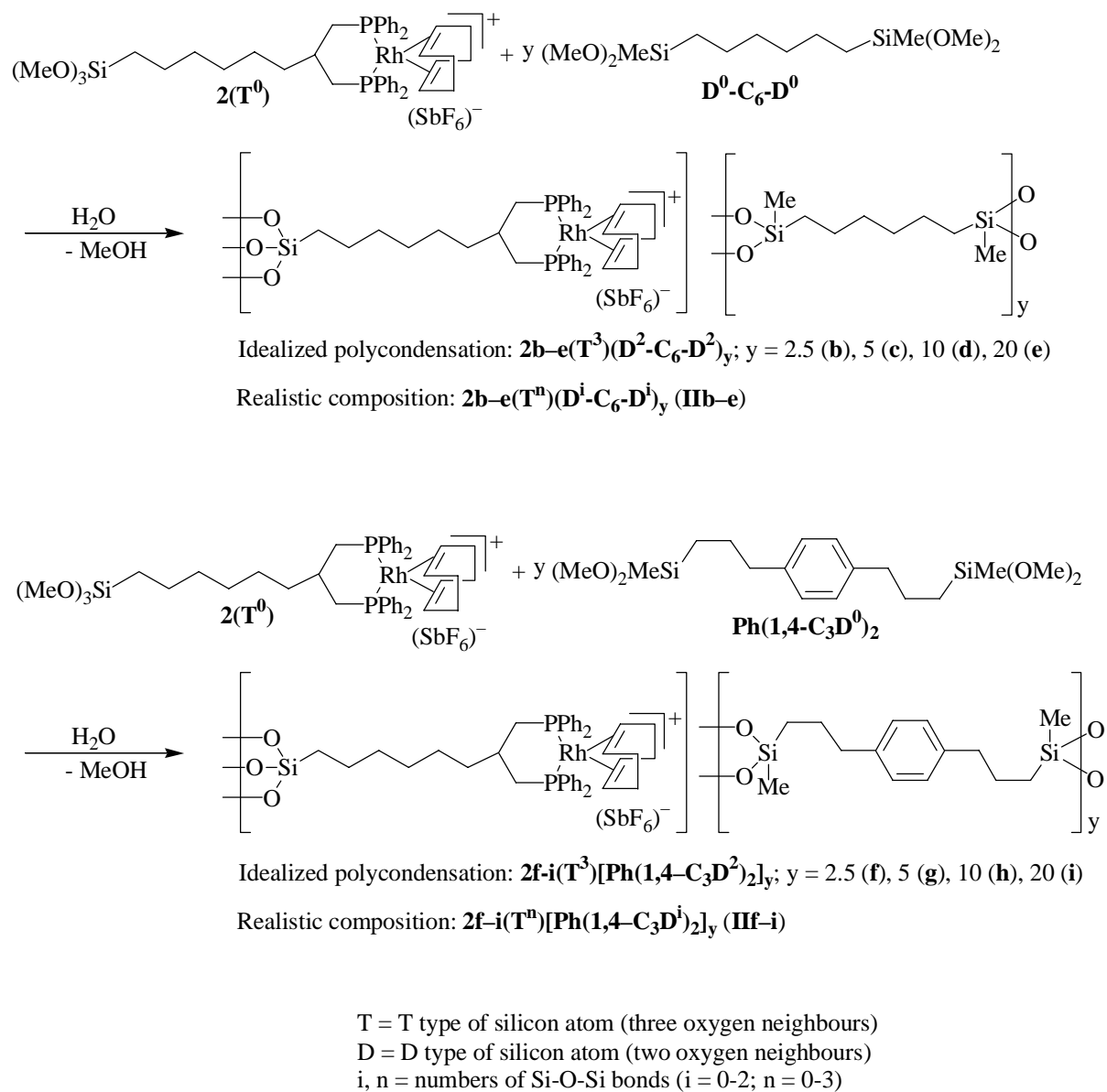
2.3.3 Sol–Gel Processing of $\mathbf{2}(\text{T}^0)$

The xerogel **IIa** was prepared by sol–gel processing of the monomeric T–functionalized rhodium(I) complex $\mathbf{2}(\text{T}^0)$ without any co–condensing agent, whereas in the case of **IIb – i** $\mathbf{2}(\text{T}^0)$ was condensed into a matrix with variable amounts of $\text{D}^0\text{-C}_6\text{-D}^0$ or $\text{Ph}(\mathbf{1,4}\text{-C}_3\text{D}^0)_2$ (Table 6, Scheme 4).

Table 6 Labeling of the xerogels **II**

Complex	Co–condensation agent	ideal T/D ratio	Compound	Xerogel
$\mathbf{2}(\text{T}^0)$			$\mathbf{2a}(\text{T}^n)$	IIa
$\mathbf{2}(\text{T}^0)$	$\text{D}^0\text{-C}_6\text{-D}^0$	5	$\mathbf{2b}(\text{T}^n)(\text{D}^i\text{-C}_6\text{-D}^i)_{2.5}$	IIb
$\mathbf{2}(\text{T}^0)$	$\text{D}^0\text{-C}_6\text{-D}^0$	10	$\mathbf{2c}(\text{T}^n)(\text{D}^i\text{-C}_6\text{-D}^i)_5$	IIc
$\mathbf{2}(\text{T}^0)$	$\text{D}^0\text{-C}_6\text{-D}^0$	20	$\mathbf{2d}(\text{T}^n)(\text{D}^i\text{-C}_6\text{-D}^i)_{10}$	IId
$\mathbf{2}(\text{T}^0)$	$\text{D}^0\text{-C}_6\text{-D}^0$	40	$\mathbf{2e}(\text{T}^n)(\text{D}^i\text{-C}_6\text{-D}^i)_{20}$	IIe
$\mathbf{2}(\text{T}^0)$	$\text{Ph}(\mathbf{1,4}\text{-C}_3\text{D}^0)_2$	5	$\mathbf{2f}(\text{T}^n)[\text{Ph}(\mathbf{1,4}\text{-C}_3\text{D}^i)_2]_{2.5}$	IIf
$\mathbf{2}(\text{T}^0)$	$\text{Ph}(\mathbf{1,4}\text{-C}_3\text{D}^0)_2$	10	$\mathbf{2g}(\text{T}^n)[\text{Ph}(\mathbf{1,4}\text{-C}_3\text{D}^i)_2]_5$	IIg
$\mathbf{2}(\text{T}^0)$	$\text{Ph}(\mathbf{1,4}\text{-C}_3\text{D}^0)_2$	20	$\mathbf{2h}(\text{T}^n)[\text{Ph}(\mathbf{1,4}\text{-C}_3\text{D}^i)_2]_{10}$	IIh
$\mathbf{2}(\text{T}^0)$	$\text{Ph}(\mathbf{1,4}\text{-C}_3\text{D}^0)_2$	40	$\mathbf{2i}(\text{T}^n)[\text{Ph}(\mathbf{1,4}\text{-C}_3\text{D}^i)_2]_{20}$	IIi

To guarantee reproducible materials uniform reaction conditions were maintained. Therefore all sol–gel processes were carried out in THF with an excess of water and $(n\text{-Bu})_2\text{Sn}(\text{OAc})_2$ as catalyst.



Scheme 4 Structure, idealized and realistic compositions of the sol-gel materials **IIb – i**.

2.3.4 Solid State NMR Spectroscopy

2.3.4.1 ^{29}Si CP/MAS NMR Spectroscopy

As a result of an incomplete condensation the ^{29}Si CP/MAS NMR spectra of the xerogels **IIb – i** reveal signals of various substructures with corresponding D^i - and T^n - functions (Figure 8). Typical chemical shifts are $\delta = -12.5$ (D^1), -21.7 (D^2), -57.1 (T^2), and -67.0 (T^3). They remain unchanged with respect to the stoichiometric ratio between the co-condensation agent and the functionalized rhodium(I) complex. All silicon atoms in the polysiloxane matrix are in direct proximity of protons, thus silyl species are detectable via cross polarization ^{27,35,36}. The degree of condensation of D - and T -groups and the real T/D -ratios were determined by contact time variation experiments (Table 7) ^{22,23,37–39}.

However, due to the low concentration of T -functions in the xerogels **IIId, e, h, i** the T -groups can hardly be detected. Therefore contact time variation experiments to determine the realistic composition of these xerogels are not feasible within a reasonable time.

With exception of **IIg** and **IIh**, in the xerogels of type **II** the degrees of condensation for the D - and T -functions range between 79 % and 95 %, which is in agreement with former investigations ^{22,48}. In the case of **IIg** the T -functions show a very low degree of condensation, whereas in the case of **IIh** T - and D -groups are highly condensed. The experimentally determined compositions do not differ significantly from the applied stoichiometries, but it seems that in each sol-gel process a small amount of the D - or T -groups were washed out during the solvent processing.

Table 7 Relative I_0 , T_{SiH} , and $T_{1\rho H}$ data of the silyl species in the xerogel **IIa – i**

Xerogel	relative I_0 data of D and T species ^a				degree of condensation [%]		real T/D moiety	T_{SiH} [ms] ^c				$T_{1\rho H}$ [ms] ^d
	D ¹	D ²	T ²	T ³	D	T		D ¹	D ²	T ²	T ³	
IIa			24.0	100		94				0.81	1.34	15.31
IIb	41.1	100	9.8	12.5	85	81	1:6.3	1.44	1.42	1.49	1.60	12.65
IIc	36.3	100	7.3	8.0	87	84	1: 8.9	1.34	1.42	1.11	1.25	8.11
IId	72.4 ^b	100 ^b	2.9 ^b	7.7 ^b	79	91	1:16.4 ^b	1.66	1.97	<i>f</i>	<i>f</i>	8.02
IIe	31.3 ^b	100 ^b	1.4 ^b	2.5 ^b	88	88	1:33.6 ^b	1.61	1.98	<i>f</i>	<i>f</i>	2.74
IIf	26.9	100	17.7	19.7	89	82	1:3.4	0.83	0.98	1.04	1.19	11.84
IIg	80.1	100	13.5	8.0	77	73	1:7.9	1.24	1.41	0.92	0.55	5.76
IIh	4.9 ^b	100 ^b	<i>e</i>	6.0 ^b	98	100	1:17.4 ^b	<i>f</i>	1.00	<i>e</i>	1.32	3.31
IIi	10.5 ^b	100 ^b	0.6 ^b	1.5 ^b	95	90	1:52.6 ^b	0.64	0.89	<i>f</i>	<i>f</i>	1.79

^a I_0 values calculated according to literature methods. ^b Determined via deconvolution of ^{29}Si CP/MAS NMR spectra ($T_c = 5$ ms). ^c Determined by contact time variation. ^d Determined via ^{29}Si with the experiment according to ref. ⁴⁰. ^e Species not detectable. ^f Intensity too low for a precise determination of T_{SiH} .

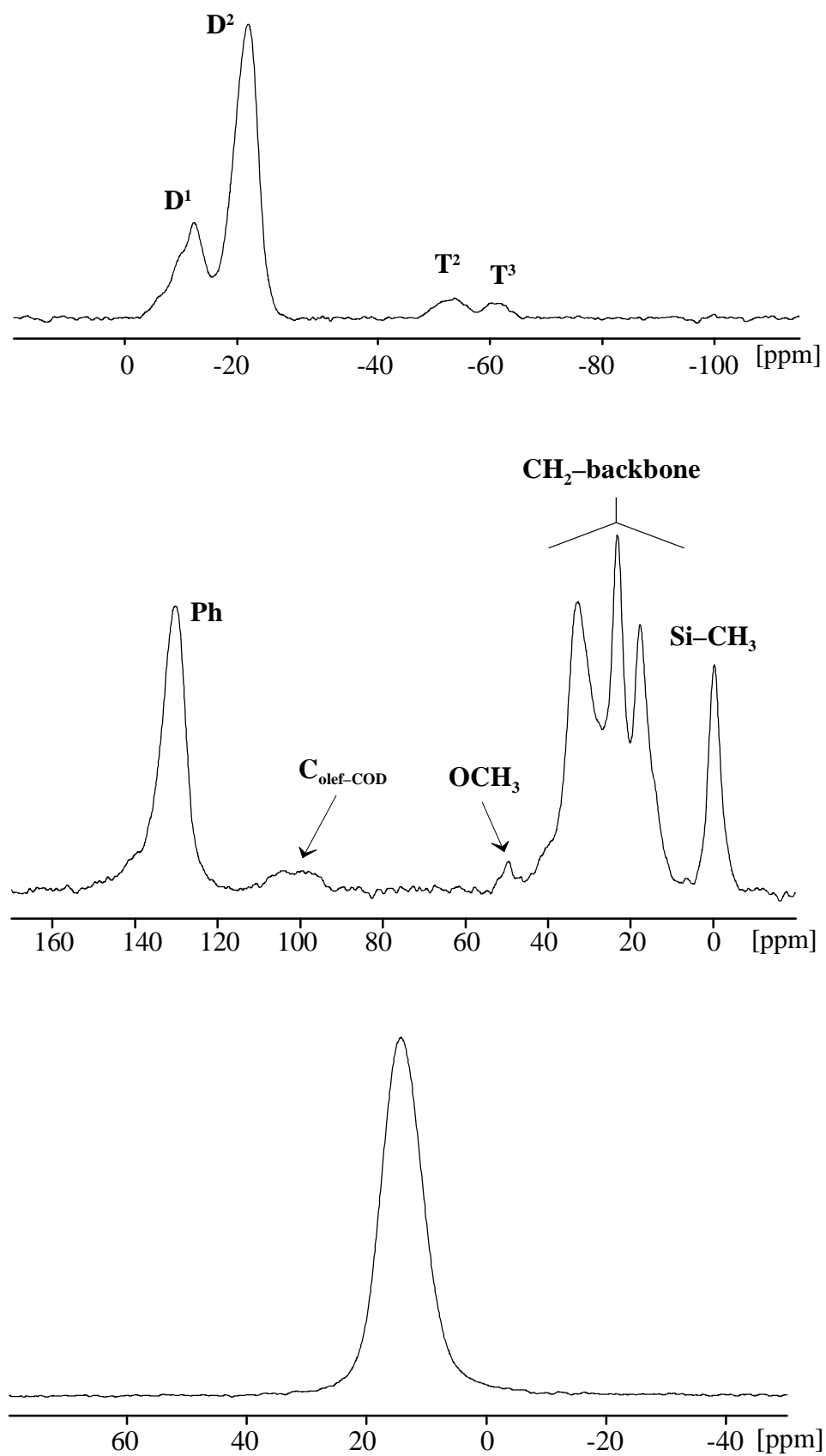


Figure 8 Solid state NMR spectra of **IIb**: ^{29}Si CP/MAS (top), ^{13}C CP/MAS (middle), ^{31}P CP/MAS (bottom).

2.3.4.2 ^{31}P and ^{13}C CP/MAS NMR Spectroscopy

In the ^{31}P CP/MAS NMR spectra of the polysiloxane-bound rhodium(I) complexes **IIa** – **i** only one broad signal is observed with chemical shifts between 10.9 and 15.3 ppm. This result reminds of the monomeric complex measured in solution. No other phosphine species is detectable in the freshly synthesized polymer, but exposure to air for some hours leads to the formation of phosphine oxide resonating at 32 ppm.

The ^{13}C CP/MAS NMR spectra of **IIa** – **e** reveal a broad signal in the aromatic region, which stems from the phenyl carbon atoms of the functionalized dppp ligand. At approximately 100 ppm two broad signals occur originating from the olefinic C-atoms of the COD ligand. The resonances of the different methylene carbon atoms between 40 and 10 ppm of **IIa** cannot be resolved. In the case of **IIb** – **e** the aliphatic region is dominated by four major signals resonating at about 33, 23, 18, and 0 ppm, which are assigned to the $\text{D}^i\text{-C}_6\text{-D}^i$ portion. In the case of the hybrid polymers **IIf** – **i** all main signals (average shifts: 139.4, 128.9, 39.1, 25.1, 16.8, and -0.3 ppm) with exception of the peaks originating from the COD ligand at approximately 100 ppm stem from the $\text{Ph}(\mathbf{1,4-C}_3\mathbf{D}^i)_2$ component. The weak or missing signal for the Si-OMe function indicates a very high degree of hydrolysis.

2.3.5 EXAFS Structure Determination of the Rhodium(I) Complexes **IIa**, **IIb**, and **IIf**

The amorphous character of the xerogels makes it impossible to get structural data with conventional X-ray diffraction. However, the properties of EXAFS (Extended X-ray Absorption Fine Structure) spectroscopy allows the determination of the local structure around the excited rhodium atoms, independent on the samples' physical state. An analysis of the EXAFS provides information on the bond distance, the coordination number, the „Debye-Waller“ factor, and the nature of the scattering atoms surrounding an excited atom^{49,50}. The

k^3 weighted EXAFS functions (Figure 9) of **IIa**, **IIb**, and **IIc** can be described by two different atom shells.

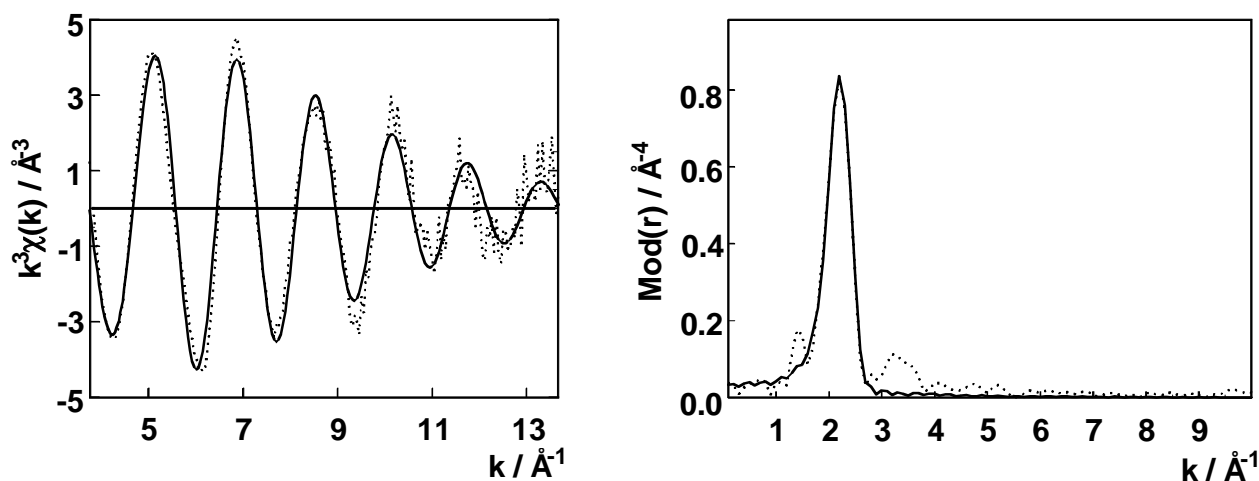


Figure 9 Calculated (solid line) and experimental (dotted line) $k^3\chi(k)$ function of **IIa** (left) and their Fourier transforms (right) (Rh–K–edge) in the k -range 3.85 – 13.00 \AA^{-1} .

For the above-mentioned complexes the first intensive peak in the corresponding Fourier transforms is mainly due to carbon and phosphorus atoms. In the case of **IIa** the assumption of four equivalent carbon atoms with a Rh – C bond length of 2.14 \AA leads to a good agreement between the experimental and the calculated functions. Additionally two equivalent phosphorus atoms were established with an average Rh – P distance of 2.28 \AA leading to a significant improvement in the fit (Table 8). In the case of **IIb** the assumption of four equivalent carbon atoms with a Rh – C distance of 2.21 \AA and two equivalent phosphorus atoms with a Rh – P bond length of 2.29 \AA leads to a good agreement between the experimental and the calculated functions. In the xerogel **IIc** the found Rh – C and Rh – P bond lengths are 2.23 and 2.31 \AA , respectively.

Table 8 EXAFS–determined structural data of the **IIa, **IIb**, and **IIf****

	IIa			IIb		IIf	
	N^b	$r [\text{Å}]^c$	$\sigma [\text{Å}]^d$	$r [\text{Å}]^c$	$\sigma [\text{Å}]^d$	$r [\text{Å}]^c$	$\sigma [\text{Å}]^d$
Rh–C ^a	4	2.14 ± 0.02	0.081 ± 0.01	2.21 ± 0.02	0.059 ± 0.02	2.23 ± 0.02	0.067 ± 0.02
Rh–P ^a	2	2.28 ± 0.02	0.109 ± 0.03	2.29 ± 0.02	0.081 ± 0.01	2.31 ± 0.02	0.063 ± 0.01

^a Absorber–backscatterer. ^b Coordination number N . ^c Interatomic distance r . ^d Debye–Waller factor σ .

The structural data are in a good agreement with the proposed structures of the **IIa**, **IIb**, and **IIf**. Furthermore, in comparison with the structural data of **IIa**, the Rh – C distances of **IIb** and **IIf** are slightly enlarged but still in agreement with determined bond lengths of similar (COD)diphosphinerhodium(I) complexes^{51,52}.

2.3.6 Studies on the Dynamic Behavior of the Xerogels **IIa – i** by Solid State NMR

Spectroscopy

2.3.6.1 Mobility of the Matrix

In the solid state the xerogels do not differ significantly in the cross polarization constant T_{SiH} . The relaxation time parameter ($T_{1\rho H}$) data extracted from the ²⁹Si CP/MAS NMR measurements of the xerogels depend on the amount of the **Dⁱ–C₆–Dⁱ** and **Ph(1,4–C₃Dⁱ)₂** components, respectively (Table 7). Shorter $T_{1\rho H}$ values were recorded for a higher amount of the co–condensing agents, thus indicating an increase of the mobility of the matrix, because, according to recent studies the $T_{1\rho H}$ values of **IIa – i** are considered to reside on the slow motion regime of the correlation time curve²². Comparing the mobilities of the two different co–condensates in these materials, it seems that there is no essential

difference between the materials with the phenyl ring in the backbone and their counterparts with the alkyl chain as main building block.

2.3.6.2 Mobility of the Reactive Center

Temperature dependent measurements of the $T_{1\rho\text{H}}$ values (via ^{31}P) are summarized in Table 9. Due to the decreasing $T_{1\rho\text{H}}$ values in the applied temperature range all rhodium containing xerogels with exception of **IIe** and **IIIi** reside on the slow motion regime of the correlation time curve²⁴. The trend of the $T_{1\rho\text{H}}$ values of compounds **IIe** and **IIIi** show a similar behavior. First they decrease, then they pass through a minimum to increase again with raising temperature. Therefore these two materials are located in the medium motion regime of the correlation time curve and show the highest mobility of all mentioned xerogels of type **II**. These results indicate that the mobility of the reactive centers as well as the mobility of the matrix (*vide supra*) increase with a higher amount of the co-condensing component. Due to the electrostatic repulsion of the cationic rhodium(I) centers the space of motion is reduced. If these positively charged complexes are diluted across the carrier matrix their mobility is enhanced, because of the enlargement of the motion radius.

Table 9 Temperature dependence of the $T_{1\rho\text{H}}$ values

Xerogel	$T_{1\rho\text{H}}$ [ms] ^a				
	295K	305 K	315 K	325 K	335 K
IIa	9.01	<i>b</i>	<i>b</i>	<i>b</i>	<i>b</i>
IIb	11.98	10.68	9.94	9.96	<i>b</i>
IIc	5.09	7.15	3.81	2.75	<i>b</i>
IId	10.20	11.30	9.36	10.46	8.85
IIe	4.15	1.25	0.91	3.08	3.13
IIf	13.81	13.17	9.22	9.79	8.06
IIg	7.55	10.14	6.21	2.87	<i>b</i>
IIh	6.82	5.88	5.30	3.29	2.49
IIIi	6.80	0.89	2.62	2.92	<i>b</i>

^a Determination via ^{31}P according to ref.⁴⁰. ^b Not determined.

2.3.7 Accessibility Studies of the Anchored Rhodium(I) Complexes by Catalytic Hydrogenation of 1-Hexene

Diphosphinerhodium(I) complexes are applied as catalysts for the hydrogenation of various olefins^{51,53-57}. Therefore the accessibility of the polysiloxane-bound rhodium(I) complexes **IIa** – **c**, **IIe** – **g**, **IIi** was investigated by hydrogenation of 1-hexene (Table 10).

Table 10 Hydrogenation of 1-hexene in toluene^a

Xerogel	Conversion [%]	hexane [%]	cis, trans 2-hexene [%]	TON ^b	TOF ^c
IIa	80.8	61.4	38.6	2811	703
IIb	40.9	86.1	13.9	2136	534
IIc	71.6	77.1	22.9	3326	832
IId ^d					
IIe	45.7	91.0	9.0	2480	620
IIf	100	84.7	13.3	5035	1259
IIg	40.4	73.3	26.7	1828	457
IIh ^d					
IIi	100	91.9	8.1	5575	1394

^a Reaction conditions: H₂ pressure 10 bar, Rh : 1-hexene = 1 : 6000, temperature 313 K, reaction time 4h. ^b Turnover number (mol_{sub} mol_{cat}⁻¹). ^c Turnover frequency (mol_{sub} mol_{cat}⁻¹ h⁻¹). ^d Not determined.

All applied complexes exhibit rather good turnover frequencies in toluene and therefore the metal centers are readily accessible for hydrogen and 1-hexene. However, due to solvation and swelling effects of the anchored rhodium(I) centers and of the matrix, respectively, it seems that there is no predictable correlation between catalytic activity, selectivity, and the type of the co-condensate. But SEM images give some evidences, that the activity depends on the particle size of the materials. Smaller particles induce a higher catalytic activity than larger particles (Figure 10).

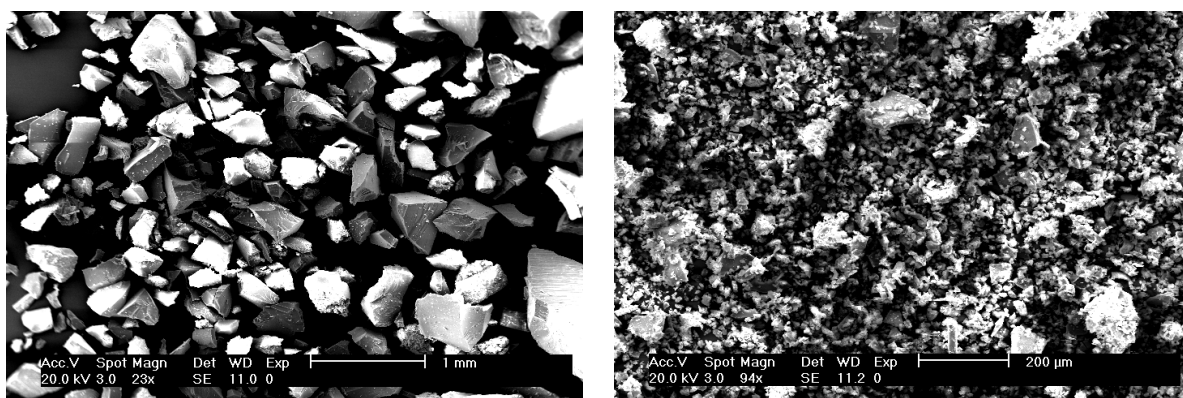


Figure 10 left: SEM image of **IIb** (large particles, lower activity); right: SEM image of **IIc** (small particles, higher activity).

An enhancement of the conversion rate was achieved with an increase of the solvent polarity (Table 11, Figure 11). In the case of **IIc** only a slight increase of the activity is observable if dioxane or methanol are used as solvent. The selectivities are comparable in each solvent. In the case of **IIg** the conversion rates and selectivities are comparable in toluene and dioxane, respectively. However, if methanol is used the selectivity is scarcely influenced by the solvent but the conversion rate is twice as high compared to the activities in toluene or dioxane. This is another example that metal catalyzed hydrogenation is favored in polar solvents, especially in alcohols, although these applied inorganic–organic hybrid materials do not exhibit good swelling abilities in polar solvents like methanol²³.

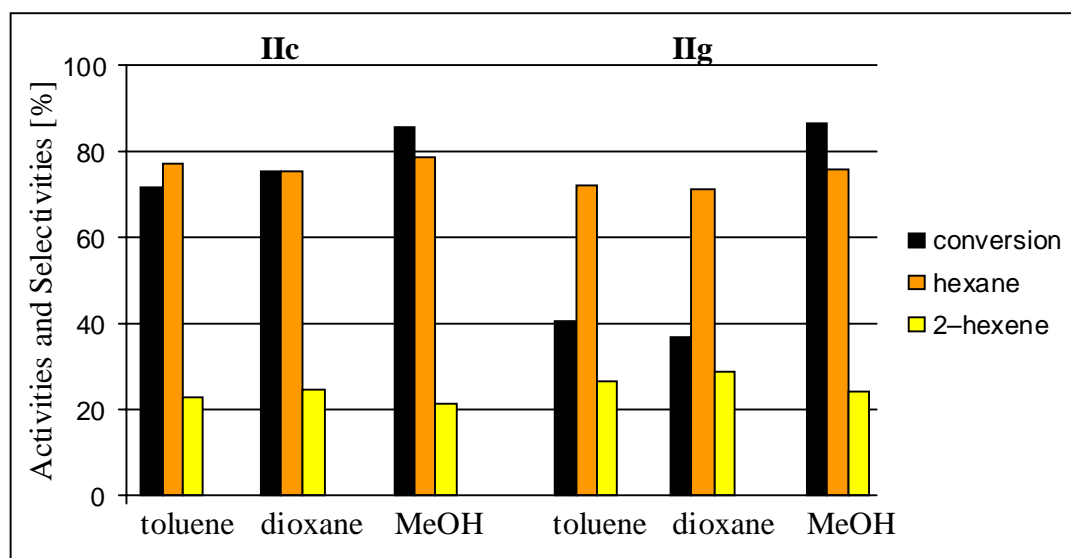


Figure 11 Dependence of activity and selectivity on the polarity of solvent at the hydrogenation of 1-hexene with **IIc** and **IIg**.

Table 11 Influence of the solvent on conversion and selectivity^a

catalyst	solvent	conversion [%]	hexane [%]	cis, trans 2-hexene [%]	TON ^b	TOF ^c
IIc	toluene	71.6	77.1	22.9	3326	832
	1,4-dioxane	75.5	75.5	24.5	3368	842
	methanol	85.5	78.7	21.3	4072	1018
IIg	toluene	40.4	72.3	26.7	1826	457
	1,4-dioxane	36.7	71.1	28.9	1571	393
	methanol	86.6	76.0	24.0	3968	992

^a Reaction conditions: H₂ pressure 10 bar, Rh : 1-hexene = 1 : 6000, temperature 313 K, reaction time 4h. ^b Turnover number (mol_{sub} mol_{cat}⁻¹). ^c Turnover frequency (mol_{sub} mol_{cat}⁻¹ h⁻¹).

To investigate the stability of the catalysts, the xerogels **IIc** and **IIg** were separated from the reaction mixture and then used again in a catalytic reaction with new solvent and 1-hexene (Table 12, Figure 12). In each case an enhancement of the conversion from run 1 to run 3 was observed, which indicates that the formation of the catalytic active species takes place after a relative long period or that the particles of materials become smaller after several

runs and therefore the activity is enhanced (*vide supra*). In the case of **IIc** the selectivity decreases from run 1 to run 2 to increase again in run 3, whereas in the case of **IIg** the highest selectivity was achieved in run 2. Leaching investigations point out, that no rhodium was found to be detached from the polysiloxane support.

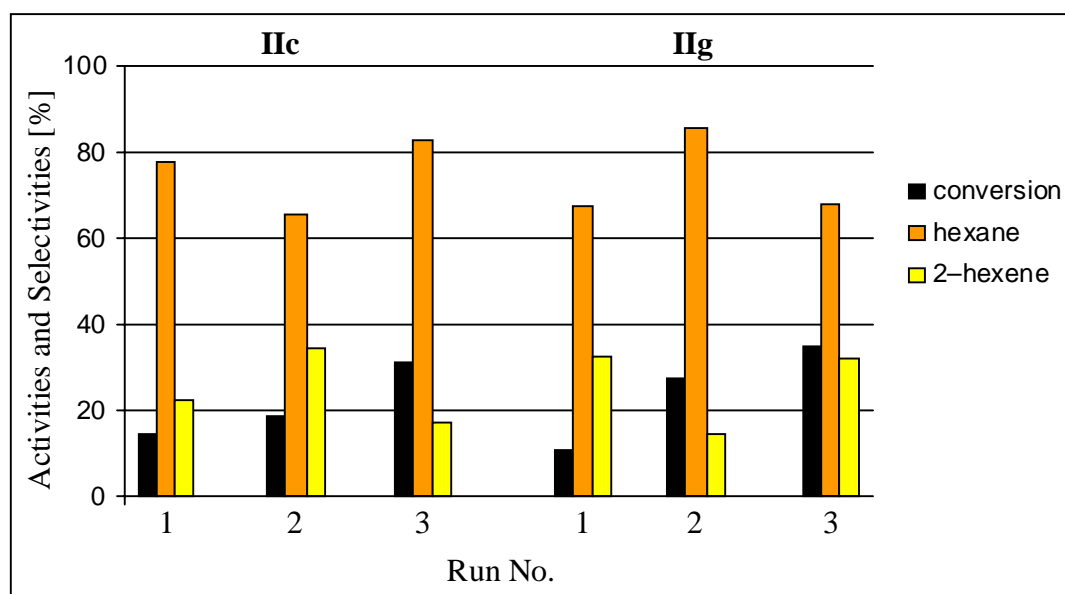


Figure 12 Activity and selectivity of three consecutive runs with a recycling of the catalyst at the hydrogenation of 1-hexene with **IIc** and **IIg**.

Table 12 Conversions and selectivities of consecutive runs with a recycling of the catalyst^a

catalyst	run No.	conversion [%]	hexane [%]	cis, trans 2-hexene [%]	TON ^b	TOF ^c
IIc	1	14.2	77.5	22.5	664	332
	2	18.5	65.4	34.6	730	365
	3	31.1	83.0	17.0	1557	778
IIg	1	10.5	67.6	32.4	427	213
	2	27.4	85.4	14.6	1407	703
	3	34.8	67.8	32.2	1419	709

^a Reaction conditions: toluene as solvent, H₂ pressure 10 bar, Rh : 1-hexene = 1 : 6000, temperature 313 K, reaction time 2h. ^b Turnover number (mol_{sub} mol_{cat}⁻¹). ^c Turnover frequency (mol_{sub} mol_{cat}⁻¹ h⁻¹).

2.3.8 Surface Area and EDX Measurements

Due to the high organic portions in these stationary phases surface area measurements according to the BET method reveal very low values ($< 3 \text{ m}^2/\text{g}$), which is in agreement with former results^{22,23,58}.

Because of difficulties in classical elemental analysis of Si-containing materials (see Experimental Section) EDX-measurements were undertaken. Figure 13 displays typical EDX spectra of **IIa** and **III** including peak assignment. Qualitative analysis confirms the presence of carbon, oxygen, silicon, fluorine, phosphorus, antimony, and rhodium. For quantification purposes, however, the measured composition has to be compared to theoretical values calculated excluding hydrogen, since it is a single electron atom and thus does not emit characteristic X-rays.

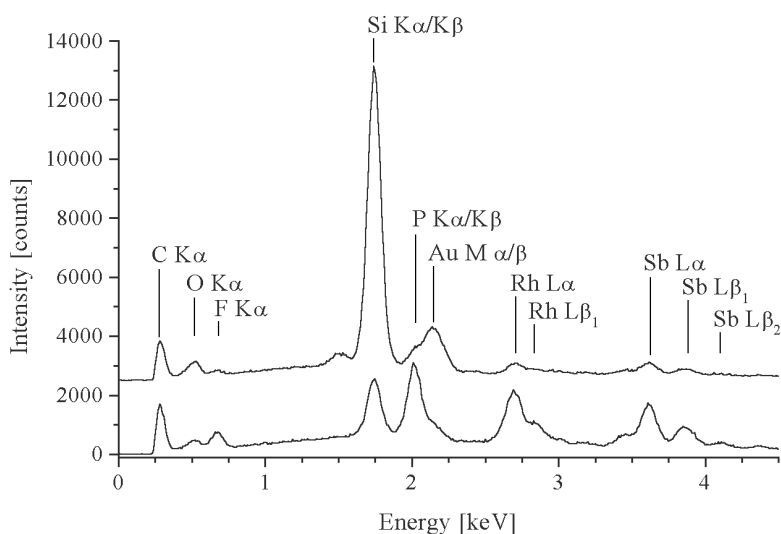


Figure 13 Typical EDX spectra of **IIa** (bottom) and **III** (top). The spectrum of **III** is omitted for clarity. Assignment of the characteristic X-ray peaks is indicated. Due to the necessity of a conductive coating, the Au M-line is also observed. Partial line overlap of the P-K line with the Au-M line introduces uncertainties to quantification.

Due to uncertainties in fundamental parameters at low X-ray energies, spectrometer calibration and the limited detector efficiency in the low energy region, correct quantification of light elements is a principal problem in EDX. Partial line overlap between the P-K and the Au-M line introduces further uncertainties to quantification. Errors are significant for the quantification of minor constituents as the bremsstrahlung background causes signal-to-background-ratios below 3 in some cases. However, all elements except for hydrogen can be detected and quantified directly, which is not possible with chemical elemental analysis. In Table 13 the quantification results of the EDX measurements are summarized and compared to reference data from NMR measurements.

Table 13 EDX data of IIa – i

Xerogel	reference data ^a							EDX (ZAF correction) ^b						
	composition [%] ^c							composition [%] ^c						
	C	O	Si	P	F	Sb	Rh	C	O	Si	P	F	Sb	Rh
IIa	52.1	2.5	3.0	6.6	12.1	12.8	10.9	55.0	5.7	4.0	6.0	4.6	13.4	11.3
IIb	51.3	9.7	13.2	4.0	7.4	7.8	6.6	55.8	11.5	8.2	4.7	6.4	7.8	5.6
IIc	52.2	9.5	15.8	3.5	6.4	6.8	5.8	51.2	11.1	18.8	3.9	4.7	5.9	4.4
IId	50.8	14.0	19.3	2.5	4.5	4.8	4.1	49.0	11.6	28.5	2.9	1.8	4.3	1.9
IIe	50.3	17.7	24.5	1.2	2.1	2.3	1.9	52.5	14.5	24.3	1.8	2.3	3.0	1.6
IIf	56.5	6.5	9.5	4.3	7.9	8.3	7.0	55.3	12.6	10.0	3.9	6.0	7.1	5.1
IIg	58.4	9.6	11.8	3.1	5.8	6.1	5.2	61.5	9.5	13.5	3.2	4.2	4.7	3.4
IIh	61.7	9.1	15.5	2.1	3.9	4.2	3.5	61.6	11.3	17.5	1.7	2.9	3.5	1.5
IIi	64.0	11.3	19.5	0.8	1.5	1.6	1.3	62.6	9.4	17.5	1.8	2.7	3.8	2.2

^a Derived from NMR data according to ref. ²². ^b Calculated according to ref. ⁴⁷. ^c Calculated excluding hydrogen.

2.3.9 Conclusion

Different xerogels **IIa** – **i** were synthesized, in which the T-functionalized (COD)(dppp)rhodium(I) complex **2(T⁰)** was incorporated into a polysiloxane matrix. The backbone of the matrices was modified by employment of the different co-condensing agents MeSi(OMe)₂(CH₂)₆(OMe)₂SiMe (**D⁰-C₆-D⁰**) and MeSi(OMe)₂(CH₂)₃(C₆H₄)(CH₂)₃(OMe)₂SiMe [**Ph(1,4-C₃D⁰)₂**] in various ratios. Multinuclear CP/MAS NMR spectroscopy and EXAFS studies proved the integrity of the complexes. According to further solid state NMR experiments, the realistic compositions do not differ significantly from the applied T/D-ratios. Studies on the mobility of the matrix and the reactive centers revealed, that an enhancement of the mobility is achieved with a larger amount of the co-condensing components and that both kinds of materials show a similar mobility. The examination of the accessibility of the incorporated rhodium(I) centers within these different types of polysiloxane matrices was carried out by hydrogenation of 1-hexene. All applied materials showed rather good turnover frequencies indicating a good accessibility of the anchored transition metal complexes. Their activity can be increased by using polar solvents. After three runs no reduction of the activity and no metal leaching were observed.

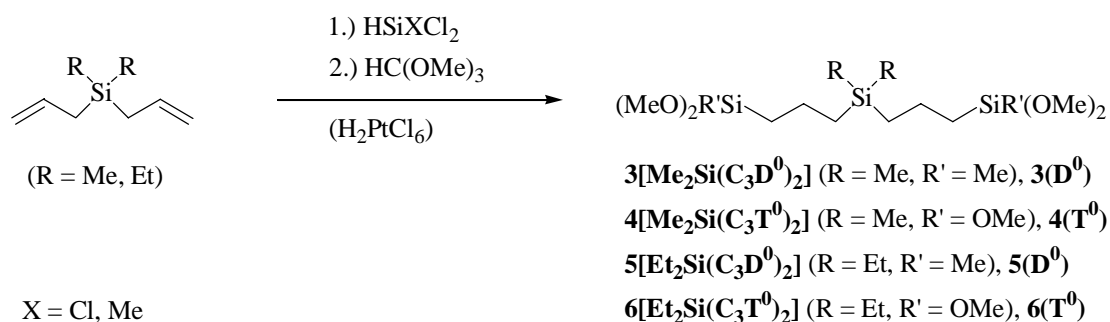
2.4 Synthesis, Sol–Gel Processing, and Investigations on the Mobility of Novel D– and T–bifunctionalized Co–condensing Agents

2.4.1 Introduction

If $\mathbf{D}^0\text{-C}_z\text{-D}^0$ materials are used as co–condensing agents the mobility of the carrier matrix and the reactive centers is induced by the high flexibility of the alkyl chain. Due to the steric demand of the phenyl ring the degree of condensation in the case of $\mathbf{Ph(1,4-C}_z\mathbf{D}^0)_2$ is somewhat lower (~80 %), which means a higher mobility of the materials ²³ (*vide supra*). In this part it was the objective to investigate novel D– and T–functionalized co–condensing agents. After the sol–gel process they combine a highly mobile alkyl chain with a low degree of condensation induced by the steric demand of the silicon attached substituents.

2.4.2 Preparation of the Monomeric Precursors $\mathbf{3(D}^0)$, $\mathbf{4(T}^0)$, $\mathbf{5(D}^0)$, and $\mathbf{6(T}^0)$

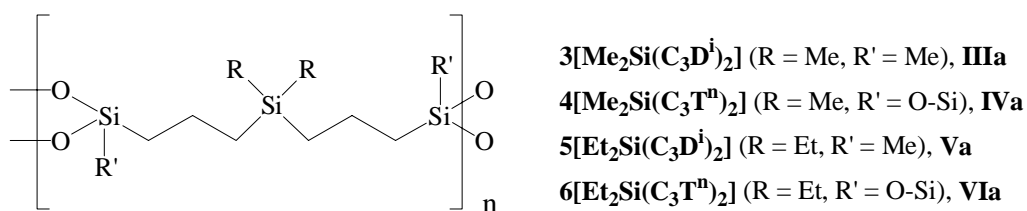
The precursors for the sol–gel process, the bis(dimethoxymethylsilylpropyl)dialkylsilanes $\mathbf{3(D}^0)$, $\mathbf{5(D}^0)$ and the bis(trimethoxysilylpropyl)dialkylsilanes $\mathbf{4(T}^0)$, $\mathbf{6(T}^0)$ were prepared by hydrosilylation of the corresponding diallyldialkylsilanes with dichloromethylsilane and trichlorosilane respectively, followed by the replacement of the chlorine atoms for methoxy groups with trimethyl orthoformate ⁵⁹ (Scheme 5). After distillation under vacuum $\mathbf{3(D}^0)$, $\mathbf{4(T}^0)$, $\mathbf{5(D}^0)$, and $\mathbf{6(T}^0)$ were obtained as colorless, analytical pure liquids, which are sensitive to moisture and soluble in common organic solvents. All monomers were characterized by ^1H , $^{13}\text{C}\{^1\text{H}\}$, and $^{29}\text{Si}\{^1\text{H}\}$ NMR spectroscopy as well as mass spectrometry.



Scheme 5 Synthesis of the monomeric precursors **3(D⁰)**, **4(T⁰)**, **5(D⁰)**, and **6(T⁰)**.

2.4.3 Sol-gel Processing of **3(D⁰)**, **4(T⁰)**, **5(D⁰)**, and **6(T⁰)**

To be able to compare the results with previous investigations (*n*-Bu)₂Sn(OAc)₂^{22,23} and a mixture of THF and methanol was employed as catalyst and solvent, respectively. According to these boundary conditions, two types of polysiloxanes were obtained (Scheme 6).



Scheme 6 Structural backbone of the xerogels.

The xerogels **IIIa, b**, **IVa, b**, and **Va, b**, **VIa, b** were prepared without and with the co-condensation agent phenyltrimethoxysilane [**Ph(T⁰)**], which was condensed into the matrix (Table 14). In this way it can be investigated whether domains are formed during the sol-gel process or if one component of the copolycondensates is washed out in the solvent processing.

Table 14 Sol–gel processes and labeling of the xerogels III, IV, V, and VI

Monomeric silanes	Co–condensation agent	Polysiloxanes	Xerogels
3[Me₂Si(C₃D⁰)₂], 3(D⁰)		3[Me₂Si(C₃D¹)₂]	IIIa
4[Me₂Si(C₃T⁰)₂], 4(T⁰)		4[Me₂Si(C₃Tⁿ)₂]	IVa
5[Et₂Si(C₃D⁰)₂], 5(D⁰)		5[Et₂Si(C₃D¹)₂]	Va
6[Et₂Si(C₃T⁰)₂], 6(T⁰)		6[Et₂Si(C₃Tⁿ)₂]	VIa
3[Me₂Si(C₃D⁰)₂], 3(D⁰)	Ph(T ⁰) ^a	3[Me₂Si(C₃D¹)₂]_x[Ph(Tⁿ)]_y	IIIb
4[Me₂Si(C₃T⁰)₂], 4(T⁰)	Ph(T ⁰)	4[Me₂Si(C₃Tⁿ)₂]_x[Ph(Tⁿ)]_y	IVb
5[Et₂Si(C₃D⁰)₂], 5(D⁰)	Ph(T ⁰)	5[Et₂Si(C₃D¹)₂]_x[Ph(Tⁿ)]_y	Vb
6[Et₂Si(C₃T⁰)₂], 6(T⁰)	Ph(T ⁰)	6[Et₂Si(C₃Tⁿ)₂]_x[Ph(Tⁿ)]_y	VIb

^aT⁰ = Si(OMe)₃

2.4.4 Solid State NMR Spectroscopic Investigations

2.4.4.1 ²⁹Si CP/MAS NMR Spectroscopy

All silicon atoms in the polysiloxane matrix are in direct proximity of protons, thus all silyl species are detectable via cross polarisation technique^{27,35,36}. The ²⁹Si CP/MAS spectra of selected polymers are depicted in Figure 14. The ²⁹Si signals of these copolymers are in the typical range for R₂Si (R = Me, Et), D–, T–, and T_{Ph}–silyl functions and their substructures D⁰–D², T⁰–T³, and T¹_{Ph}–T³_{Ph}, which indicates an incomplete condensation. Average chemical shifts are Et₂Si, 4.8; Me₂Si, 1.4; D⁰, –2.4; D¹, –12.4; D², –22.2; T⁰, –42.4; T¹, –50.6; T², –59.3; T³, –68.3; T¹_{Ph}, –62.8; T²_{Ph}, –71.4; T³_{Ph}, –79.8. D⁰–, and T⁰– species, which are attached to the polymeric matrix via the second silyl function, cannot be removed during solvent processing.

The degree of condensation of the D–, T–, and T_{Ph}–species and the real ratios of T_{Ph}/D and T_{Ph}/T (Table 15) were determined by generally known methods^{22,23,37,38}. The degrees of condensation range between 70 and 96 % for the D–functions and 52 and 70 % for the T–groups. The T_{Ph}–species show a degree of condensation between 68 and 93 %. These values

are lower than the degrees of condensation which were determined in the case of the bifunctionalized silanes $(\text{MeO})_2\text{MeSi}(\text{CH}_2)_z\text{SiMe}(\text{OMe})_2$ ($\mathbf{D}^0\text{-C}_z\text{-D}^0$, $z = 6, 8, 14$; $> 92\%$)²², $(\text{MeO})_2\text{MeSi}(\text{CH}_2)_z(\text{C}_6\text{H}_4)(\text{CH}_2)_z\text{SiMe}(\text{OMe})_2$ ($\mathbf{Ph(1,4-C}_z\mathbf{D}^0)_2$, $z = 3, 4$; $> 77\%$), and $(\text{MeO})_3\text{Si}(\text{CH}_2)_3(\text{C}_6\text{H}_4)(\text{CH}_2)_3\text{Si}(\text{OMe})_3$ ($\mathbf{Ph(1,4-C}_3\mathbf{T}^0)_2$, $> 67\%$)²³. The steric demand of the internal organosilicon function influences the kinetics and seems to be responsible for the rather low degree of condensation. The experimentally determined stoichiometries of the $\text{T}_{\text{Ph}}/\text{D-}$ and $\text{T}_{\text{Ph}}/\text{T-}$ polymers do not differ significantly from the applied stoichiometries. Neither D-, T-, nor T_{Ph} -functions were washed out during the solvent processing. Thus the monomeric co-condensing agents $\mathbf{3(D}^0)$, $\mathbf{4(T}^0)$, $\mathbf{5(D}^0)$, and $\mathbf{6(T}^0)$ are useful precursors to generate carrier matrices for 'Chemistry in Interphases'.

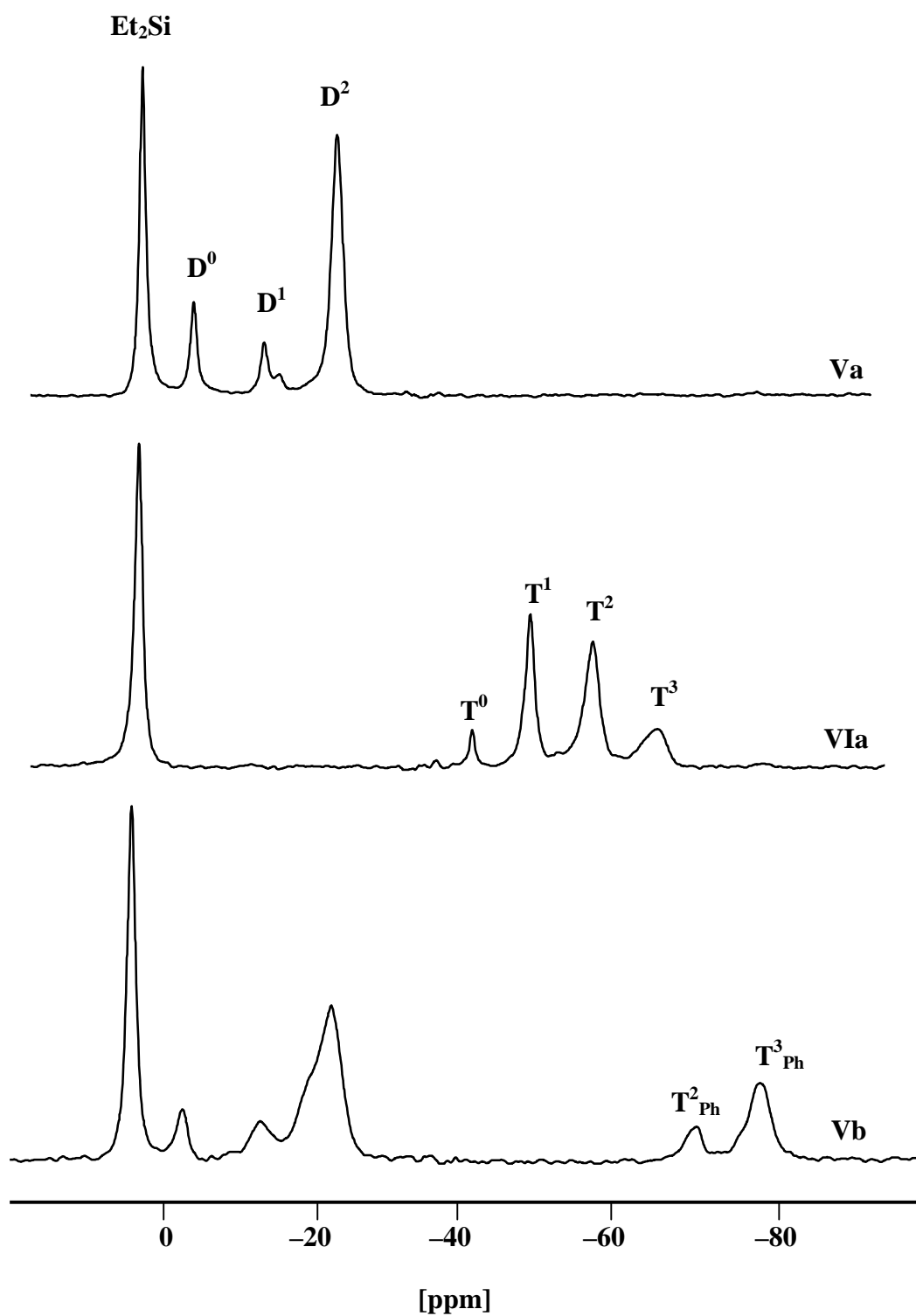


Figure 14 ^{29}Si CP/MAS NMR spectra of selected xerogels.

Table 15 Relative I_0 data, degree of condensation, degree of hydrolysis of the silyl species in the copolymers

Xerogel	relative I_0 data of D-, T- and T _{Ph} -species ^a										degree of condensation [%]			real T _{Ph} /D- and T _{Ph} /T- moiety	degree of hydrolysis [%] ^b
	D ⁰	D ¹	D ²	T ⁰	T ¹	T ²	T ³	T ¹ _{Ph}	T ² _{Ph}	T ³ _{Ph}	D	T	T _{Ph}		
IIIa	<i>c</i>	7.7	100								96				97
IVa				13.4	100	95.9	24.5					52			80
Va	22.5	18.2	100								78				89
VIa				13.9	90.3	100	43.8					57			70
IIIb	9.6	100	88.2					3.5	40.7	43.6	70		82	1 : 2.2	92
IVb				7.0	77.2	100	51.3	24.5	46.4	28.6		61	68	1 : 2.4	72
Vb	14.6	26.6	100					<i>c</i>	14.3	56.3	80		93	1 : 2.0	92
VIb				2.8	48.5	100	81.1	23.7	40.0	61.9		70	77	1 : 1.9	83

^a Determination via ²⁹Si SPE/MAS experiment. ^b For the determination of the degree of hydrolysis see ref.²². ^c Species not detectable.

2.4.4.2 ^{13}C CP/MAS NMR Spectroscopy

The ^{13}C CP/MAS NMR spectra of the pure D-polymers show a small peak at 49.6 ppm for the non-hydrolyzed Si-OMe functions. In the aliphatic region a broad peak occurs between 20 and 14 ppm, which originates from the three methylene units connecting the internal silicon atom and the D-group. In the ^{13}C CP/MAS NMR spectrum of **IIIa** two sharp signals at 0.1 and -2.8 ppm are ascribed to the methyl groups adjacent to the silicon atoms. In the case of **Va** the ethyl groups attached to the internal silicon atom give rise to two signals at 7.6 and 4.0 ppm. The methyl group of the D-fragment resonates at -0.1 ppm.

A relative high intense peak of the non-hydrolyzed Si-OMe functions in the spectra of the pure T-polymers indicates a rather low degree of hydrolysis. An unresolved signal group between 21 and 14 ppm originates from the three methylene units connecting the internal silicon atom and the T-group. In the case of **IVa** the methyl groups attached to the internal silicon atom resonate at -3.3 ppm and in the spectrum of **VIa** the two peaks of the ethyl groups are located at 7.5 and 4.0 ppm.

In the aliphatic region the T_{Ph}/D - and T_{Ph}/T -polymers reveal the same patterns as the above-mentioned materials, but two broad signals at 134 and 127 ppm are observed caused by the phenyl ring of the **Ph(Tⁿ)** moiety.

2.4.5 Studies on the Dynamic Behavior of the Polysiloxanes by Solid State and Suspension State NMR Spectroscopy

The values of the spin-lattice relaxation time of the protons in the rotating frame ($T_{1\rho\text{H}}$) were determined via a ^{29}Si direct spin lock- τ -CP experiment⁴⁰. The observed decays of the magnetization were monoexponential in each of the samples. Thus the relaxation mechanism

is spin–diffusion controlled and the occurrence of domains within 1 – 2 nm is excluded. Therefore the materials are considered as homogenous. In the solid state all polymers do not differ significantly in the relaxation parameters $T_{1\rho\text{H}}$ and T_{SiH} (Table 16).

Table 16 T_{SiH} and $T_{1\rho\text{H}}$ data of the silyl species in the xerogels

Xerogel	$R_2\text{Si}^c$	T_{SiH} [ms] ^a										$T_{1\rho\text{H}}$ [ms] ^b	
		D^0	D^1	D^2	T^0	T^1	T^2	T^3	T^1_{Ph}	T^2_{Ph}	T^3_{Ph}		
IIIa	0.92	<i>d</i>	<i>e</i>	1.96									2.54
IVa	0.92				<i>e</i>	1.96	0.95	0.95					2.36
Va	0.76	1.99	1.12	0.65									2.08
VIa	1.42				<i>e</i>	2.07	1.84	1.46					1.57
IIIb	1.37	<i>d</i>	1.89	0.75					<i>e</i>	0.76	1.04		1.94
IVb	0.90				<i>e</i>	1.29	0.97	0.95	0.60	0.90	<i>e</i>		2.12
Vb	1.20	1.78	0.95	1.08					<i>d</i>	2.32	1.73		2.45
VIb	0.88				1.02	1.37	1.17	1.27	1.12	1.47	2.50		2.31

^a Determination via contact time variation. ^b Determination via ^{29}Si according to ref. ⁴⁰. ^c R = Me, Et. ^d Species not detectable. ^e Intensity too low for precise determination.

With rising temperature for all samples, except for **IIIa**, **Va**, and **Vb**, the increasing $T_{1\rho\text{H}}$ values indicate that they are in the fast–motion regime of the correlation time curve. This high mobility is due to the rather low degree of condensation (Table 15). The polymers **IIIa**, **Va**, and **Vb** do not show a constant trend of the $T_{1\rho\text{H}}$ values with an increase of the temperature. This fact indicates that these materials are in a broad minimum of the correlation time curve, and therefore no precise prediction on the mobility can be made (Table 17).

Table 17 Temperature dependence of the $T_{1\rho\text{H}}$

Xerogel	$T_{1\rho\text{H}}$ [ms] ^a			
	300 K	310 K	320 K	330 K
IIIa	2.54	2.04	2.52	1.01
IVa	2.36	3.33	6.19	6.78
Va	2.08	1.21	2.63	0.98
VIa	1.57	3.51	6.38	<i>b</i>
IIIb	1.94	4.40	5.56	<i>b</i>
IVb	2.12	1.21	4.10	4.28
Vb	2.45	3.33	1.47	2.72
VIb	2.31	4.12	6.00	6.70

^a Determination via ²⁹Si according to ref. ⁴⁰. ^b Not determined.

For ‘Chemistry in Interphases’ it is necessary to study the mobility and dynamics of the materials in the suspension state. Therefore ¹H High Resolution Magic Angle Spinning (HR/MAS) experiments and $T_{1\rho\text{H}}$ measurements of suspensions ²³ of all polymers in different solvents (methanol, tetrahydrofuran, and chloroform) were carried out (Tables 18 and 19). Representative ¹H HR/MAS NMR spectra of **IIIb** are depicted in Figure 15. If solvents of a medium polarity (CDCl₃ and THF-*d*₈) are used nearly all signals of the aliphatic and aromatic protons are resolved in contrast to spectra obtained in methanol.

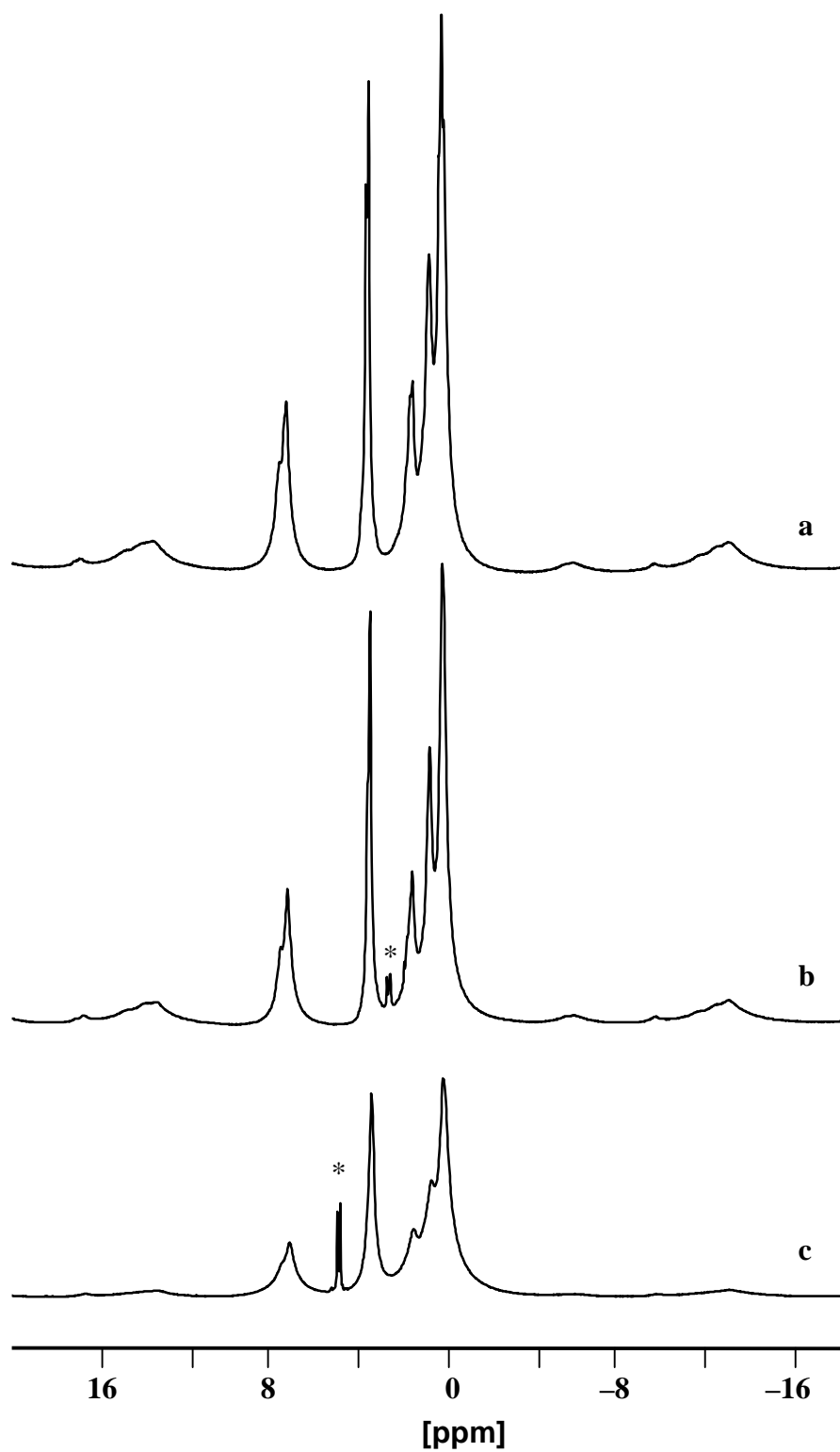


Figure 15 ^1H HR/MAS NMR spectra of **IIIb** in CDCl_3 (a), THF-d_8 (b), MeOH-d_4 (c).
Peak assignment: δ 7.4 – 7.1 (aromatic protons), δ 3.5 (MeO), δ 1.5 – 0.0 (aliphatic protons);
peaks originating from the solvent are denoted with *.

Table 18 $T_{1\rho\text{H}}$ data in suspension of the polymers IIIa, b and IVa, b

δ (^1H)	IIIa			IVa			IIIb			IVb		
	$T_{1\rho\text{H}}$ [ms]			$T_{1\rho\text{H}}$ [ms]			$T_{1\rho\text{H}}$ [ms]			$T_{1\rho\text{H}}$ [ms]		
[ppm]	CDCl_3	THF	MeOH	CDCl_3	THF	MeOH	CDCl_3	THF	MeOH	CDCl_3	THF	MeOH
0.0	38.2	23.6	2.7	55.9	48.4	7.8	68.9	62.4	9.2	55.0	46.3	12.1
0.6	28.7	21.2		28.7	47.1	6.6	58.7	56.0	5.6	46.2	38.0	
1.5	31.9	29.2		54.0	55.7	6.2	63.3	63.4	5.5	52.6	38.0	
3.5	38.1	36.6	4.3	71.8	70.3	14.3	86.8	84.8	16.2	66.9	49.6	9.0
7.1							66.2	60.5	7.8	64.4	50.6	7.2
7.4							67.4	57.1	7.7	58.1	46.1	7.2

Table 19 $T_{1\rho\text{H}}$ data in suspension of the polymers Va, b and VIa, b

δ (^1H)	Va			VIa			Vb			VIb		
	$T_{1\rho\text{H}}$ [ms]			$T_{1\rho\text{H}}$ [ms]			$T_{1\rho\text{H}}$ [ms]			$T_{1\rho\text{H}}$ [ms]		
[ppm]	CDCl_3	THF	MeOH	CDCl_3	THF	MeOH	CDCl_3	THF	MeOH	CDCl_3	THF	MeOH
0.0	28.6	22.8	7.6				37.1	33.7				
0.4				36.4	22.8					41.0	18.4	
0.7	26.1	19.6		36.4	22.9	6.0		23.6	5.5	26.0	18.4	7.1
0.9	26.1	19.7	5.7	36.4	22.8		25.5					
1.5	22.6	23.8		36.4	22.3					18.9	19.7	7.1
3.5	42.4	31.1	12.3	45.9	29.3	13.3	37.7	40.0	19.7	35.0	22.8	6.6
7.1								24.1		29.7	20.8	7.5
7.4							26.9	24.1	5.4	29.7	20.8	

$T_{1\rho\text{H}}$ values determined in suspension increase by an order of magnitude except if MeOH is used as a solvent. In solvents of medium polarity all investigated xerogels form highly mobile interphases and the relaxation times $T_{1\rho\text{H}}$ are located on the fast motion regime of the correlation time curve²³. In suspension spin diffusion does not longer play the dominating role of the relaxation processes. The different proton sites relax in varying rates. By these measurements it is corroborated, that the non-hydrolyzed methoxy protons (3.5 ppm) are most mobile followed by the protons of the methyl (0.0 ppm) or ethyl groups (0.9 and 0.4 ppm) adjacent to the internal silicon atom. Due to the low swelling capability, the determination of the $T_{1\rho\text{H}}$ values of the mentioned polymers swollen in MeOH is rather difficult.

With the exception of **VIb**, the pure D-polymers show the lowest $T_{1\rho\text{H}}$ values and therefore the lowest mobility in suspension, which can be explained by the rather high degree of condensation.

2.4.6 Surface Area Measurements, SEM Images, and EDX Measurements

Due to the high organic portions in these inorganic-organic hybrid materials the surface area measurements according to the BET method reveal very low values ($< 10 \text{ m}^2/\text{g}$), which is in agreement with former results^{22,23}.

SEM images of the polymers **IIIa** and **IVa** are depicted in Figure 16. In contrast to **IVa**, which consists of smaller particles due to the higher brittleness of T-polymers, **IIIa** as a pure D-polymer is rubber-like with mainly large particles.

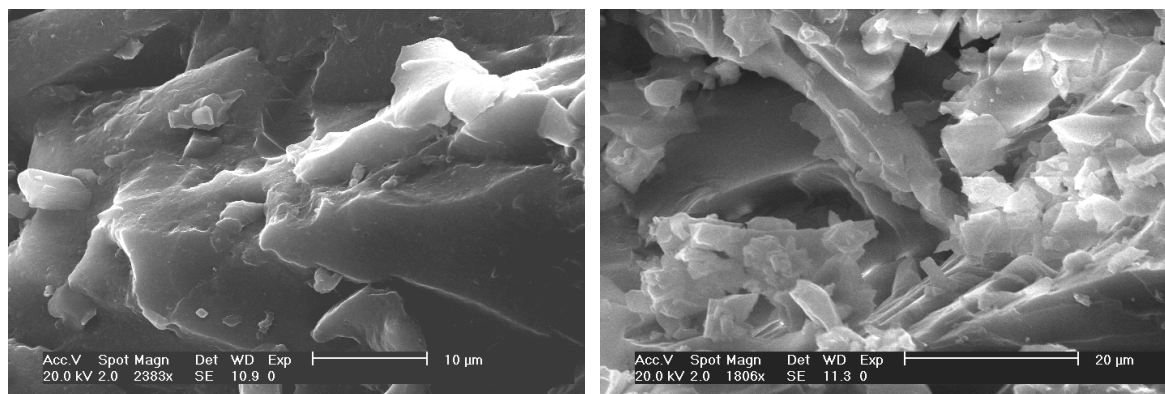


Figure 16 SEM images of **IIIa** (left) and **IVa** (right).

Figure 17 illustrates typical EDX spectra of **IIIa** and **VIa** including peak assignment. A qualitative analysis confirms the presence of carbon, oxygen and silicon. For purposes of quantification, however, the measured composition has to be compared with theoretical values calculated excluding hydrogen, since hydrogen is a single electron atom and thus does not emit characteristic X-rays. In Table 20 the quantification results of the EDX measurements are summarized and compared to reference data from NMR measurements.

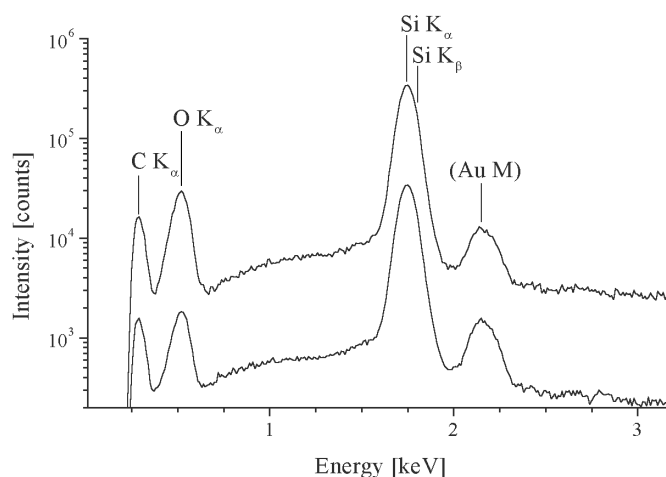


Figure 17 EDX spectra of **VIa** (top) and **IIIa** (bottom). The spectrum of **VIa** is offset by a factor of 10 for clarity. It can be seen that the oxygen content of **VIa** is significantly higher than in **IIIa**.

Table 20 EDX data of IIIa, b, IVa, b, Va, b, and VIa, b

Xerogel	Reference data ^a			EDX [ZAF correction] ^b			EDX [$\phi(\rho z)$ -correction] ^b		
	Composition [%] ^c			Composition [%] ^c			Composition [%] ^c		
	C	O	Si	C	O	Si	C	O	Si
IIIa	49.2	16.4	34.4	50.0	14.9	35.1	51.1	15.9	33.0
IVa^d	40.9	27.2	31.9	–	–	–	–	–	–
IIIb	51.9	17.3	30.8	54.6	19.4	26.0	54.7	20.7	24.6
IVb^d	45.1	26.2	28.7	–	–	–	–	–	–
Va	53.7	14.9	31.4	53.2	12.9	33.9	54.2	13.9	31.9
VIa	45.8	25.0	29.2	47.2	20.9	31.9	48.0	22.0	30.0
Vb	55.1	16.3	28.6	56.6	17.2	26.2	56.7	18.5	24.8
VIb	49.6	23.3	27.1	50.6	21.4	28.0	51.0	22.6	26.4

^a Derived from NMR data according to ref. ²². ^b Calculated according to ref. ⁴⁷. ^c Calculated excluding hydrogen. ^d Sample topography does not allow quantification.

2.4.7 Conclusion

A new type of polysiloxanes with tunable T/T– and T/D–ratios was synthesized by sol–gel processing of the novel monomeric precursors $R'Si(OMe)_2(CH_2)_3R_2Si(CH_3)Si(OMe)_2R'$ ($R = Me, Et$; $R' = Me, OMe$) [**3(D⁰)**, **4(T⁰)**, **5(D⁰)**, **6(T⁰)**]. Since they combine the advantages of a mobile alkyl chain with a lower degree of condensation, which is induced by the steric demand of the internal organosilicon function, the mentioned precursors are suitable to form highly mobile carrier matrices for ‘Chemistry in Interphases’. As a result of the $T_{1\rho H}$ measurements in the solid state the formation of domains is excluded, which means that the materials are homogenous. 1H HR/MAS NMR spectroscopy and $T_{1\rho H}$ measurements in suspension furnish evidence that the xerogels form highly mobile interphases if solvents of a medium polarity like chloroform or tetrahydrofuran are used. Due to the lower degree of condensation the polymers with T–silyl functions seem to be more mobile in the solid and in the suspension state than the pure D–polymers. Despite low degrees of condensation the cross–linking in these novel inorganic–organic hybrid materials is sufficient to resist even a

partial decomposition during sol–gel processing. These properties afford the precondition that leaching of catalytically active transition metal complexes is reduced in ‘Chemistry in Interphases’.

3. Experimental Section

3.1 General Remarks

All reactions and manipulations were carried out under argon with the usual Schlenck techniques. Methanol was dried with magnesium and distilled. All other solvents were distilled from sodium benzophenone or calcium hydride. H₂O and (*n*-Bu)₂Sn(OAc)₂ were distilled under inert gas prior to use. All solvents and reagents were stored under argon.

3.1.1 Reagents

RhCl₃ and PdCl₂ were a gift from Degussa AG. Dichloromethylsilane and trichlorosilane were purchased from Aldrich. Trimethyl orthoformate, phenyltrimethoxysilane and 1-hexene were purchased from Fluka. (COD)PdCl₂⁶⁰, (NBD)Mo(CO)₄⁶¹, [μ-ClRh(COD)]₂⁶², the T-functionalized diphosphine **1**(T⁰)⁴¹, the co-condensation agents **D**⁰-C₆-**D**⁰²² and **Ph**(**1,4-C**₃**D**⁰)₂²³ as well as diallyldimethylsilane⁶³ and diallyldiethylsilane⁶⁴ were synthesized as previously described.

3.1.2 Elemental Analyses, IR, and Mass Investigations

Elemental analyses were carried out on a Vario EL (Elementar Analytische Systeme Hanau). IR data were obtained on a Bruker IFS 48 FT-IR spectrometer. Mass spectra (FD) were acquired on a Finnigan MAT 711A instrument (8 kV, 333 K), EI-spectra were recorded on a TSQ Finnigan (70 eV, 473 K) and reported as mass/charge (*m/z*).

3.1.3 NMR Spectroscopy in Solution

Solution nuclear magnetic resonance spectra were recorded on a Bruker DRX 250 spectrometer (field strength 5.87 T) at 296 K. Frequencies are as follows: ^1H NMR: 250.13 MHz, $^{31}\text{P}\{^1\text{H}\}$ NMR: 101.25 MHz (referenced to 85 % H_3PO_4), $^{13}\text{C}\{^1\text{H}\}$ NMR: 62.90 MHz, $^{29}\text{Si}\{^1\text{H}\}$ NMR: 49.69 MHz (referenced to TMS). ^{103}Rh NMR resonances were measured using a 2D (^{31}P , $^{103}\text{Rh}\{^1\text{H}\}$) experiment⁶⁵. Chemical shifts in the ^1H and $^{13}\text{C}\{^1\text{H}\}$ NMR spectra were measured relative to partially deuterated solvent peaks which are reported relative to TMS. The ^{103}Rh chemical shift values are referred $\Xi(\text{Rh}) = 3.16 \text{ Mhz}$ ⁶⁶.

3.1.4 Solid State NMR Measurements

CP/MAS solid state NMR spectra were recorded on Bruker DSX 200 and Bruker ASX 300 (temperature dependent measurements) multinuclear spectrometers equipped with wide bore magnets (field strength 4.7 T and 7.05 T). Magic angle spinning was applied up to 10 kHz (4 mm ZrO_2 rotors) and 3 – 4 kHz (7 mm ZrO_2 rotors), respectively. Frequencies and standards: ^{31}P , 81.961 MHz (4.7 T), 121.442 MHz (7.05 T) [85% H_3PO_4 , $\text{NH}_4\text{H}_2\text{PO}_4$ ($\delta = 0.8$) as second standard]; ^{13}C , 50.228 MHz (4.7 T), 75.432 MHz (7.05 T), [TMS, carbonyl resonance of glycine ($\delta = 176.05$) as second standard]; ^{29}Si , 39.73 MHz (4.7 T), 59.595 MHz (7.05 T), (Q_8M_8 as second standard). All samples were packed under exclusion of molecular oxygen. The cross polarization constants T_{XH} were determined by variation of the contact time T_c (14 – 16 experiments). The proton relaxation times in the rotating frame $T_{1\rho\text{H}}$ were measured by direct proton spin lock- τ -CP experiments⁴⁰. The relaxation parameters were obtained using Bruker software SIMFIT. Peak deconvolution of the spectra were performed with the Bruker software WINFIT using Voigtian line shapes. For the quantification of the silyl species in the

polysiloxanes, ^{29}Si CP/MAS NMR contact time variations experiments were carried out and the obtained quasi 2D–data set was analyzed with XWINNMR. The relative amounts I_0 of each of the D^i and T^n species in one sample were calculated by inserting their peak areas of the deconvoluted spectra $I(T_c)$, the individual T_{SiH} data, and the common $T_{1\rho\text{H}}$ value into the following equation ³⁷.

$$I(T_c) = \frac{I_0}{(1 - T_{\text{SiH}}/T_{1\rho\text{H}})} (e^{-T_c/T_{1\rho\text{H}}} - e^{-T_c/T_{\text{SiH}}}) \quad (1)$$

If the boundary condition $T_{\text{SiH}} \ll T_{1\rho\text{H}}$ ³⁹ could not be considered, the quantification of the silyl species was performed by deconvolution of the ^{29}Si CP/MAS spectra ($T_c = 5$ ms) ³⁸ or by a ^{29}Si HPDEC/MAS NMR experiment [recycle delay 20 s, pulse length 3.5 μs ($\sim 45^\circ$)] followed by peak deconvolution.

3.1.5 Suspension NMR Measurements

The ^1H HR/MAS suspension state NMR spectra were recorded on a Bruker ASX 300 spectrometer equipped with a wide bore magnet (field strength 7.05 T, proton resonance frequency 300.13 MHz). Acquisition parameters: 90° proton pulse length 3.5 μs , recycle delay 3 s, sweep width 50 kHz, 16 K data points in the time domain. The chemical shifts were referenced with respect to TMS. The $T_{1\rho\text{H}}$ values in suspension were determined by a spin lock–SPE–experiment via ^1H (90° proton pulse length 3.5 μs , recycle delay 3 s, spectral width 50 kHz, 16 K data points in the time domain) ²³. The polysiloxanes were allowed to swell in solvents at least for one hour in 4 mm rotors with inserts. In all cases the rotation frequency was 4 kHz. Samples were employed in amounts of 20 mg.

3.1.6 EXAFS Measurements

EXAFS measurements were performed at the Rh–K–edge (23220 eV) at the beamline X1.1 of the Hamburger Synchrotron–Strahlungslabor (HASYLAB) at DESY, Hamburg with a Si(311) double crystal monochromator under ambient conditions (5.46 GeV, beam current 93 mA). Data were collected in transmission mode with ion chambers. Energy calibration was monitored with a 20 μm thick rhodium metal foil at the K–edge (23220 eV). All measurements were performed under an inert gas atmosphere. The samples were prepared of a mixture of the xerogels and polyethylene. Data were analyzed with a program package specially developed for the requirements of amorphous samples⁶⁷. The program AUTOBK of the University of Washington⁶⁸ was used for background removal, and the program EXCURV92⁶⁹ was used for evaluation of the XAFS function. The resulting EXAFS function was weighted with k^3 . Data analysis in k space was performed according to the curved–wave multiple–scattering formalism of the program EXCURV92. The mean free path of the scattered electrons was calculated from the imaginary part of the potential (VPI was set to –4.00), the amplitude reduction factor AFAC was fixed at 0.8, and an overall energy shift ΔE_0 was introduced to fit the data. In the fitting procedure the intermolecular coordination numbers were varied and the intramolecular coordination numbers were fixed according to the known values of the ligands around the rhodium atom.

3.1.7 SEM and EDX Investigations

Scanning electron micrographs and energy dispersive X–ray analysis (EDX) were performed on a Philips XL 30 scanning electron microscope (SEM) equipped with a DX–4 X–ray detection system by EDAX. This consists of an energy dispersive Si(Li)–detector with an

active area of 10 mm² and the eDX software package. The primary beam energy was set to 20 keV for all measurements. Micrographs were recorded detecting secondary electrons generated by a probe current of approximately 50 or 168 pA, whereas a probe current of 575 or 623 pA was applied for carrying out elemental analysis by EDX. Quantification of X-ray emission spectra was achieved employing the ZAF as well as the $\phi(\rho z)$ correction procedure to convert X-ray intensities to elemental amounts⁴⁷. The sample powder was placed on a specimen stub covered with a conductive adhesive tab and subsequently provided with a sputtered 20 nm gold layer to avoid specimen charging. Spectra were recorded with spot illumination of the sample for 240 or 300 seconds, yielding count rates of about 2000 s⁻¹. Spectra were acquired several times at different sample positions to ensure reproducibility. The various measurements were found to differ to about 3 % which is within the limits of error, especially for light element samples with pronounced topography. For this reason, special care was taken to find specimen areas exhibiting flat surfaces to ensure the validity of the correction models. All measurements were performed at ambient temperature.

3.1.8 Catalysis

Hydrogenation experiments were carried out in a 100 ml stainless steel autoclave equipped with a mechanical stirring bar. The autoclave was flushed with argon prior to the introduction of the reaction mixture (1 – 10 μ mol catalyst with respect to rhodium, 6 – 60 mmol of 1-hexene and 25 ml of the solvent). The suspension was set under hydrogen pressure and stirred prior to heating to the desired temperature. The quantitative analyses were performed on a GC 6000 Vega Series 2 (Carlo Erba Instruments) with an FID and a capillary column CP Sil 88 [17 m, carrier gas helium (50 kPa); integrator Hewlett Packard 3390 A].

Leaching investigations were carried out with a Varian Spectr AA 20 Plus atomic absorption spectrometer.

3.2 Preparation of the Compounds

3.2.1 Synthesis of the Monomers

3.2.1.1 Preparation of the Rhodium(I) Complex $2(\mathbf{T}^0)$

η^4 -1,5-Cyclooctadiene[2-diphenylphosphinylmethyl-1-diphenylphosphinyl-8-trimethoxy-silyloctanerrhodium(I)]hexafluoroantimonate(V) [$2(\mathbf{T}^0)$]: To a solution of AgSbF_6 (164 mg, 0.48 mmol) in 3 ml of THF a solution of $[\mu\text{-ClRh}(\text{COD})]_2$ (118 mg, 0.24 mmol) in 3 ml of THF was added under exclusion of light. After stirring for 1 h a solution of $1(\mathbf{T}^0)$ (295 mg, 0.48 mmol) in 3 ml of THF was added. The reaction mixture was stirred for 2 h and the precipitated AgCl was removed by centrifugation. Then the solvent was removed under reduced pressure. The residue was dissolved in 3 ml of THF and 10 ml of *n*-pentane was added to this solution. After stirring for 10 min, filtration (P3) and drying for 1 h 452 mg (88 %) of $2(\mathbf{T}^0)$ was obtained as a microcrystalline, orange-yellow solid.

^1H NMR (CDCl_3): $\delta = 7.56 - 7.19$ (m, 20H, H-phenyl), 4.86, 4.24 [br, 4H, H-olefin (COD)], 3.47 (s, 9H, OCH_3), 2.60 - 1.05 (m, 23H, CH_2 , CH), 0.53 - 0.47 (m, 2H, $\text{CH}_2\text{-CH}_2\text{-Si}$). $^{13}\text{C}\{^1\text{H}\}$ NMR (CDCl_3): $\delta = 134.6 - 126.3$ (m, C-phenyl), 102.2, 95.6 [br, C-olefin (COD)], 48.7 (OCH_3), 38.4 (m, CH_2P), 31.0 - 20.7 (CH_2 , CH), 7.2 ($\text{CH}_2\text{-CH}_2\text{-Si}$). $^{31}\text{P}\{^1\text{H}\}$ NMR (CDCl_3): $\delta = 15.5$ (d, $^1J(\text{RhP}) = 141.4$ Hz). $^{103}\text{Rh}\{^1\text{H}\}$ NMR (CDCl_3): $\delta = -350$. IR (KBr, cm^{-1}): 1096 s [$\nu(\text{Si-OMe})$], 669 m [$\nu(\text{SbF}_6^-)$]. MS (FD): m/z 827.1 [$\text{M}^+ - \text{SbF}_6$]. $\text{C}_{44}\text{H}_{58}\text{F}_6\text{O}_3\text{P}_2\text{RhSbSi}$: calcd C 49.69, H 5.50 %; found C 49.32, H 4.87 %.

3.2.1.2 Synthesis of the Co-condensing Agents 3(D⁰), 4(T⁰), 5(D⁰), and 6(T⁰)

Bis[3-(dimethoxymethylsilyl)propyl]dimethylsilane [3(D⁰)]: A mixture of diallyldimethylsilane (6.27 g, 44.7 mmol), dichloromethylsilane (17.25 g, 150 mmol) and hexachloroplatinic acid (15.0 mg, 0.029 mmol) in 75 ml of THF was stirred for 2 d at room temperature. Then the solvent was removed under reduced pressure. To the remaining viscous oil trimethyl orthoformate (100 ml, 960 mmol) was added. After stirring for 4 d all volatile components were removed under reduced pressure and distillation under vacuum afforded 11.68 g (75 %) of 3(D⁰), which was obtained as a colorless, airstable liquid sensitive to moisture, b.p. 110 °C (4 mbar).

¹H NMR (C₆D₆): δ = 3.43 (s, 12H, Si-OCH₃), 1.49 (m, 4H, Si-CH₂-CH₂-CH₂-Si), 0.73 (t, ³J(HH) = 7.69 Hz, 4H, (H₃C)₂Si-CH₂-CH₂), 0.63 (m, 4H, H₃C(H₃CO)₂Si-CH₂-CH₂-), 0.11 (s, 6H, Si(OCH₃)₂CH₃), 0.00 (s, 6H, Si(CH₃)₂). ¹³C{¹H} NMR (C₆D₆): δ = 49.7 (Si-OCH₃), 19.8 ((H₃C)₂Si-CH₂-), 18.1 (Si-CH₂-CH₂-CH₂-Si), 17.8 (H₃C(H₃CO)₂Si-CH₂-), -3.3 (Si(CH₃)₂), -5.5 (Si(OCH₃)₂CH₃). ²⁹Si{¹H} NMR (C₆D₆): δ = 1.1 (Si(CH₃)₂), -2.8 (Si(OCH₃)₂CH₃). IR (KBr, cm⁻¹): 1258 s [ν(Si-CH₃)], 1190 s [ν(Si-CH₂-)], 1087 vs [ν(Si-OCH₃)]. MS (EI): m/z = 337 [M⁺ - CH₃], 291 [M⁺ - 2CH₃ - OCH₃], 205 [H₃C(H₃CO)₂Si(CH₂)₃Si(CH₃)₂⁺]. C₁₄H₃₆O₄Si₃: calcd C 47.68, H 10.29 %; found C 46.98, H 10.25 %.

Bis[3-(trimethoxysilyl)propyl]dimethylsilane [4(T⁰)]: A mixture of diallyldimethylsilane (13.62 g, 97.0 mmol), trichlorosilane (39.5 g, 300 mmol) and hexachloroplatinic acid (15.0 mg, 0.029 mmol) in 150 ml of THF was stirred for 2 d at room temperature. Then the solvent was removed under reduced pressure. To the remaining viscous oil trimethyl orthoformate (200 ml, 1.92 mol) was added. After stirring for 4 d all volatile components were removed

under reduced pressure and distillation under vacuum afforded 9.98 g (27 %) of **4(T⁰)**, which was obtained as a colorless, airstable liquid sensitive to moisture, b.p. 110 °C (3 mbar).

¹H NMR (C₆D₆): δ = 3.53 (s, 18H, Si–OCH₃), 1.54 (m, 4H, Si–CH₂–CH₂–CH₂–Si), 0.74 (t, ³J(HH) = 7.85 Hz, 4H, (H₃C)₂Si–CH₂–CH₂–), 0.64 (m, 4H, (H₃CO)₃Si–CH₂–CH₂–), 0.00 (s, 6H, Si(CH₃)₂). ¹³C{¹H} NMR (C₆D₆): δ = 50.5 (Si–OCH₃), 20.0 ((H₃C)₂Si–CH₂–), 18.2 (Si–CH₂–CH₂–CH₂–Si), 14.6 ((H₃CO)₃Si–CH₂–), –3.0 (Si(CH₃)₂). ²⁹Si{¹H} NMR (C₆D₆): δ = 1.2 (Si(CH₃)₂), –42.4 (Si(OCH₃)₃). IR (KBr, cm^{–1}): 1248 s [ν(Si–CH₃)], 1192 s [ν(Si–CH₂–)], 1077 vs [ν(Si–OCH₃)]. MS (EI): *m/z* = 369 [M⁺ – CH₃], 307 [M⁺ – CH₃ – 2OCH₃], 221 [(H₃CO)₃Si(CH₂)₃Si(CH₃)₂⁺]. C₁₄H₃₆O₆Si₃: calcd C 43.71, H 9.43 %; found C 43.63, H 9.39 %.

Bis[3-(dimethoxymethylsilyl)propyl]diethylsilane [5(D⁰)]: A mixture of diallyldiethylsilane (7.69 g, 45.7 mmol), dichloromethylsilane (17.25 g, 150 mmol) and hexachloroplatinic acid (15.0 mg, 0.029 mmol) in 75 ml of THF was stirred for 2 d at room temperature. Then the solvent was removed under reduced pressure. To the remaining viscous oil trimethyl orthoformate (100 ml, 960 mmol) was added. After stirring for 4 d all volatile components were removed under reduced pressure and distillation under vacuum afforded 5.26 g (54 %) of **5(D⁰)**, which was obtained as a colorless, airstable liquid sensitive to moisture, b.p. 135 °C (4 mbar).

¹H NMR (C₆D₆): δ = 3.30 (s, 12H, Si–OCH₃), 1.49 (m, 4H, Si–CH₂–CH₂–CH₂–Si), 0.93 (t, ³J(HH) = 7.85 Hz, 6H, Si–CH₂–CH₃), 0.70 (t, ³J(HH) = 8.01 Hz, 4H, (H₅C₂)₂Si–CH₂–CH₂–), 0.61 (m, 4H, H₃C(H₃CO)₂Si–CH₂–CH₂–), 0.48 (q, ³J(HH) = 7.85 Hz, 4H, Si–CH₂–CH₃), 0.07 (s, 6H, Si(OCH₃)₂CH₃). ¹³C{¹H} NMR (C₆D₆): δ = 49.9 (Si–OCH₃), 18.5 ((H₅C₂)₂Si–CH₂–), 18.0 (Si–CH₂–CH₂–CH₂–Si), 16.5 (H₃C(H₃CO)₂Si–CH₂–), 7.8 (Si–CH₂–CH₃), 4.2 (Si–CH₂–CH₃), –5.3 (Si(OCH₃)₂CH₃). ²⁹Si{¹H} NMR (C₆D₆): δ = 4.5 (Si(CH₂–CH₃)₂), –2.6

(Si(OCH₃)₂CH₃). IR (KBr, cm⁻¹): 1258 s [ν(Si-CH₃)], 1190 s [ν(Si-CH₂-)], 1089 vs [ν(Si-OCH₃)]. MS (EI): m/z = 351 [M⁺ - C₂H₅], 305 [M⁺ - C₂H₅ - CH₃ - OCH₃], 233 [H₃C(H₃CO)₂Si(CH₂)₃Si(C₂H₅)₂⁺]. C₁₆H₄₀O₄Si₃: C 50.47, H 10.59 %; found C 50.40, H 10.50 %.

Bis[3-(trimethoxysilyl)propyl]diethylsilane [6(T⁰)]: A mixture of diallyldiethylsilane (9.68 g, 57.5 mmol), trichlorosilane (24.5 g, 190 mmol) and hexachloroplatinic acid (15.0 mg, 0.029 mmol) in 75 ml of THF was stirred for 2 d at room temperature. Then the solvent was removed under reduced pressure. To the remaining viscous oil trimethyl orthoformate (100 ml, 960 mmol) was added. After stirring for 4 d all volatile components were removed under reduced pressure and distillation under vacuum afforded 14.57 g (62 %) of **6(T⁰)**, which was obtained as a colorless, airstable liquid sensitive to moisture, b.p. 120 °C (3 mbar).

¹H NMR (C₆D₆): δ = 3.53 (s, 18H, Si-OCH₃), 1.49 (m, 4H, Si-CH₂-CH₂-CH₂-Si), 0.89 (t, ³J(HH) = 8.06 Hz, 6H, Si-CH₂-CH₃), 0.68 (t, ³J(HH) = 7.85 Hz, 4H, (H₅C₂)₂Si-CH₂-CH₂-), 0.57 (m, 4H, (H₃CO)₃Si-CH₂-CH₂-), 0.43 (q, ³J(HH) = 8.06 Hz, 4H, Si(CH₂-CH₃)₂). ¹³C{¹H} NMR (C₆D₆): δ = 50.2 (Si-OCH₃), 17.9 ((H₅C₂)₂Si-CH₂-), 16.2 (Si-CH₂-CH₂-CH₂-Si), 14.5 ((H₃CO)₃Si-CH₂-), 7.6 (Si-CH₂-CH₃), 4.0 (Si-CH₂-CH₃). ²⁹Si{¹H} NMR (C₆D₆): δ = 4.7 Si(CH₂-CH₃)₂, -42.3 (Si(OCH₃)₃). IR (KBr, cm⁻¹): 1192 s [ν(Si-CH₂-)], 1092 vs [ν(Si-OCH₃)]. MS (EI): m/z = 383 [M⁺ - C₂H₅], 337 [M⁺ - C₂H₅ - CH₃ - OCH₃], 249 [(H₃CO)₃Si(CH₂)₃Si(C₂H₅)₂⁺]. C₁₆H₄₀O₆Si₃: calcd C 46.56, H 9.77 %; found C 46.39, H 9.78 %.

3.2.2 Synthesis of the Xerogels **Ia** – **d**

General Procedure for Sol–Gel Processing

To a solution of 2–diphenylphosphinylmethyl–1–diphenylphosphinyl–8–trimethoxysilyloctan **1(T⁰)** in 7 ml of THF/MeOH (6:1) the corresponding amount of the co–condensation agent **D⁰–C₆–D⁰** or **Ph(1,4–C₃D⁰)₂**, H₂O, and 30 mg of the catalyst (*n*–Bu)₂Sn(OAc)₂ were added. This mixture was stirred for 48 h at room temperature until a gel was formed. Then the solvent was removed under reduced pressure and the obtained gels were dried for 1 h. The crude gels were washed three times with toluene (5 ml), Et₂O (5 ml), and *n*–pentane (10 ml). After aging was performed by drying for 8h in vacuo the xerogels **Ia** – **d** were obtained as colorless solids.

(2–Diphenylphosphinylmethyl–1–diphenylphosphinyl–8–polysiloxanyloctane)(Dⁱ–C₆–Dⁱ)_{2.5}

(Ia): 1(T⁰) (0.97 g, 1.57 mmol) and **D⁰–C₆–D⁰** (1.16 g, 3.93 mmol) were sol–gel processed with water (0.2 g, 11.1 mmol). After purification and aging a colorless gel was obtained. Yield: 1.48 g (88 %).

³¹P CP/MAS NMR: $\delta = -22.1$. ¹³C CP/MAS NMR: $\delta = 139.0, 133.0, 129.6$ (br, C–phenyl), 49.9 (SiOCH₃), 44.1 – 7.6 (CH₂ of matrix and spacer), –0.1 (O_{2/2}SiCH₃), –5.4 ((H₃CO)₂SiCH₃). ²⁹Si CP/MAS NMR: $\delta = -1.7$ (D⁰), –14.0 (D¹), –22.5 (D²), –58.8 (T²), –67.0 (T³). C₁₀₆H₁₆₄P₄Si₁₂O₁₃ (idealized stoichiometry): calcd C 59.91, H 7.73 %; corrected stoichiometry²²: C 61.21, H 7.77 %; found C 59.33, H 6.95 %⁷⁰.

(2–Diphenylphosphinylmethyl–1–diphenylphosphinyl–8–polysiloxanyloctane)(Dⁱ–C₆–Dⁱ)₅

(Ib): 1(T⁰) (0.83 g, 1.35 mmol) and **D⁰–C₆–D⁰** (1.98 g, 6.75 mmol) were sol–gel processed with water (0.4 g, 22.2 mmol). After purification and aging a colorless gel was obtained. Yield: 1.75 g (83 %).

^{31}P CP/MAS NMR: $\delta = -22.5$. ^{13}C CP/MAS NMR: $\delta = 139.5, 133.0, 128.3$ (br, C-phenyl), 49.6 (SiOCH_3), 41.7 – 8.6 (CH_2 of matrix and spacer), -0.2 ($\text{O}_{2/2}\text{SiCH}_3$), -5.6 ($(\text{H}_3\text{CO})_2\text{SiCH}_3$). ^{29}Si CP/MAS NMR: $\delta = -2.0$ (D^0), -12.2 (D^1), -22.5 (D^2), -58.9 (T^2), -67.6 (T^3). $\text{C}_{146}\text{H}_{254}\text{P}_4\text{Si}_{22}\text{O}_{23}$ (idealized stoichiometry): calcd C 56.23, H 8.21 %; corrected stoichiometry²²: C 55.94, H 8.23 %; found C 51.95, H 7.67 %⁷⁰.

(2-Diphenylphosphinylmethyl-1-diphenylphosphinyl-8-polysiloxanyloctane)[Ph(1,4- C_3D^i)₂]_{2.5} (Ic): $\mathbf{1}(\text{T}^0)$ (0.83 g, 1.35 mmol) and $\mathbf{Ph}(1,4-\text{C}_3\text{D}^0)_2$ (1.25 g, 3.38 mmol) were sol-gel processed with water (0.2 g, 11.1 mmol). After purification and aging a colorless gel was obtained. Yield: 1.43 g (85 %).

^{31}P CP/MAS NMR: $\delta = -22.6$. ^{13}C CP/MAS NMR: $\delta = 139.4, 128.6$ (br, C-phenyl), 49.8 (SiOCH_3), 44.4 – 8.2 (CH_2 of matrix and spacer), -0.1 ($\text{O}_{2/2}\text{SiCH}_3$), -5.2 ($(\text{H}_3\text{CO})_2\text{SiCH}_3$). ^{29}Si CP/MAS NMR: $\delta = -2.2$ (D^0), -11.8 (D^1), -22.2 (D^2), -58.1 (T^2), -67.7 (T^3). $\text{C}_{136}\text{H}_{184}\text{P}_4\text{Si}_{12}\text{O}_{13}$ (idealized stoichiometry): calcd C 65.66, H 7.45 %; corrected stoichiometry²²: C 67.84, H, 7.08 %; found C 65.20, H 6.89 %⁷⁰.

(2-Diphenylphosphinylmethyl-1-diphenylphosphinyl-8-polysiloxanyloctane)[Ph(1,4- C_3D^i)₂]₅ (Id): $\mathbf{1}(\text{T}^0)$ (0.83 g, 1.35 mmol) and $\mathbf{Ph}(1,4-\text{C}_3\text{D}^0)_2$ (2.5 g, 6.75 mmol) were sol gel processed with water (0.4 g, 22.2 mmol). After purification and aging a colorless gel was obtained. Yield: 1.69 g (87 %).

^{31}P CP/MAS NMR: $\delta = -22.5$. ^{13}C CP/MAS NMR: $\delta = 139.2, 128.8$ (br, C-phenyl), 49.7 (SiOCH_3), 45.1 – 6.2 (CH_2 of matrix and spacer), -0.5 (SiCH_3). ^{29}Si CP/MAS NMR: $\delta = -12.1$ (D^1), -21.8 (D^2), -58.0 (T^2), -67.1 (T^3). $\text{C}_{206}\text{H}_{294}\text{P}_4\text{Si}_{22}\text{O}_{23}$ (idealized stoichiometry): calcd C 63.76, H 7.64 %; corrected stoichiometry²²: C 63.60, H 7.65 %; found C 63.35, H 7.35 %.

3.2.3 Synthesis of the Xerogels **I_Ab** and **I_Ad**

{[1,3-Bis(diphenylphosphinyl)-2-(8-polysiloxanyloctyl)propane]dioxide}[(Dⁱ-C₆-Dⁱ)₅

(I_{Ab}): To a suspension of **Ib** (192 mg, 0.24 mmol) in 5 ml of *i*-propanol 0.5 ml (6.0 mmol) of an aqueous solution of H₂O₂ (35 %) was added. After stirring over night, the suspension was filtered (P3), washed with ethanol (5 ml), acetone (5 ml), ethyl acetate (5 ml), and petroleum ether (10 ml). After drying in vacuo for 6 h a colorless powder was obtained. Yield: 177 mg (~ 100 %).

³¹P CP/MAS NMR: δ = 30.5. ¹³C CP/MAS NMR: δ = 137.8, 123.4 (br, C-phenyl), 49.6 (SiOCH₃), 42.6 – 9.4 (CH₂ of matrix and spacer), -0.2 (O₂SiCH₃), -5.4 ((H₃CO)₂SiCH₃). ²⁹Si CP/MAS NMR: δ = -2.4 (D⁰), -12.4 (D¹), -22.6 (D²), -58.7 (T²), -66.8 (T³). IR (KBr, cm⁻¹): 1197 m (P=O). C₇₅₀H₁₃₁₅P₂₀Si₁₁₅O₁₄₀: calcd C 54.85, H 8.07 %; found C 50.33, H 8.33 % ⁷⁰.

{[1,3-Bis(diphenylphosphinyl)-2-(8-polysiloxanyloctyl)propane]dioxide}[Ph(1,4-C₃Dⁱ)₂]₅

(I_{Ad}): To a suspension of **Id** (181 mg, 0.18 mmol) in 5 ml of *i*-propanol 0.5 ml (6.0 mmol) of an aqueous solution of H₂O₂ (35 %) was added. After stirring over night, the suspension was filtered (P3), washed with ethanol (5 ml), acetone (5 ml), ethyl acetate (5 ml), and petroleum ether (10 ml). After drying in vacuo for 6 h a colorless powder was obtained. Yield: 179 mg (~ 100 %).

³¹P CP/MAS NMR: δ = 31.5. ¹³C CP/MAS NMR: δ = 139.4, 128.4 (br, C-phenyl), 49.9 (SiOCH₃), 46.2 – 11.4 (CH₂ of matrix and spacer), -0.1 (SiCH₃). ²⁹Si CP/MAS NMR: δ = -12.7 (D¹), -22.3 (D²), -58.4 (T²), -68.1 (T³). IR (KBr, cm⁻¹): 1185 m (P=O). C₁₀₇₉H₁₅₄₇P₂₀Si₁₁₇O₁₄₂: calcd C 62.62, H 7.53 %; found C 61.18, H 7.54 % ⁷⁰.

3.2.4 Synthesis of the Xerogels **I_{Bb}** and **I_{Bd}**

{[1,3-Bis(diphenylphosphinyl)-2-(8-polysiloxanyloctyl)propane]disulphide} (*Dⁱ-C₆-Dⁱ*)₅

(I_{Bb}): A suspension of **Ib** (280 mg, 0.35 mmol) and of S₈ (26 mg, 0.81 mmol) in 10 ml of toluene was stirred at 80°C for 8 h. After removing toluene in vacuo the crude product was washed three times with CS₂ (5 ml), ethyl acetate (5 ml), finally *n*-pentane (10 ml). After drying in vacuo for 3 h a colorless powder was obtained. Yield: 260 mg (~ 100 %).

³¹P CP/MAS NMR: δ = 38.5. ¹³C CP/MAS NMR: δ = 142.0 – 120.6 (C-phenyl), 49.8 (SiOCH₃), 44.5 – 8.9 (CH₂ of matrix and spacer), -0.1 (O_{2/2}SiCH₃), -5.4 ((H₃CO)₂SiCH₃). ²⁹Si CP/MAS NMR: δ = -2.1 (D⁰), -12.3 (D¹), -22.5 (D²), -57.7 (T²), -67.6 (T³). IR (KBr, cm⁻¹): 626 w (P=S). C₇₅₀H₁₃₁₅P₂₀S₂₀Si₁₁₅O₁₂₀: calcd C 53.80, H 7.92, S 3.83 %; found C 50.37, H 8.15, S 3.81 % ⁷⁰.

{[1,3-Bis(diphenylphosphinyl)-2-(8-polysiloxanyloctyl)propane]disulphide} [*Ph(1,4-*

C₃Dⁱ)₂]₅ **(I_{Bd})**: A suspension of **Id** (210 mg, 0.21 mmol) and of S₈ (18 mg, 0.56 mmol) in 10 ml of toluene was stirred at 80°C for 8 h. After removing toluene in vacuo the crude product was washed three times with CS₂ (5 ml), ethyl acetate (5 ml), finally *n*-pentane (10 ml). After drying in vacuo for 3 h a colorless powder was obtained. Yield: 212 mg (~ 100 %).

³¹P CP/MAS NMR: δ = 38.5. ¹³C CP/MAS NMR: δ = 139.4, 128.5 (br, C-phenyl), 49.7 (SiOCH₃), 46.4 – 7.6 (CH₂ of matrix and spacer), -0.2 (SiCH₃). ²⁹Si CP/MAS NMR: δ = -12.3 (D¹), -22.0 (D²), -57.7 (T²), -67.6 (T³). IR (KBr, cm⁻¹): 624 w (P=S). C₁₀₇₉H₁₅₄₇P₂₀S₂₀Si₁₁₇O₁₂₂: calcd C 61.66, H 7.42, S 3.05 %; found C 59.88, H 7.34, S 4.50 % ⁷⁰.

3.2.5 Synthesis of the Xerogels **I_{Cb}** and **I_{Cd}**

[[1,3-Bis(diphenylmethylphosphonium)-2-(8-polysiloxanyloctyl)propane]diiodide](Dⁱ-C₆-Dⁱ)₅ (I_{Cb}**):** To a suspension of **Ib** (190 mg, 0.24 mmol) in 5 ml of CH₂Cl₂ 0.05 ml (0.80 mmol) of methyl iodide was added. After stirring at room temperature for 8 h the solvent was removed in vacuo and the crude product was washed three times with *n*-pentane (10 ml). After drying in vacuo for 3 h a colorless powder was obtained. Yield: 226 mg (~ 100 %).

³¹P CP/MAS NMR: δ = 22.4. ¹³C CP/MAS NMR: δ = 133.3, 130.6 (br, C-phenyl), 122.5 (*ipso*-C), 49.8 (SiOCH₃), 46.1 – 7.6 (CH₂ of matrix and spacer, PCH₃), -0.1 (O_{2/2}SiCH₃), -5.5 ((H₃CO)₂SiCH₃). ²⁹Si CP/MAS NMR: δ = -2.3 (D⁰), -12.5 (D¹), -22.6 (D²), -58.8 (T²), -67.0 (T³). C₇₇₀H₁₃₇₅I₂₀P₂₀Si₁₁₅O₁₂₀: calcd C 48.83, H 7.32, I 13.40 %; found C 45.91, H 7.84, I 9.05 % ⁷⁰.

[[1,3-Bis(diphenylmethylphosphonium)-2-(8-polysiloxanyloctyl)propane]diiodide]

[Ph(1,4-C₃Dⁱ)₂]₅ (I_{Cd}**):** To a suspension of **Id** (220 mg, 0.22 mmol) in 5 ml of CH₂Cl₂ 0.05 ml (0.80 mmol) of methyl iodide was added. After stirring at room temperature for 8 h the solvent was removed in vacuo and the crude product was washed three times with *n*-pentane (10 ml). After drying in vacuo for 3 h a colorless powder was obtained. Yield: 244 mg (~ 100 %).

³¹P CP/MAS NMR: δ = 21.9. ¹³C CP/MAS NMR: δ = 139.4, 128.4 (br, C-phenyl), 121.9 (*ipso*-C), 49.7 (SiOCH₃), 45.1 – 6.2 (CH₂ of matrix and spacer, PCH₃), -0.3 (SiCH₃). ²⁹Si CP/MAS NMR: δ = -12.5 (D¹), -22.4 (D²), -59.1 (T²), -68.0 (T³). C₁₀₉₉H₁₆₀₇I₂₀P₂₀Si₁₁₇O₁₂₂: calcd C 56.86, H 6.98, I 10.93 %; found C 53.57, H 6.27, I 9.06 % ⁷⁰.

3.2.6 Synthesis of the Xerogels I_{Db} and I_{Dd}

[(2-Diphenylphosphinylmethyl-1-diphenylphosphinyl-8-polysiloxanyloctane)molybdenumtetracarbonyl](Dⁱ-C₆-Dⁱ)₅ (I_{Db}): To a suspension of **Ib** (172 mg, 0.21 mmol) in 5 ml of CH₂Cl₂ a solution of (NBD)Mo(CO)₄ (60 mg, 0.20 mmol) in 5 ml of CH₂Cl₂ was added. After stirring at room temperature for 8 h the solvent was removed in vacuo and the crude product was washed three times with toluene (5 ml) and *n*-pentane (10 ml). After drying in vacuo for 3 h a slight yellow powder was obtained. Yield: 190 mg (~ 100 %).

³¹P CP/MAS NMR: $\delta = 24.6$. ¹³C CP/MAS NMR: $\delta = 215.4, 212.7$ (CO), 144.7 – 122.9 (C-phenyl), 49.7 (SiOCH₃), 45.4 – 7.9 (CH₂ of matrix and spacer), -0.1 (O_{2/2}SiCH₃), -5.5 ((H₃CO)₂SiCH₃). ²⁹Si CP/MAS NMR: $\delta = -2.3$ (D⁰), -12.2 (D¹), -22.5 (D²), -58.8 (T²), -66.7 (T³). IR (KBr, cm⁻¹) 2018 s, 1927 s, 1897 vs (CO). C₇₉₀H₁₃₁₅Mo₁₀P₂₀Si₁₁₅O₁₆₀: calcd C 52.19, H 7.29 %; found C 46.41, H 7.38 % ⁷⁰.

[(2-Diphenylphosphinylmethyl-1-diphenylphosphinyl-8-polysiloxanyloctane)molybdenumtetracarbonyl][Ph(1,4-C₃Dⁱ)₂]₅ (I_{Dd}): To a suspension of **Id** (184 mg, 0.18 mmol) in 5 ml of CH₂Cl₂ a solution of (NBD)Mo(CO)₄ (60 mg, 0.20 mmol) in 5 ml of CH₂Cl₂ was added. After stirring at room temperature for 8 h the solvent was removed in vacuo and the crude product was washed three times with toluene (5 ml) and *n*-pentane (10 ml). After drying in vacuo for 3 h a slight yellow powder was obtained. Yield: 191 mg (~ 100 %).

³¹P CP/MAS NMR: $\delta = 24.6$. ¹³C CP/MAS NMR: $\delta = 215.2, 211.7$ (CO), 139.6, 128.5 (br, C-phenyl), 49.7 (SiOCH₃), 45.8 – 8.2 (CH₂ of matrix and spacer), -0.4 (SiCH₃). ²⁹Si CP/MAS NMR: $\delta = -12.5$ (D¹), -21.7 (D²), -58.2 (T²), -66.6 (T³). IR (KBr, cm⁻¹) 2017 s, 1925 s, 1893 vs (CO). C₁₁₁₉H₁₅₄₇Mo₁₀P₂₀Si₁₁₇O₁₆₂: calcd C 59.85, H 6.94 %; found C 59.04, H 6.03 % ⁷⁰.

3.2.7 Synthesis of the Xerogels **I_Eb** and **I_Ed**

[Dichloro(2-diphenylphosphinylmethyl-1-diphenylphosphinyl-8-polysiloxanyloctane)-palladium(II)](Dⁱ-C₆-Dⁱ)₅ (I_Eb**):** To a suspension of **Ib** (172 mg, 0.21 mmol) in 5 ml of CH₂Cl₂ a solution of (COD)PdCl₂ (58 mg, 0.20 mmol) in 5 ml of CH₂Cl₂ was added. After stirring at room temperature for 8 h the solvent was removed in vacuo and the crude product was washed three times with acetone (5 ml), toluene (5ml), and *n*-pentane (10 ml). After drying in vacuo for 3 h a yellow powder was obtained. Yield: 178 mg (~ 100 %).

³¹P CP/MAS NMR: δ = 16.6. ¹³C CP/MAS NMR: δ = 142.7 – 122.5 (C-phenyl), 49.8 (SiOCH₃), 42.1 – 8.6 (CH₂ of matrix and spacer), -0.1 (O_{2/2}SiCH₃), -5.5 ((H₃CO)₂SiCH₃). ²⁹Si CP/MAS NMR: δ = -2.4 (D⁰), -12.3 (D¹), -22.6 (D²), -58.4 (T²), -67.4 (T³). C₇₅₀H₁₃₁₅Cl₂₀P₂₀Pd₁₀Si₁₁₅O₁₂₀: calcd C 50.93, H 7.41, Cl 3.97 %; found C 49.35, H 8.04, Cl 3.35 % ⁷⁰.

[Dichloro(2-diphenylphosphinylmethyl-1-diphenylphosphinyl-8-polysiloxanyloctane)-palladium(II)][Ph(1,4-C₃Dⁱ)₂]₅ (I_Ed**):** To a suspension of **Id** (179 mg, 0.17 mmol) in 5 ml of CH₂Cl₂ a solution of (COD)PdCl₂ (50 mg, 0.18 mmol) in 5 ml of CH₂Cl₂ was added. After stirring at room temperature for 8 h the solvent was removed in vacuo and the crude product was washed three times with acetone (5 ml), toluene (5ml), and *n*-pentane (10 ml). After drying in vacuo for 3 h a yellow powder was obtained. Yield: 166 mg (~ 100 %).

³¹P CP/MAS NMR: δ = 17.4. ¹³C CP/MAS NMR: δ = 139.6, 128.5 (br, C-phenyl), 49.6 (SiOCH₃), 45.1 – 9.9 (CH₂ of matrix and spacer), -0.3 (SiCH₃). ²⁹Si CP/MAS NMR: δ = -9.5 (D¹), -21.9 (D²), -58.7 (T²), -66.4 (T³). C₁₀₇₉H₁₅₄₇Cl₂₀P₂₀Pd₁₀Si₁₁₇O₁₂₂: calcd C 58.51, H 7.04, Cl 3.20 %; found C 57.32, H 7.98, Cl 3.31 % ⁷⁰.

3.2.8 Synthesis of the Xerogels IIa – i

General Procedure for Sol–Gel Processing

To a solution of $2(\mathbf{T}^0)$ in 10 ml of THF the corresponding amount of the co-condensing agent $\mathbf{D}^0\text{-C}_6\text{-D}^0$ or $\mathbf{Ph}(1,4\text{-C}_3\mathbf{D}^0)_2$, 500 mg (28 mmol) of H_2O and the catalyst $(n\text{-Bu})_2\text{Sn}(\text{OAc})_2$ (30 mg, 0.087 mmol) was added. The reaction mixture was stirred at room temperature for 24 h until a gel was formed. Then the solvent was removed under reduced pressure and the crude product was dried for 2 h. After washing three times with toluene (5 ml), diethyl ether (5 ml), and *n*-pentane (10 ml) and drying in vacuum overnight the xerogels **IIa – i** were obtained as yellow powders.

$\eta^4\text{-1,5-Cyclooctadiene[2-diphenylphosphinylmethyl-1-diphenylphosphinyl-8-polysiloxanyloctanerhodium(I)]hexafluoroantimonate(V)$ (IIa): Initial weight of $2(\mathbf{T}^0)$ 513 mg (0.48 mmol). Yield: 467 mg (97.8 %).

^{31}P CP/MAS NMR: $\delta = 15.3$. ^{13}C CP/MAS NMR: $\delta = 144.4 - 121.1$ (br, C-phenyl), 103.8, 98.0 [br, C-olefin (COD)], 40.2, 31.1, 28.8, 23.7, 12.0 (br, CH_2 , CH). ^{29}Si CP/MAS NMR: $\delta = -57.7$ (T^2), -64.8 (T^3). $\text{C}_{82}\text{H}_{98}\text{F}_{12}\text{O}_3\text{P}_4\text{Rh}_2\text{Sb}_2\text{Si}_2$ (idealized stoichiometry): calcd C 49.52, H 4.97 %; corrected stoichiometry²²: C 49.47, H 5.06 %; found C 42.87, H 3.07 %⁷⁰.

$\{\eta^4\text{-1,5-Cyclooctadiene[2-diphenylphosphinylmethyl-1-diphenylphosphinyl-8-polysiloxanyloctanerhodium(I)]hexafluoroantimonate(V)}(\mathbf{D}^i\text{-C}_6\text{-D}^i)_{2.5}$ (IIb): Initial weight of $2(\mathbf{T}^0)$ 500 mg (0.47 mmol) and of $\mathbf{D}^0\text{-C}_6\text{-D}^0$ 345 mg (1.18 mmol). Yield: 730 mg (93.5 %).

^{31}P CP/MAS NMR: $\delta = 13.9$. ^{13}C CP/MAS NMR: $\delta = 145.4 - 120.1$ (br, C-phenyl), 103.7, 97.9 [br, C-olefin (COD)], 42.7 – 10.5 (br, CH_2 , CH of backbone and spacer), -0.2 (Si- CH_3). ^{29}Si CP/MAS NMR: $\delta = -9.8$ (D^1), -20.8 (D^2), -57.1 (T^2), -65.4 (T^3).

$C_{122}H_{188}F_{12}O_{13}P_4Rh_2Sb_2Si_{12}$ (idealized stoichiometry): calcd C 48.83, H 6.31 %; corrected stoichiometry²²: C 47.87, H 6.61 %; found C 42.21, H 5.13 %⁷⁰.

**{ η^4 -1,5-Cyclooctadiene[2-diphenylphosphinylmethyl-1-diphenylphosphinyl-8-polysilox-
anyloctanerhodium(I)]hexafluoroantimonate(V)}(Dⁱ-C₆-Dⁱ)₅ (IIc)**: Initial weight of **2(T⁰)**
315 mg (0.38 mmol) and of **D⁰-C₆-D⁰** 559 mg (1.90 mmol). Yield: 705 mg (97.4 %).

³¹P CP/MAS NMR: $\delta = 14.1$. ¹³C CP/MAS NMR: $\delta = 145.0 - 120.3$ (br, C-phenyl), 104.2, 98.1 [br, C-olefin (COD)], 49.5 (OCH₃), 44.1 – 7.3 (br, CH₂, CH of backbone and spacer), – 0.4 (Si-CH₃). ²⁹Si CP/MAS NMR: $\delta = -11.5$ (D¹), –22.2 (D²), –59.0 (T²), –67.9 (T³).

$C_{162}H_{278}F_{12}O_{23}P_4Rh_2Sb_2Si_{22}$ (idealized stoichiometry): calcd C 48.49, H 6.98 %; corrected stoichiometry²²: C 48.54, H 6.88 %; found C 45.44, H 6.70 %⁷⁰.

**{ η^4 -1,5-Cyclooctadiene[2-diphenylphosphinylmethyl-1-diphenylphosphinyl-8-polysilox-
anyloctanerhodium(I)]hexafluoroantimonate(V)}(Dⁱ-C₆-Dⁱ)₁₀ (II d)**: Initial weight of **2(T⁰)**
185 mg (0.17 mmol) and of **D⁰-C₆-D⁰** 510 mg (1.74 mmol). Yield: 466 mg (98.8 %).

³¹P CP/MAS NMR: $\delta = 14.1$. ¹³C CP/MAS NMR: $\delta = 140.2 - 116.1$ (br, C-phenyl), 106.8 – 90.7 [br, C-olefin (COD)], 49.8 (OCH₃), 44.7 – 7.9 (br, CH₂, CH of backbone and spacer), –0.2 (Si-CH₃). ²⁹Si CP/MAS NMR: $\delta = -12.4$ (D¹), –22.2 (D²), –59.0 (T²), –68.0 (T³).

$C_{242}H_{458}F_{12}O_{43}P_4Rh_2Sb_2Si_{42}$ (idealized stoichiometry): calcd C 48.15, H 7.65 %; corrected stoichiometry²²: C 46.93, H 7.57 %; found C 46.04, H 7.38 %⁷⁰.

**{ η^4 -1,5-Cyclooctadiene[2-diphenylphosphinylmethyl-1-diphenylphosphinyl-8-polysilox-
anyloctanerhodium(I)]hexafluoroantimonate(V)}(Dⁱ-C₆-Dⁱ)₂₀ (II e)**: Initial weight of **2(T⁰)**
205 mg (0.19 mmol) and of **D⁰-C₆-D⁰** 1130 mg (3.86 mmol). Yield: 1080 mg (97.8 %).

^{31}P CP/MAS NMR: $\delta = 14.2$. ^{13}C CP/MAS NMR: $\delta = 145.3 - 120.8$ (br, C-phenyl), $110.5 - 91.4$ [br, C-olefin (COD)], 49.8 (OCH₃), $44.4 - 8.2$ (br, CH₂, CH of backbone and spacer), -0.2 (Si-CH₃). ^{29}Si CP/MAS NMR: $\delta = -11.5$ (D¹), -20.6 (D²), -56.6 (T²), -64.2 (T³). C₄₀₂H₈₁₈F₁₂O₈₃P₄Rh₂Sb₂Si₈₂ (idealized stoichiometry): calcd C 47.88, H 8.18 %, corrected stoichiometry²²: C 46.08, H 8.36 %; found C 46.63, H 7.56 %.

{ η^4 -1,5-Cyclooctadiene[2-diphenylphosphinylmethyl-1-diphenylphosphinyl-8-polysiloxanyloctanerhodium(I)]hexafluoroantimonate(V)}[Ph(1,4-C₃Dⁱ)₂]_{2.5} (II_f): Initial weight of **2(T⁰)** 500 mg (0.47 mmol) and of **Ph(1,4-C₃D⁰)₂** 437 mg (1.18 mmol). Yield: 665 mg (91.5 %).

^{31}P CP/MAS NMR: $\delta = 14.3$. ^{13}C CP/MAS NMR: $\delta = 148.6 - 115.1$ (br, C-phenyl), $103.4 - 98.5$ [br, C-olefin (COD)], $47.1 - 9.5$ (br, CH₂, CH of backbone and spacer), -0.2 (Si-CH₃). ^{29}Si CP/MAS NMR: $\delta = -9.6$ (D¹), -20.5 (D²), -55.5 (T²), -65.5 (T³). C₁₅₂H₂₀₈F₁₂O₁₃P₄Rh₂Sb₂Si₁₂ (idealized stoichiometry): calcd C 53.99, H 6.20 %; corrected stoichiometry²²: C 53.04, H 6.05 %; found C 53.35, H 9.23 %.

{ η^4 -1,5-Cyclooctadiene[2-diphenylphosphinylmethyl-1-diphenylphosphinyl-8-polysiloxanyloctanerhodium(I)]hexafluoroantimonate(V)}[Ph(1,4-C₃Dⁱ)₂]₅ (II_g): Initial weight of **2(T⁰)** 315 mg (0.38 mmol) and of **Ph(1,4-C₃D⁰)₂** 704 mg (1.9 mmol). Yield: 764 mg (94.7 %).

^{31}P CP/MAS NMR: $\delta = 14.0$. ^{13}C CP/MAS NMR: $\delta = 144.4 - 122.6$ (br, C-phenyl), $102.5 - 95.4$ [br, C-olefin (COD)], 49.8 (OCH₃), $44.1 - 7.3$ (br, CH₂, CH of backbone and spacer), -0.1 (Si-CH₃). ^{29}Si CP/MAS NMR: $\delta = -12.5$ (D¹), -21.7 (D²), -54.7 (T²), -67.0 (T³). C₂₂₂H₃₁₈F₁₂O₂₃P₄Rh₂Sb₂Si₂₂ (idealized stoichiometry): calcd C 55.85, H 6.71 %; corrected stoichiometry²²: C 54.49, H 6.69 %; found C 52.40, H 6.08 %⁷⁰.

*{η⁴-1,5-Cyclooctadiene[2-diphenylphosphinylmethyl-1-diphenylphosphinyl-8-polysilox-
anyloctanerrhodium(I)]hexafluoroantimonate(V)}[Ph(1,4-C₃Dⁱ)₂]₁₀ (IIIh)*: Initial weight of **2(T⁰)** 185 mg (0.17 mmol) and of **Ph(1,4-C₃D⁰)₂** 644 mg (1.7 mmol). Yield: 496 mg (94.2 %).

³¹P CP/MAS NMR: δ = 10.9. ¹³C CP/MAS NMR: δ = 149.3 – 115.8 (br, C-phenyl), 108.4 – 97.3 [br, C-olefin (COD)], 48.4 – 8.2 (br, CH₂, CH of backbone and spacer), –0.1 (Si-CH₃). ²⁹Si CP/MAS NMR: δ = –12.8 (D¹), –22.5 (D²), –67.7 (T³). C₃₆₂H₅₃₈F₁₂O₄₃P₄Rh₂Sb₂Si₄₂ (idealized stoichiometry): calcd C 57.52, H 7.17 %; corrected stoichiometry ²²: C 56.89, H 7.00 %; found C 57.90, H 7.02 %.

*{η⁴-1,5-Cyclooctadiene[2-diphenylphosphinylmethyl-1-diphenylphosphinyl-8-polysilox-
anyloctanerrhodium(I)]hexafluoroantimonate(V)}[Ph(1,4-C₃Dⁱ)₂]₂₀ (IIIi)*: Initial weight of **2(T⁰)** 205 mg (0.19 mmol) and of **Ph(1,4-C₃D⁰)₂** 1430 mg (3.86 mmol). Yield: 1420 mg (89.2 %).

³¹P CP/MAS NMR: δ = 14.3. ¹³C CP/MAS NMR: δ = 148.3 – 117.9 (br, C-phenyl), 108.3 – 92.4 [br, C-olefin (COD)], 46.5 – 8.9 (br, CH₂, CH of backbone and spacer), –0.1 (Si-CH₃). ²⁹Si CP/MAS NMR: δ = –11.8 (D¹), –21.1 (D²), –54.7 (T²), –65.8 (T³). C₆₄₂H₉₇₈F₁₂O₈₃P₄Rh₂Sb₂Si₈₂ (idealized stoichiometry): calcd C 58.73, H 7.51 %; corrected stoichiometry ²²: C 59.09, H 7.61 %; found C 58.74, H 6.07 %.

3.2.9 Synthesis of the Xerogels IIIa, b, IVa, b, Va, b, and VIa, b

General Procedure for Sol–Gel Processing

To a solution of the monomeric precursors in 4 ml of THF/MeOH (3:1) water and the catalyst (*n*-Bu)₂Sn(OAc)₂ was added. This mixture was stirred for 12 h at room temperature until a gel was formed. Then the solvent was removed under reduced pressure and the obtained gels were dried for 1h. The crude gels were washed three times with toluene (5 ml), Et₂O (5 ml) and *n*-pentane (10 ml). After aging by drying for 8h in a vacuum the gels were obtained as rubber-like colorless solids.

Bis[3-(polymethylsiloxanyl)propyl]dimethylsilane (IIIa): A mixture of **3(D⁰)** (1.51 g, 4.3 mmol), water (440 mg, 24.6 mmol) and (*n*-Bu)₂Sn(OAc)₂ (30 mg, 0.087 mmol) in 4 ml of THF/MeOH (3:1) was sol–gel processed to give a colorless swollen gel. After purification and aging 1.11 g (95.4 %) of a colorless powder were formed.

¹³C CP/MAS NMR: δ = 49.7 (Si–OCH₃), 26.1 – 14.3 (Si–CH₂–CH₂–CH₂–Si), 0.1 (O_{2/2}Si–CH₃), –2.8 (Si(CH₃)₂). ²⁹Si CP/MAS NMR: δ = 1.5 (Si(CH₃)₂), –11.6 (D¹), –22.0 (D²). C₁₀H₂₄O₂Si₃ (idealized stoichiometry): calcd C 46.10, H 9.28 %; corrected stoichiometry ²²: C 44.39, H 9.69 %; found C 44.46, H 9.54 %.

Bis[3-(polysiloxanyl)propyl]dimethylsilane (IVa): A mixture of **4(T⁰)** (1.38 g, 3.6 mmol), water (440 mg, 24.6 mmol) and (*n*-Bu)₂Sn(OAc)₂ (30 mg, 0.087 mmol) in 4 ml of THF/MeOH (3:1) was sol–gel processed to give a colorless swollen gel. After purification and aging 0.95 g (91.8 %) of a colorless powder were formed.

¹³C CP/MAS NMR: δ = 49.8 (Si–OCH₃), 19.4 – 15.5 (Si–CH₂–CH₂–CH₂–Si), –3.3 (Si(CH₃)₂). ²⁹Si CP/MAS NMR: δ = 1.6 (Si(CH₃)₂), –42.3 (T⁰), –50.5 (T¹), –59.4 (T²),

-68.8 (T³) . C₈H₁₈O₃Si₃ (idealized stoichiometry): calcd C 38.98, H 7.36 %, corrected stoichiometry²²: C 37.60, H 8.06 %; found C 37.55, H 8.35 %.

Bis[3-(polymethylsiloxanyl)propyl]diethylsilane (Va): A mixture of **5(D⁰)** (1.35 g, 3.6 mmol), water (440 mg, 24.6 mmol) and (*n*-Bu)₂Sn(OAc)₂ (30 mg, 0.087 mmol) in 4 ml of THF/MeOH (3:1) was sol-gel processed to give a colorless swollen gel. After purification and aging 1.01 g (94.3 %) of a colorless powder were formed.

¹³C CP/MAS NMR: δ = 49.6 (Si-OCH₃), 20.2 – 14.3 (Si-CH₂-CH₂-CH₂-Si), 7.6 (Si-CH₂-CH₃), 4.0 (Si-CH₂-CH₃), -0.1 (O₂/Si-CH₃). ²⁹Si CP/MAS NMR: δ = 4.8 (Si(C₂H₅)₂), -2.5 (D⁰), -12.6 (D¹), -23.1 (D²). C₁₂H₂₈O₂Si₃ (idealized stoichiometry): calcd C 49.94, H 9.78 %; corrected stoichiometry²²: C 48.43, H 9.82 %; found C 48.63, H 9.48 %.

Bis[3-(polysiloxanyl)propyl]diethylsilane (VIa): A mixture of **6(T⁰)** (1.42 g, 3.5 mmol), water (440 mg, 24.6 mmol) and (*n*-Bu)₂Sn(OAc)₂ (30 mg, 0.087 mmol) in 4 ml of THF/MeOH (3:1) was sol-gel processed to give a colorless swollen gel. After purification and aging 1.07 g (96.9 %) of a colorless powder were formed.

¹³C CP/MAS NMR: δ = 49.7 (Si-OCH₃), 21.3 – 14.0 (Si-CH₂-CH₂-CH₂-Si), 7.4 (Si-CH₂-CH₃), 4.0 (Si-CH₂-CH₃). ²⁹Si CP/MAS NMR: δ = 4.9 (Si(C₂H₅)₂), -42.4 (T⁰), -50.7 (T¹), -59.6 (T²), -68.8 (T³). C₁₀H₂₂O₃Si₃ (idealized stoichiometry): calcd C 43.75, H 8.08 %; corrected stoichiometry²²: C 41.87, H 8.62 %; found C 43.48, H 8.67 %.

Bis[3-(polymethylsiloxanyl)propyl]dimethylsilane[Ph(Tⁿ)] (IIIb): A mixture of **3(D⁰)** (0.87 g, 2.5 mmol), phenyltrimethoxysilane (0.49 g, 2.5 mmol), water (440 mg, 24.6 mmol) and (*n*-Bu)₂Sn(OAc)₂ (30 mg, 0.087 mmol) in 4 ml of THF/MeOH (3:1) was sol-gel processed to give a colorless swollen gel. After purification and aging 0.96 g (96.9 %) of a colorless powder were formed.

^{13}C CP/MAS NMR: $\delta = 134.3 - 127.7$ (C_6H_5), 49.6 (Si-OCH_3), 26.1 - 14.3 ($\text{Si-CH}_2\text{-CH}_2\text{-CH}_2\text{-Si}$), -0.3 ($\text{O}_{2/2}\text{Si-CH}_3$), -3.1 ($\text{Si}(\text{CH}_3)_2$). ^{29}Si CP/MAS NMR: $\delta = 1.3$ ($\text{Si}(\text{CH}_3)_2$), -2.0 (D^0), -12.5 (D^1), -21.6 (D^2), -62.8 (T^1_{Ph}), -71.4 (T^2_{Ph}), -80.3 (T^3_{Ph}). $\text{C}_{32}\text{H}_{58}\text{O}_7\text{Si}_8$ (idealized stoichiometry): calcd C 49.31, H 7.50 %; corrected stoichiometry ²²: C 47.81, H 7.93 %; found C 48.18, H 7.97 %.

Bis[3-(polysiloxanyl)propyl]dimethylsilane[Ph(T^n)] (IVb): A mixture of **4(T^0)** (0.92 g, 2.4 mmol), phenyltrimethoxysilane (0.47 g, 2.4 mmol), water (440 mg, 24.6 mmol) and (*n*-Bu)₂Sn(OAc)₂ (30 mg, 0.087 mmol) in 4 ml of THF/MeOH (3:1) was sol-gel processed to give a colorless swollen gel. After purification and aging 0.91 g (90.3 %) of a colorless powder were formed.

^{13}C CP/MAS NMR: $\delta = 134.4 - 127.8$ (C_6H_5), 49.8 (Si-OCH_3), 26.0 - 14.0 ($\text{Si-CH}_2\text{-CH}_2\text{-CH}_2\text{-Si}$), -3.4 ($\text{Si}(\text{CH}_3)_2$). ^{29}Si CP/MAS NMR: $\delta = 1.3$ ($\text{Si}(\text{CH}_3)_2$), -42.3 (T^0), -50.6 (T^1), -59.2 (T^2), -62.9 (T^1_{Ph}), -68.1 (T^3), -71.6 (T^2_{Ph}), -79.8 (T^3_{Ph}). $\text{C}_{32}\text{H}_{58}\text{O}_7\text{Si}_8$ (idealized stoichiometry): calcd C 44.76, H 6.17 %; corrected stoichiometry ²²: C 42.14, H 6.75 %; found C 43.09, H 7.04 %.

Bis[3-(polymethylsiloxanyl)propyl]diethylsilane[Ph(T^n)] (Vb): A mixture of **5(D^0)** (0.85 g, 2.2 mmol), phenyltrimethoxysilane (0.44 g, 2.2 mmol), water (440 mg, 24.6 mmol) and (*n*-Bu)₂Sn(OAc)₂ (30 mg, 0.087 mmol) in 4 ml of THF/MeOH (3:1) was sol-gel processed to give a colorless swollen gel. After purification and aging 0.94 g (99.3 %) of a colorless powder were formed.

^{13}C CP/MAS NMR: $\delta = 134.2 - 127.8$ (C_6H_5), 49.7 (Si-OCH_3), 26.0 - 14.3 ($\text{Si-CH}_2\text{-CH}_2\text{-CH}_2\text{-Si}$), 7.6 ($\text{Si-CH}_2\text{-CH}_3$), 4.0 ($\text{Si-CH}_2\text{-CH}_3$), -0.3 ($\text{O}_{2/2}\text{Si-CH}_3$), ^{29}Si CP/MAS NMR: $\delta = 4.7$ ($\text{Si}(\text{C}_2\text{H}_5)_2$), -2.1 (D^0), -12.6 (D^1), -22.1 (D^2), -71.1 (T^2_{Ph}), -79.6 (T^3_{Ph}). $\text{C}_{36}\text{H}_{66}\text{O}_7\text{Si}_8$

(idealized stoichiometry): calcd C 51.75, H 7.96 %; corrected stoichiometry ²²: C 50.42, H 8.46 %; found C 50.35, H 8.04 %.

Bis[3-(polysiloxanyl)propyl]diethylsilane[Ph(Tⁿ)] (VIb): A mixture of **6(T⁰)** (0.93 g, 2.2 mmol), phenyltrimethoxysilane (0.47 g, 2.2 mmol), water (440 mg, 24.6 mmol) and (*n*-Bu)₂Sn(OAc)₂ (30 mg, 0.087 mmol) in 4 ml of THF/MeOH (3:1) was sol-gel processed to give a colorless swollen gel. After purification and aging 0.98 g (99.8 %) of a colorless powder were formed.

¹³C CP/MAS NMR: δ = 134.3 – 127.7 (C₆H₅), 49.8 (Si-OCH₃), 26.2 – 13.3 (Si-CH₂-CH₂-CH₂-Si), 7.4 (Si-CH₂-CH₃), 3.9 (Si-CH₂-CH₃). ²⁹Si CP/MAS NMR: δ = 4.8 (Si(C₂H₅)₂), -42.4 (T⁰), -50.5 (T¹), -59.0 (T²), -62.8 (T¹_{Ph}), -67.9 (T³), -71.4 (T²_{Ph}), -79.5 (T³_{Ph}).
C₃₂H₅₄O₉Si₈ (idealized stoichiometry): calcd C 47.60, H 6.74 %; corrected stoichiometry ²²: C 46.01, H 7.21 %; found C 46.55, H 7.47 %.

4. References

- ¹ F. R. Hartley, *Supported Metal Complexes*, D. Reidel Publishing Company, Dordrecht, 1985.
- ² E. Lindner, F. Auer, T. Schneller and H. A. Mayer, *Angew. Chem. Int. Ed.*, 1999, **38**, 2154.
- ³ U. Schubert, *New J. Chem.*, 1994, **18**, 1049.
- ⁴ I. S. Khatib, R. V. Parish, *J. Organomet. Chem.*, 1989, **369**, 9.
- ⁵ E. Lindner, M. Kemmler, T. Schneller, H. A. Mayer, *Inorg. Chem.*, 1995, **34**, 5489.
- ⁶ E. Lindner, T. Schneller, F. Auer, P. Wegner, H. A. Mayer, *Chem. Eur. J.*, 1997, **3**, 1833.
- ⁷ E. Lindner, F. Auer, A. Baumann, P. Wegner, H. A. Mayer, H. Bertagnolli, U. Reinöhl, T. S. Ertel, A. Weber, *J. Mol. Catal. A*, 2000, **157**, 97.
- ⁸ E. Lindner, A. Baumann, P. Wegner, H. A. Mayer, U. Reinöhl, A. Weber, T. S. Ertel, H. Bertagnolli, *J. Mater. Chem.*, 2000, **10**, 1655.
- ⁹ L. L. Hench, J. K. West, *Chem. Rev.*, 1990, **90**, 33.
- ¹⁰ C. J. Brinker, G. W. Scherer, *Sol Gel Science*, Academic Press, London, 1990.
- ¹¹ R. J. P. Corriu, D. Leclercq, *Angew. Chem. Int. Ed.*, 1996, **35**, 1420.
- ¹² J.-P. Bezombes, C. Chuit, R. J. P. Corriu, C. Reye, *J. Mater. Chem.*, 1998, **8**, 1749.
- ¹³ B. Breitscheidel, J. Zieder, U. Schubert, *Chem. Mater.*, 1991, **3**, 559.
- ¹⁴ A. Adima, J. J. E. Moreau, M. Wong Chi Man, *Chirality*, 2000, **12**, 411.
- ¹⁵ F. R. Hartley, P. N. Vezey, *Adv. Organomet. Chem.*, 1977, **15**, 189.
- ¹⁶ W. Dumont, J.-C. Poulin, T.-P. Dang, H. B. Kagan, *J. Am. Chem. Soc.*, 1973, **95**, 8295.
- ¹⁷ R. J. P. Corriu, C. Hoarau, A. Mehdi, C. Reye, *Chem. Commun.*, 2000, 71.
- ¹⁸ E. Lindner, A. Jäger, T. Schneller, H. A. Mayer, *Chem. Mater.*, 1997, **9**, 81.
- ¹⁹ E. Lindner, M. Kemmler, H. A. Mayer, P. Wegner, *J. Am. Chem. Soc.*, 1994, **116**, 348.
- ²⁰ J. Büchele, H. A. Mayer, *Chem Commun.*, 1999, 2165.

-
- ²¹ E. Lindner, R. Schreiber, M. Kemmler, T. Schneller, H. A. Mayer, *Chem. Mater.*, 1995, **7**, 951.
- ²² E. Lindner, T. Schneller, H. A. Mayer, H. Bertagnolli, T. S. Ertel, W. Hörner, *Chem. Mater.*, 1997, **9**, 1524.
- ²³ E. Lindner, T. Salesch, F. Hoehn, H. A. Mayer, *Z. Anorg. Allg. Chem.*, 1999, **625**, 2133.
- ²⁴ C. A. Fyfe, *Solid State NMR for Chemists*, CRC Press, Gulph, ON, 1984.
- ²⁵ H. Eckert, *Prog. Nucl. Magn. Reson. Spectrosc.*, 1992, **24**, 159.
- ²⁶ K. Schmidt-Rohr, H. W. Spiess, *Multidimensional Solid State NMR and Polymers*, Academic Press, London, 1994.
- ²⁷ G. Engelhardt, D. Michel, *High-Resolution NMR of Silicates and Zeolithes*, J. Wiley & Sons, Chichester, New York, Brisbane, Toronto, Singapore, 1987.
- ²⁸ U. Schubert, N. Hüsing, A. Lorenz, *Chem. Mater.*, 1995, **7**, 2010.
- ²⁹ S. R. Hartmann, E. L. Hahn, *Phys. Rev.*, 1962, **128**, 2042.
- ³⁰ A. Pines, M. G. Gibby, J. S. Waugh, *J. Chem. Phys.*, 1973, **59**, 569.
- ³¹ E. R. Andrew, *Prog. Nucl. Magn. Reson. Spectrosc.*, 1971, **8**, 1.
- ³² J. Schaefer, E. O. Stejskal, R. Buchdahl, *Macromolecules*, 1977, **10**, 384.
- ³³ A. D. Tochia, *J. Magn. Res.*, 1978, **30**, 613.
- ³⁴ J. L. Koenig, M. Andreis, *Solid State NMR of Polymers*, (Ed.: L. J. Mathias), Plenum Press, New York, 1991.
- ³⁵ D. W. Sindorf, G. E. Maciel, *J. Am. Chem. Soc.*, 1983, **105**, 3767.
- ³⁶ E. Bayer, K. Albert, J. Reiners, M. Nieder, D. Müller, *J. Chromatogr.*, 1983, **33**, 197.
- ³⁷ M. Mehring, *Principles of High Resolution NMR in Solids*, 2nd ed., Springer-Verlag, Berlin, 1983.
- ³⁸ R. Voelkel, *Angew. Chem. Int. Ed.*, 1988, **27**, 1468.
- ³⁹ R. K. Harris, *Analyst*, 1985, **110**, 649.

- ⁴⁰ R. S. Aujla, R. K. Harris, K. J. Packer, M. Parameswaran, B. J. Say, A. Bunn, M. E. A. Cudby, *Polym. Bull.*, 1982, **8**, 253.
- ⁴¹ E. Lindner, A. Enderle, A. Baumann, *J. Organomet. Chem.*, 1998, **558**, 235.
- ⁴² L. Maier, *Helv. Chim. Acta*, 1968, **51**, 406.
- ⁴³ A. R. J. Genge, A. M. Gibson, N. K. Guymer, G. Reid, *J. Chem. Soc., Dalton Trans.*, 1996, **21**, 4099.
- ⁴⁴ P. Leglaye, B. Donnadiou, J.-J. Brunet, R. Chauvin, *Tetrahedron Lett.*, 1998, **39**, 9179.
- ⁴⁵ C. Kayran, F. Kozanoglu, S. Özkar, S. Saldamli, A. Tekkaya, C. G. Kreiter, *Inorg. Chim. Acta.*, 1999, **284**, 229.
- ⁴⁶ S. O. Grim, R. C. Barth, J. D. Mitchell, J. D. Gaudio, *Inorg. Chem.*, 1977, **16**, 1777.
- ⁴⁷ J. I. Goldstein, D. E. Newbury, P. Echlin, D. C. Joy, A. D. Romig, C. E. Lyman, C. Fiori, E. Lifshin, *Scanning Electron Microscopy and X-Ray Microanalysis*, 2nd ed., Plenum Press, New York/London, 1992.
- ⁴⁸ E. Lindner, W. Wielandt, A. Baumann, H. A. Mayer, U. Reinöhl, A. Weber, T. S. Ertel, H. Bertagnolli, *Chem. Mater.*, 1999, **11**, 1833.
- ⁴⁹ E. A. Stern, *Phys. Rev. B*, 1974, **10**, 3027.
- ⁵⁰ F. W. Lytle, D. E. Sayers, E. A. Stern, *Phys. Rev. B*, 1975, **11**, 4825.
- ⁵¹ J. Karas, G. Huttner, K. Heinze, P. Rutsch, L. Zsolnai, *Eur. J. Inorg. Chem.*, 1999, **3**, 405.
- ⁵² A. Jacobi, G. Huttner, U. Winterhalter, *J. Organomet. Chem.*, 1998, **571**, 231.
- ⁵³ Y.-Y. Yan, T. V. RajanBabu, *Org. Lett.*, 2000, **26**, 4137.
- ⁵⁴ P. A. MacNeil, N. K. Roberts, B. Bosnich, *J. Am. Chem. Soc.*, 1981, **103**, 2273.
- ⁵⁵ G. Descotes, D. Lafont, D. Sinou, J. M. Brown, P. A. Chaloner, D. Parker, *New J. Chem.*, 1981, **3**, 167.
- ⁵⁶ U. Nagel, A. Bublewitz, *Chem. Ber.*, 1992, **125**, 1061.
- ⁵⁷ O. Pamies, G. Net, A. Ruiz, C. Claver, *Eur. J. Inorg. Chem.*, 2000, **9**, 2011.
- ⁵⁸ E. Lindner, A. Jäger, F. Auer, W. Wielandt, P. Wegner, *J. Mol. Catal. A*, 1998, **129**, 91.

-
- ⁵⁹ M. E. Childs, W. P. Weber, *J. Organomet. Chem.*, 1975, **86**, 169.
- ⁶⁰ P. Drew, J. R. Doyle, *Inorg. Synth.*, 1972, **13**, 52.
- ⁶¹ J. J. Eisch, R. B. King (Editors), *Organometallic synthesis Vol.1*, Academic Press, New York, 1965.
- ⁶² G. Giordano, R. H. Crabtree, *Inorg. Synth.*, 1990, **28**, 88.
- ⁶³ E. W. Abel, R. J. Rowley, *J. Organomet. Chem.*, 1975, **84**, 199.
- ⁶⁴ B. I. Yakovlev; *Zh. Obshch. Khim.*, 1949, **19**, 1969; *Chem. Abstr.*, 1950, 1016.
- ⁶⁵ R. Benn, C. Brevard, *J. Am. Chem. Soc.*, 1986, **108**, 5622.
- ⁶⁶ B. E. Mann, in: P. S. Pregosin, *Transition Metal Nuclear Magnetic Resonance*, Elsevier, Amsterdam, 1991.
- ⁶⁷ T. S. Ertel, H. Bertagnolli, S. Hückmann, U. Kolb, D. Peter, *Appl. Spectrosc.*, 1992, **46**, 690.
- ⁶⁸ M. Newville, P. Livins, Y. Yakobi, J. J. Rehr, E. A. Stern, *Phys. Rev. B*, 1993, **47**, 14126.
- ⁶⁹ S. J. Gurman, N. Binsted, I. Ross, *J. Phys. C*, 1986, **19**, 1845.
- ⁷⁰ The low carbon value is due to incomplete combustion of silicon containing compounds, which may be responsible for the formation of SiC: R. Kalfat, F. Babonneau, N. Gharbi, H. Zarrouk, *J. Mater. Chem.*, 1996, **6**, 1673.

5. Summary

The anchoring of reactive centers, especially catalytically active transition metal complexes, to an inert support matrix is a field of increasing interest in terms of academic as well as commercial research. Such materials are able to combine the advantages of homogenous and heterogeneous catalysis: the catalyst becomes easily separable from the reaction products and it can be reused in several runs without an essential loss of activity. On the other hand, the reactive centers are well defined and the improvement of their properties is not only empirical. Due to the homogenous character of the catalytic reaction the activities and selectivities are high.

However, there are still specific problems with such systems which inhibited the commercial breakthrough of these types of catalysts. They can leach from the support during the catalytic reaction. Furthermore the heterogenization of complexes leads to reduced mobility of the reactive centers causing lower activities and selectivities of the anchored catalysts compared to their homogenous counterparts.

A versatile approach to reduce or even eliminate these problems is the introduction of the concept of interphase. In the presence of a stationary phase (e. g. an anchored metal complex) and a mobile phase (solvent, gaseous or liquid reactant) a penetration of both phases on a molecular level takes place. This state is designated as 'interphase' since no homogenous phase is formed. However, interphases are able to imitate homogenous conditions providing favorable activities in different types of catalytic reactions without any essential metal leaching. A typical approach for the generation of stationary phases in interphase chemistry is the sol-gel process, which offers a convenient route for the preparation of suitable polysiloxane networks under smooth and low temperature conditions. Simultaneous co-condensation of T-functionalized metal complexes or ligands with various alkoxysilanes or

organosilanes provides materials, in which the reactive centers are nearly homogeneously distributed across a chemical and thermal inert carrier matrix.

The objective of the present work is the synthesis and systematic investigation of novel stationary phases for 'Chemistry in Interphases'. Thereby structural and dynamic parameters were discussed and the accessibility of the reactive centers was probed by model as well as catalytic reactions.

In the first chapter of this thesis the T-functionalized 1,3-bis(diphenylphosphinyl)propane $[(\text{MeO})_3\text{Si}(\text{CH}_2)_6\text{CH}(\text{CH}_2\text{PPh}_2)_2; \text{PP}(\text{T}^0)]$ was sol-gel processed with the D-bifunctionalized co-condensing agents $\text{MeSi}(\text{OMe})_2(\text{CH}_2)_6(\text{MeO})_2\text{SiMe}$ ($\text{D}^0\text{-C}_6\text{-D}^0$) and $\text{MeSi}(\text{OMe})_2(\text{CH})_3(\text{C}_6\text{H}_4)(\text{CH}_2)_3(\text{MeO})_2\text{SiMe}$ [$\text{Ph}(\mathbf{1,4-C}_3\mathbf{D}^0)_2$] in two different ratios to yield the polysiloxane-bound diphos ligands $[\text{PP}(\text{T}^n)](\text{D}^i\text{-C}_6\text{-D}^i)_y$ ($y = 2.5, 5$) and $[\text{PP}(\text{T}^n)][\text{Ph}(\mathbf{1,4-C}_3\mathbf{D}^i)_2]_y$ ($y = 2.5, 5$). By means of ^{29}Si solid state NMR spectroscopy the real T/D-ratios of all copolymers were determined. No significant washing out of the monomers after the sol-gel process was detectable. It was found, that the materials with the phenyl ring in the backbone show lower degrees of condensation than their counterparts with alkyl chains as main building blocks. ^{31}P and ^{13}C CP/MAS NMR measurements give evidence that the ligands and the matrices are preserved during the entire sol-gel process.

For the investigation of the dynamic properties of the polysiloxane-bound ligands detailed ^{29}Si and ^{31}P CP/MAS NMR relaxation time studies were carried out. The diphos ligands with the phenyl ring containing co-condensation agents are found to be more mobile than those with alkyl chains. This fact can be explained by the lower degree of condensation, which is induced by the sterical demand of the phenyl ring.

To scrutinize the accessibility of the phosphorus centers in these different kinds of stationary phases both polysiloxane-bound diphos ligands $[\text{PP}(\text{T}^n)](\text{D}^i\text{-C}_6\text{-D}^i)_5$ and $[\text{PP}(\text{T}^n)][\text{Ph}(\mathbf{1,4-C}_3\mathbf{D}^i)_2]_5$ were subjected to various classical phosphine reactions. The

oxidation of these diphosphines swollen in *i*-propanol with H₂O₂ resulted quantitatively in the formation of the corresponding phosphine oxides. Polymers with thiophosphoryl centers were obtained when the mentioned diphosphines were reacted with S₈ at 80 °C in toluene. Upon treatment of a suspension of the diphosphines [PP(Tⁿ)](Dⁱ-C₆-Dⁱ)₅ and [PP(Tⁿ)] [Ph(1,4-C₃Dⁱ)₂]₅ in dichloromethane with methyl iodide both phosphorus atoms were quantitatively quaternized. With the quantitative reaction of the diphosphine ligands with (NBD)Mo(CO)₄ and (COD)PdCl₂, respectively, it could be demonstrated, that the phosphorus centers incorporated into both kind of materials are even accessible by rather bulky substrates.

Cationic diphosphinerhodium(I) complexes proved to be highly active in hydrogenation reactions of various olefins. Thus, the second part of the work features the synthesis and characterization of a (COD)diphosphinerhodium(I) complex bound to a polysiloxane network and accessibility studies by the catalytic hydrogenation of 1-hexene. The monomeric precursor complex {(C₈H₁₂)Rh[(Ph₂PCH₂)₂CH(CH₂)₆Si(OMe)₃]}[SbF₆]{(COD)Rh[PP(T⁰)]} was synthesized in a one-pot reaction starting from [μ-ClRh(COD)]₂ by consecutive chloride abstraction with AgSbF₆ and addition of the T-functionalized diphos ligand (MeO)₃Si(CH₂)₆CH(CH₂PPh₂)₂ [PP(T⁰)]. This complex was sol-gel processed with various amounts of the co-condensing agents D⁰-C₆-D⁰ and Ph(1,4-C₃D⁰)₂ to give the novel stationary phases {(COD)Rh[PP(Tⁿ)]}(Dⁱ-C₆-Dⁱ)_y (y = 0, 2.5, 5, 10, 20) and {(COD)Rh[PP(Tⁿ)]}[Ph(1,4-C₃Dⁱ)₂]_y (y = 0, 2.5, 5, 10, 20).

Multinuclear solid state NMR experiments (¹³C, ²⁹Si, ³¹P) reveal the integrity of the rhodium centers and of the polysiloxane matrices. The found T/D-ratios do not differ significantly from the applied stoichiometric compositions and the degrees of condensation range between 77 and 98 % and 73 and 100 % for the D-functions and T-groups, respectively.

The distances in the next coordination sphere of the rhodium atom in the polysiloxane-bound complexes were determined by EXAFS spectroscopy.

Dynamic NMR investigations on the matrix and the reactive centers point out that the mobility increases with higher amounts of the co-condensing components, which can be explained with the electrostatic repulsion of the cationic rhodium centers. If the positively charged metal complexes are diluted across the support matrix, the radius of motion is enhanced and therefore the mobility increases.

The accessibility of the polysiloxane-bound diphosphinerhodium(I) complexes was investigated by the catalytic hydrogenation of 1-hexene. All applied complexes show rather good turnover frequencies and are therefore readily accessible for substrates. But due to solvation and swelling effects there is no predictable correlation between the catalytic activity and the type of the co-condensing component. However, SEM images give some evidence, that the activity depends on the size of the particles of the materials: smaller particles induce a higher catalytic activity than larger particles. An enhancement of the conversion rate was achieved by the use of polar solvents (1,4-dioxane, methanol). If the catalysts were reused in three consecutive runs, no loss of activity and metal leaching was found.

The focus of the last section is the synthesis of novel co-condensing agents, which combine – after the sol-gel process– a highly mobile alkyl chain with a low degree of condensation to achieve an increase of mobility. The monomeric D- and T-functionalized co-condensates $\mathbf{R}_2\text{Si}(\text{C}_3\text{D}^0)_2$ [$\text{MeSi}(\text{OMe})_2(\text{CH}_2)_3\text{SiR}_2(\text{CH}_2)_3(\text{OMe})_2\text{SiMe}$; $\text{R} = \text{Me}, \text{Et}$] and $\mathbf{R}_2\text{Si}(\text{C}_3\text{T}^0)_2$ [$(\text{MeO})_3\text{Si}(\text{CH}_2)_3\text{SiR}_2(\text{CH}_2)_3\text{Si}(\text{OMe})_3$; $\text{R} = \text{Me}, \text{Et}$] were prepared by hydrosilylation of the corresponding diallyldialkylsilanes with dichloromethylsilane and trichlorosilane respectively, followed by the replacement of the chlorine atoms for methoxy groups with trimethyl orthoformate.

These precursors were sol-gel processed without and with phenyltrimethoxysilane as the co-condensing agent. The obtained xerogels were investigated by means of solid state NMR experiments (^{13}C , ^{29}Si). According to ^{13}C CP/MAS NMR data the pure D-polymers show a higher degree of hydrolysis than the pure T-, $\text{T}_{\text{Ph}}/\text{D}$ -, and $\text{T}_{\text{Ph}}/\text{T}$ -copolymers. ^{29}Si SPE/MAS measurements and dynamic NMR studies (via ^{29}Si) corroborate that the pure T-xerogels as well as the $\text{T}_{\text{Ph}}/\text{D}$ - and $\text{T}_{\text{Ph}}/\text{T}$ -materials are lower condensed and exhibit a higher mobility than the pure D-polymers. However, the observed mobilities of these new materials are higher compared with those of $\text{D}^i\text{-C}_6\text{-D}^i$, $\text{Ph}(\mathbf{1,4-C}_3\mathbf{D}^i)_2$, and $\text{Ph}(\mathbf{1,4-C}_3\mathbf{T}^n)_2$.

In order to examine the mobilities and dynamics of these new materials in interphases ^1H HR/MAS experiments and $T_{1\rho\text{H}}$ measurements of suspensions of all polymers in different solvents were carried out. In solvents of medium polarity (CDCl_3 , THF) all xerogels form highly mobile interphases in contrast to polar solvents (MeOH). The pure D-polymers are found to exhibit the lowest mobilities of all applied xerogels, which can be explained by the high degree of condensation.

Meine akademische Ausbildung verdanke ich:

K. Albert, G. Bach, H. Bertagnolli, W. Brunn, H. Eckstein, W. Dammertz, W. Dilger, A. Donges, M. Hanack, H.-P. Hagenmaier, W. Höhle, P. Horn, G. Jung, B. Koppenhöfer, N. Kuhn, E. Lindner, M. Maier, H. A. Mayer, H.-J. Meyer, K. Müller, U. Nagel, D. Oelkrug, H. Pauschmann, E. Plies, H.-G. v. Schnering, V. Schurig, F. F. Seelig, H. Sorber, B. Speiser, J. Strähle, R. Thalacker, W. Voelter.

Lebenslauf

Persönliche Daten

Name: Stefan Michael Brugger
Geburtstag/–ort: 18. Juni 1971 in Kempten/Allgäu
Eltern: Wilhelm Brugger
Hannelore Brugger, geb. Bresele
Staatsangehörigkeit: deutsch

Schulbildung

Sept. 1977 – Juli 1981 Grundschule Martinszell
Sept. 1981 – Juli 1982 Hauptschule Waltenhofen
Sept. 1982 – Juli 1991 Allgäu Gymnasium Kempten
10. Juli 1991 Erhalt der Allgemeinen Hochschulreife

Wehrdienst

Juli 1991 – Sept. 1992 Artilleriekaserne Kempten

Studium

Okt. 1992 – Dez. 1996 Chemie mit Schwerpunkt Allgemeine Chemie an der Fachhochschule der Naturwissenschaftlichen – technischen Akademie Isny
März 1996 – Okt. 1996 Diplomarbeit über das Thema „Beiträge zur Charakterisierung von Silanen und Siloxanen mit homo- und heteronuklear gebundenen Si-Partialstrukturen“ bei Prof. Dr. H.-G. v. Schnering am MPI für Festkörperforschung in Stuttgart
06. Dez. 1996 Zeugnis über die Diplomprüfung
April 1997 – Juni 1998 Eignungsfeststellungsverfahren an der Universität Tübingen
10. Juni 1998 Zulassung als Doktorand durch die Fakultät für Chemie und Pharmazie der Universität Tübingen
Juni 1998 – Mai 2001 Dissertation unter der Leitung von Prof. Dr. E. Lindner am Institut für Anorganische Chemie der Universität Tübingen mit dem Thema „Synthesis and Characterization of Novel Stationary Phases for Model and Catalytic Reactions in Interphases and New Polysiloxane Matrices“
Okt. 1998 – Mai 2001 Promotionsstipendium im Graduiertenkolleg „Chemie in Interphasen“